Chapter 8

Modelling of particulate matter

Key points

- Models for predicting PM concentrations are essential for assessing pollutant levels at locations without monitors, for making future projections and for investigating the potential of different air pollutant mitigation policies.

- In view of the many different sources and the diverse chemical make-up of particulates in the atmosphere, no model is able to fully describe all the processes related to their generation and spatial variation in concentration. However, a range of different types of model of varying sophistication are currently available for predicting concentrations for different spatial scales and averaging times.

- Models routinely used for scales up to the national scale are either empirically based or make use of dispersion algorithms or a combination of the two. The empirical models are generally fast to run, make full use of available data and are able to provide both source apportionment and predictions of annual means. However, they are not able to provide reliable daily peak concentrations nor are they easily transferable to areas with few observations. In addition, both estimated mass concentration and source apportionment depend critically on the measurement technique employed.

- Dispersion models are able to predict concentrations at smaller averaging times and at greater spatial resolution. They can provide source apportionment for each emission category defined within the relevant emission inventory. However, they make less direct use of available data and may require increased run times. Dispersion models are not able to account for the variation of roadside concentration with road type unless they consider local effects such as surface roughness changes, vehicle-induced turbulence, exhaust height, presence of street canyons and so on. For this reason, empirical models have made use of roadside adjustment factors; however, these are based on limited data and little quantitative understanding of the processes involved.

- Both types of models have significant uncertainties connected with the residual largely coarse component, which is not modelled explicitly. The different empirical models are at variance in their estimates of the background coarse component as shown by the source apportionment, whereas dispersion models generally add a constant based on monitoring data to take account of this contribution. Neither approach can be projected forward in a satisfactory manner. The modelling of the traffic-related coarse component is also poorly formulated.

- Regional models continue to be developed by including more sophisticated parameterisations of the physical and secondary inorganic chemical processes. These models are now used routinely to investigate future projections and

emission scenarios for policy development across the UK and Europe. Because of the large areas considered, their spatial resolution is much lower so that they are only able to predict background concentrations.

- The national model and London-based calculations suggest that in a typical meteorological year, the annual average PM_{10} will generally achieve the 2005 limit value (40 µg m^{-3}) in 2005, but that there are likely to be widespread exceedences of the Stage II indicative limit value of 20 µg m^{-3} in 2010, especially in urban areas. The extent of these exceedences varies significantly according to the model employed. Exceedences of the daily average will be close to the limit value in major urban areas, especially London in 2005; however, the extent of exceedence of the 2010 daily limit value depends markedly on whether this parameter is calculated from annual mean or directly from daily averages, as in dispersion models.

- Regional models are able to reproduce the main observed features of distributors of particulate sulphate, nitrate and ammonium across Northwest Europe and the southeast-northwest gradient across the British Isles.

- $PM_{2.5}$ modelling has been calculated both nationally and for London. However, the reliability of these models is currently difficult to determine because of the wide divergence in measurements of the different monitoring devices and lack of agreed conversion (or scaling) factors.

8.1 Introduction

739. This chapter presents details of local, urban and regional models used for calculating PM concentrations in the UK. It also includes maps and tables of calculated PM concentrations of relevance to compliance with PM_{10} air quality limits and policy development in the UK. Although monitors can give information about PM concentrations at specific points, they can only give limited information about the spatial distribution of concentration, source apportionment and future concentrations. Models are therefore an essential tool for assessing future policy and for understanding the physical and chemical processes that determine PM concentrations and trends.

740. A fully comprehensive model for PM would include source modelling, particle condensation and accumulation models, advection/dispersion/deposition and chemical transformation models on a range of spatial scales from local to long range. The compilation of such a model is not scientifically viable at the moment because some important processes (for example, non-exhaust traffic emissions) are not well understood compared to other processes; it would not be practically useful either. However, a great number of models do exist for different aspects of the problem. These tend to focus on specific scale ranges or physical/chemical processes and either ignore other important processes/effects or take account of them through simple assumptions or parameterisation and/or use appropriate monitoring of PM concentrations to complement the modelling. It is not possible to describe or even mention the full range of models available and so prominence is given to the models that are informing policy development and assisting with air quality assessment in the UK. For convenience these are presented in four separate categories, although sometimes – for certain aspects of the models – the distinctions between the different categories are not clear cut.

741. The models that have been used routinely to calculate concentrations (both current and projected) across the UK are the APEG Receptor Model and the Mapping Model developed by Netcen. This first group of models is semi-empirical, relying to a large extent on monitored data, but they also include a local dispersion modelling component. The second group of models covers those designed for calculating concentrations at high spatial resolution across urban areas. These vary in the relative extent to which they rely on either dispersion modelling and/or monitoring data as the basis for their calculations. The third major group are the regional or long range models. These cover greater spatial scales at lower spatial resolution than the urban models. These models require meteorological fields as input and include both Eulerian and Lagrangian models for advection and dispersion. They may also include advanced routines for droplet condensation/accumulation and chemical transformation. The remaining category consists of road emission models and finally there is some discussion of a miscellaneous set of models, including particle accumulation models, particle source models and other models/modelling studies prominent in Europe or North America but which have not been used for policy development in the UK.

742. This chapter starts by presenting each of these model groups in turn, including validation and case studies as appropriate. Section 8.3 compares and contrasts the different modelling approaches to important effects/contributions. Section 8.4 presents model outputs mainly from the first three groups described above. This section includes current and future projections, at both national and urban scales, maps and receptor point output and detailed source apportionment; where possible, appropriate comparisons are made between different models. Finally, Section 8.5 includes discussion of model uncertainty before conclusions and recommendations are made in Section 8.6.

8.2 Current modelling and mapping methods

8.2.1 National models – Receptor and Mapping

8.2.1.1 Site-specific source apportionment using the APEG receptor model

743. This model – developed for APEG (APEG, 1999; Stedman *et al*., 2001a) – calculates the source apportionment of PM_{10} and $PM_{2.5}$concentrations at locations where concentrations of these pollutants are measured. The basic assumption is that the daily average PM concentration can be considered as three distinct components, namely:

- primary combustion PM;
- secondary PM; and
- 'other' PM.

744. It is further assumed that the primary PM is related directly to co-located NO_X measurements and that secondary PM can be determined from rural sulphate measurements. Then a regression analysis is carried out for the calendar year of monitoring data for each site to determine the coefficients A and B as follows:

$$[\text{measured } PM_{10} (\mu g\ m^{-3}, \text{TEOM})] = A\ [\text{measured } NO_X (\mu g\ m^{-3}, \text{as } NO_2)] + B\ [\text{measured sulphate } (\mu g\ m^{-3})] + C\ (\mu g\ m^{-3}, \text{TEOM}).$$

Note that the analysis presented here is generally based on TEOM instruments.

745. The contribution from primary PM is further subdivided into the contributions from each emission sector (traffic, domestic, industry and so on). The contribution from individual point sources is calculated using ADMS 3.1.

746. The contribution from secondary PM is divided into the contribution from sulphate and nitrate by assuming that all of the sulphate is present as ammonium sulphate and that the remainder of the secondary PM within the secondary fraction determined from the regression analysis is present as nitrate. Thus, all of the site-to-site variation in the relationship between sulphate and secondary PM concentrations is assumed to be due to variation in the nitrate component, as is apparent from the results for 2002 listed in Tables 8.6–8.13. Note the nitrate concentration is greater for gravimetric PM_{10} measurements than for TEOM PM_{10} measurements and very low for TEOM $PM_{2.5}$ measurements, as might be expected due to the losses of ammonium nitrate for the TEOM measurement and the relatively larger size ranges of sodium nitrate particles.

747. The site-specific source apportionment has been combined with temporal trends in emissions to calculate site-specific projections both backwards and forwards in time, as described in the AQEG NO_2 report (AQEG, 2004). The primary PM concentration from each source sector has been projected according to published emission trends for each sector. The contributions from sulphate and nitrate particles have been projected forward by assuming that sulphate and nitrate concentrations will follow the predicted emissions reductions required to meet the National Emissions Ceilings Directive targets. The trends in previous years have been derived from the trends in measured rural mean sulphate and nitrate across the UK. The concentration of 'other' particles (the residual) for which emissions cannot currently be specified is assumed to remain unchanged in all years. The projected total annual mean PM concentration from all sources is calculated as the sum of the contributions in each year.

8.2.1.2 Netcen mapping model

748. The Netcen mapping model (Stedman *et al*., 2003) is designed to calculate UK-wide maps of annual average pollutant concentration at sufficient speed that extensive scenario testing can be conducted. The background maps provide concentrations at 1-km resolution, and a single representative concentration for each road segment is used to represent a roadside increment.

749. The maps of background concentrations are made up of the following components:

- large point sources of primary particles;
- small point sources of primary particles;
- area sources of primary particles;
- secondary particles; and
- the residual component (usually be dominated by particles within the PM_{coarse} fraction).

8.2.1.2.1 Contributions from point sources

750. The contribution to annual mean PM_{10} concentrations from 58 PM_{10} point sources with >200 tonnes per annum emission, is modelled using ADMS 3.1 and sequential meteorological data for 2002 from Waddington. Concentrations of PM_{10} point sources with less than 200 tonnes per annum release are modelled on the assumption that they all disperse in a similar manner i.e., the sources are assumed to have the same height, buoyancy and momentum (Stedman *et al.*, 2003).

8.2.1.2.2 Contributions from area sources

751. Figure 8.1 shows the calibration of the area source model. The modelled large point and small point source and mapped secondary PM_{10} has been subtracted from the measured annual mean PM_{10} concentration at background sites. This is compared with the modelled area source contribution to annual mean PM_{10} concentration calculated with ADMS 3.1 using emissions from a 33 km x 33 km square in which the receptor point is at the centre. It is assumed that all area sources disperse with initial buoyancy or momentum and in identical meteorological conditions in this case 10-year average meteorological data for 1993–2002 from Heathrow have been used. Calibration plots are shown in μg m^{-3} (TEOM), since TEOM measurements have been used to calibrate the models. Following the same approach that used for NO_X, the monitoring sites are split into two groups: 'inner conurbations' and 'elsewhere', but the scatter is large. It is clear from the figure that the calibration relationships are much weaker than the corresponding relationships for NO_X (AQEG, 2004). This is due to the smaller contribution of local area sources to ambient PM concentrations compared with regional contributions relative to NO_X. Robust relationships have been found for NO_X and the same method has, therefore, been applied to PM. The modelled area source contribution is multiplied by the relevant empirical coefficient to calculate the calibrated area source contribution for each grid square in the country.

Figure 8.1 Calibration of a PM_{10} area source model.

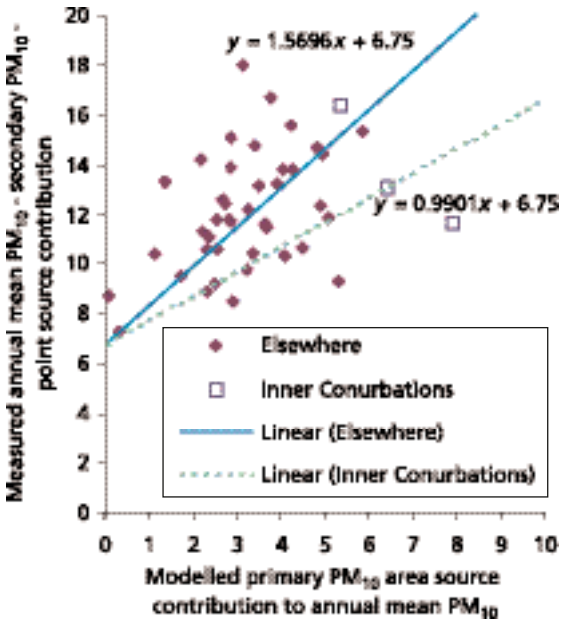

8.2.1.2.3 Secondary particle contributions

752. Secondary particles are assumed to consist of sulphates and nitrates only, as in the receptor model. A map of secondary PM_{10} particle concentrations across the UK is calculated from rural measurements of sulphate and nitrate concentrations by interpolation onto a 20 km x 20 km grid. Sulphate and nitrate particle concentrations were measured on a monthly basis at 12 rural sites using a denuder method during 2002 (CEH, 2003).

753. Sulphate is assumed to be present as ammonium sulphate, and sulphate concentrations were multiplied by 1.354 to take the presence of the counter ion into account. The mean value of the APEG receptor model coefficient B, described above and relating secondary PM_{10} concentrations to sulphate concentrations in 2002, was 2.71, averaged over 11 background monitoring sites. A comparison of interpolated sulphate and nitrate concentrations at these locations indicates that a scaling factor for nitrate concentrations of 1.0 is equivalent (along with a sulphate scaling factor of 1.354) to the sulphate to nitrate ratio implied by the coefficient derived from the APEG receptor model. (The equivalent B factor derived from the interpolated concentration fields at these 11 locations was 2.76.) TEOM instruments are subject to partial losses of the more volatile particle components, such as ammonium nitrate. This may explain why a scaling factor of greater than 1.0 is not required to take account of the counter ions associated with the measured nitrate concentrations.

8.2.1.2.4 Coarse and other particles not included explicitly in the modelling

754. A constant residual particle concentration c above of 8.8 µg m^{-3} (gravimetric) (6.75 µg m^{-3}, TEOM) is the final component of the mapped PM_{10} concentration at background locations. This represents emissions of particles more especially in the larger size or coarser range and includes other sources such as wind-blown dusts, sea salt and agricultural activities, which are not generally included in emission inventories.

8.2.1.2.5 Roadside concentrations

755. The annual mean concentration of PM_{10} at a roadside location is assumed to be made up of two parts: the background concentration (as described above) and a roadside increment dependent on traffic flow:

roadside increment (µg m^{-3},TEOM) = 0.242 (g m^{-1} s^{-1})
* road link emissions (adjusted traffic flow).

Figure 8.2 Calibration of PM_{10} roadside increment mode.

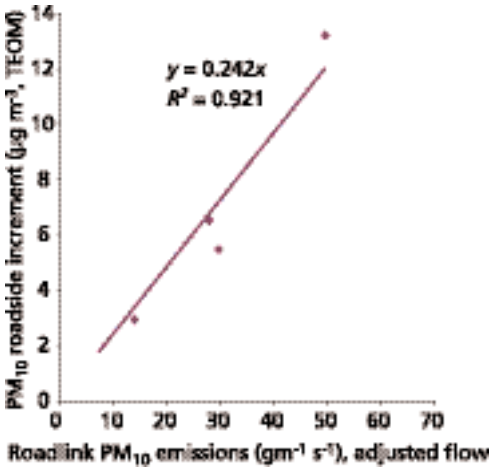

756. The NAEI provides estimates of PM_{10} emissions for major road links in the UK for 2001 (Dore *et al.*, 2003) and these have been adjusted to provide estimates of emissions in 2002. Figure 8.2 shows a comparison of the roadside increment of annual mean PM_{10} concentrations at roadside or kerbside national automatic monitoring sites with PM_{10} emission estimates for the individual road links alongside which these sites are located. Emissions were adjusted for annual average daily traffic flow using the method described in Section 8.3.2.

8.2.1.2.6 Verification of mapped values

757. Figures 8.3 and 8.4 show comparisons of modelled and measured annual mean PM_{10} concentration in 2002 at both background and roadside monitoring site locations. Both the national network sites used to calibrate the models and verification sites are shown.

Figure 8.3 Verification of background annual mean PM_{10} model 2002.

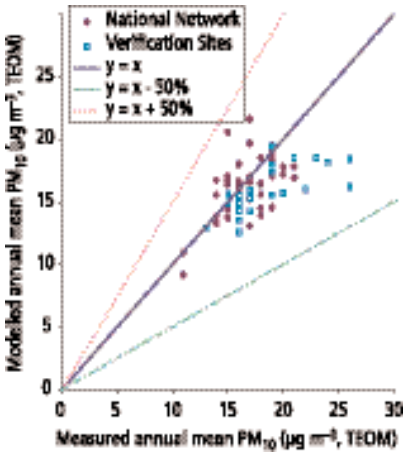

Figure 8.4 Verification of roadside annual mean PM_{10} model 2002.

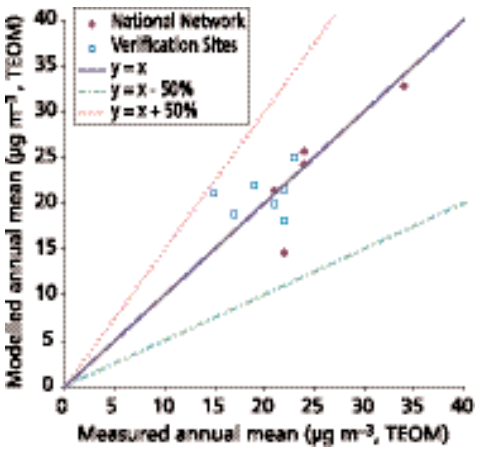

758. The PM_{10} models were calibrated using measurement data from TEOM instruments. Measurements of PM_{10} concentrations using gravimetric instruments (KFG and Partisol instruments) are now available for a number of sites in the UK. These measurements provide an additional independent verification of the model results. A comparison of measured annual mean concentrations in 2002 with estimates calculated by multiplying the modelled PM_{10} concentrations by 1.3 is shown in Figure 8.5.

Figure 8.5 Verification of annual mean TEOM PM_{10} * 1.3 model 2002: comparison with gravimetric measurements.

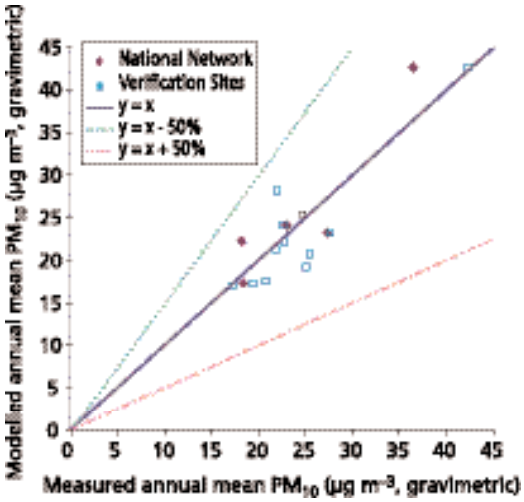

759. The 24-h mean concentrations are not explicitly modelled for comparison with the 24-h limit values. Instead an annual mean concentration of 31.5 µg m^{-3} (gravimetric) is taken to be equivalent to 35 days with 24-h mean concentrations greater than 50 µg m^{-3} (gravimetric; the Stage I 24-h limit value). This equivalence is derived from an analysis of recent monitoring data (Stedman *et al.*, 2001b) and is reproduced in Figure 8.6. The relationship between the number of days with concentrations >50 µg m^{-3}, gravimetric and annual mean become increasingly uncertain at lower numbers of exceedences.

Figure 8.6 The relationship between the number of days with PM_{10} concentrations ≥50 µg m^{-3} and annual mean concentration (1992–1999).

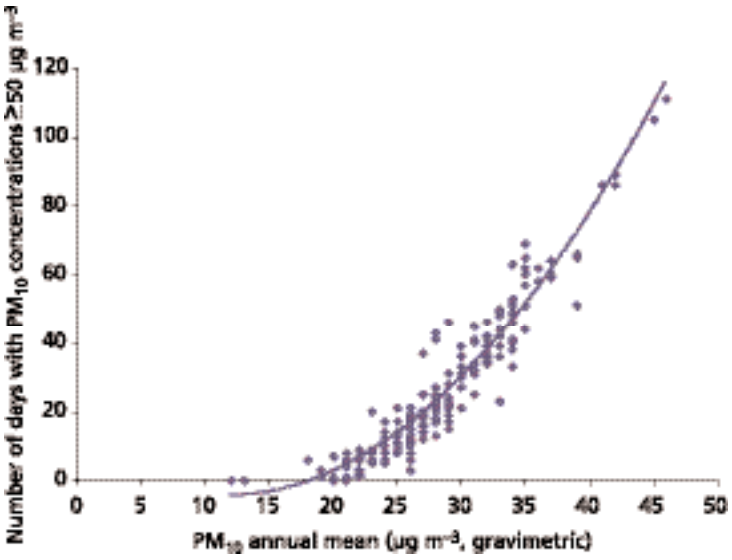

8.2.1.2.7 $PM_{2.5}$ maps

760. Maps of $PM_{2.5}$ concentrations are calculated using similar models to those applied to calculate the national maps of PM_{10} concentrations. Measurement data for $PM_{2.5}$ are only available for a much smaller number of sites and a generally applicable scaling factor between the different measurement methods is not available and so no equivalent factor to 1.3 for PM_{10} has been used for $PM_{2.5}$ in the Netcen mapping model. A factor of 1.3 has, however, been used in the ADMS-Urban calculations.

761. The NAEI PM_{10} emission inventory was used to calculate the $PM_{2.5}$ maps. The emissions from sectors for which the majority of the emission is expected to be in the size range greater than 2.5 µm were excluded (construction and quarries). Table 8.1 shows the separate scaling factors for TEOM and gravimetric measurements within the national mapping model for secondary PM concentrations and the concentrations of PM not modelled explicitly.

762. There is clearly some inconsistency between the models adopted for PM_{10} and $PM_{2.5}$ because a factor of 1.3 has been applied to the PM_{10} TEOM maps to scale to the PM_{10} gravimetric maps, whereas the different $PM_{2.5}$ maps account for the difference between the monitoring methods by applying different scaling factors for nitrate alone.

Table 8.1 Assumptions within the national modelling of PM_{10} and $PM_{2.5}$.

	Sulphate factor	Nitrate factor	Residual PM ($\mu g\ m^{-3}$)
PM_{10} TEOM	1.354	1.000	6.75
PM_{10} gravimetric[a]	1.760	1.300	8.80
$PM_{2.5}$ TEOM	1.354	0.333	4.50
$PM_{2.5}$ gravimetric	1.354	1.500	4.50

[a]Assumed to be TEOM * 1.3.

8.2.2 Urban models

763. The urban models described in this section are used to calculate the pollutant concentrations at high resolution in an urban area. The impacts of road sources are fully resolved so that spatial variations in concentration across and near roads can be calculated.

8.2.2.1 ERG PM_{10} model and predictions

764. For predictions of PM_{10} in London, ERG has utilised the measurements available in London to derive a receptor-based PM_{10} model. Regression analyses of NO_X and PM_{10} have been extended to include $PM_{2.5}$, and thus PM_{10} has been divided into four components: $PM_{2.5}$ that is related to NO_X:$PM_{2.5}$ $f(NO_X)$; $PM_{2.5}$ that is not related to NO_X:$PM_{2.5}$ <> $f(NO_X)$; coarse particles that are related to NO_X:PM_C $f(NO_X)$; and coarse particles that are not related to NO_X:PM_C <> $f(NO_X)$. The NO_X and non-NO_X components can be combined to produce PM_{10} that is related to NO_X:PM_{10} $f(NO_X)$ and PM_{10} that is not related to NO_X:PM_{10}<>$f(NO_X)$.

Where: $PM_{10}\ f(NO_X) = PM_{2.5}\ f(NO_X) + PM_C\ f(NO_X)$
$PM_{10}<>f(NO_X) = PM_{2.5}<>f(NO_X) + PM_C<>f(NO_X)$.

Total PM_{10} can be calculated:
$PM_{10} = PM_{10}\ f(NO_X) + PM_{2.5}<>f(NO_X) + PM_C<>f(NO_X)$.

765. In the formulation above it is assumed that the particle fractions that are related to NO_X are related to primary emissions. Fine particles, which cannot be related to NO_X, are assumed to comprise secondary aerosol. Coarse particles that are not related to NO_X might be expected to consist of wind-blown dusts and other natural particles. The particle fraction definitions include a coarse component that can be related to concentrations of NO_X.

766. Annual mean values of NO_X, PM_{10} and $PM_{2.5}$ were calculated, at monthly intervals, at sites with co-located measurements. Annual means were chosen to eliminate the effects of seasonality and a minimum of 75% data capture was required to ensure that the measurement was representative of the year. Relationships between annual mean NO_X, and PM_{10} and between NO_X and $PM_{2.5}$ were established using linear regression. Each monthly analysis used annual mean measurements from all site types, including kerbside, roadside, urban background, suburban and rural locations. A maximum of 22 sites have been used for the

PM_{10} analysis and a maximum of five sites for $PM_{2.5}$. Linear regressions have been derived of the form:

$$PM_{10}\ (\mu g\ m^{-3}) = A\ NO_X\ (ppb) + B\ (\mu g\ m^{-3})$$
$$PM_{2.5}\ (\mu g\ m^{-3}) = C\ NO_X\ (ppb) + D\ (\mu g\ m^{-3})$$

767. The gradient (A and C) enables the calculation of the PM_{10} and $PM_{2.5}$ that is related to NO_X, for example, combustion-related particles. The intercept (B and D) gives the annual mean of the PM_{10} and $PM_{2.5}$ that is not related to NO_X, which would include the secondary aerosol, for example. The time series of gradients and intercepts is shown in Figures 8.7 and 8.8. Only results from annual mean NO_X against PM_{10} regressions with $r^2 > 0.8$ have been used to produce the time series of A and B. Fewer sites were available for $PM_{2.5}$, therefore NO_X against $PM_{2.5}$ regressions with $r^2 > 0.75$ and more than three sites have been used to produce the time series of C and D. The variation in the gradients shown in Figure 8.7 is reasonably consistent over the period of analysis, as indicated by the small standard deviation ( ) in Equation 1. For PM_{10}, for example, over 5 years the gradient has not varied much above or below 0.086. Assuming that the underlying ratios of PM_{10} and $PM_{2.5}$ to NO_X are constant, the mean gradients can be used to derive the overall relationships which are applicable across the range of site types:

$$PM_{10} f(NO_X) = 0.086\ [NO_X]\ (= 0.005)\ (\mu g\ m^{-3}\ ppb^{-1}) \quad (1)$$
$$PM_{2.5} f(NO_X) = 0.072\ [NO_X]\ (= 0.002)\ (\mu g\ m^{-3}\ ppb^{-1}) \quad (2)$$

Figure 8.7 Regression gradients for PM_{10} and $PM_{2.5}$.

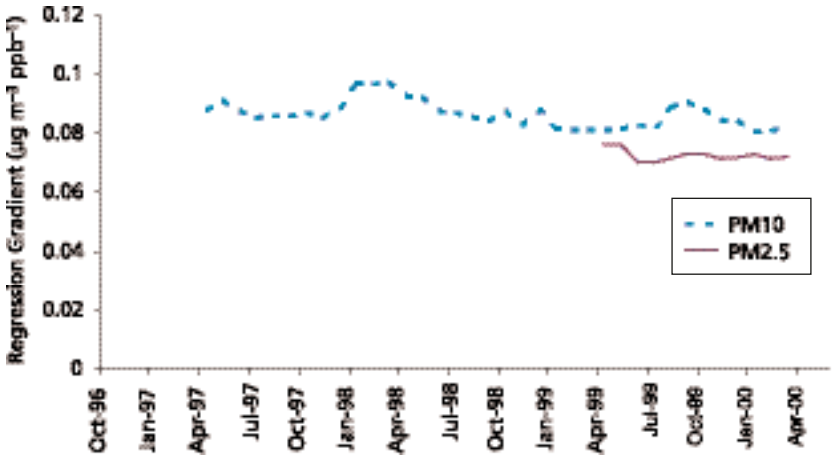

768. The annual mean concentrations of the two components that are independent of NO_X can be seen in Figure 8.8. From this analysis of annual means it appears that $PM_{10}<>f(NO_X)$ has declined considerably during the 4-year period (unlike the gradients shown in Figure 8.7), from around 18.4 µg m^{-3} to 15.3 µg m^{-3}. This decline might be due to the differing meteorology in each year. However, it is more likely that the decline is due to reductions in the emissions that result in the formation of secondary aerosol arising from measures being taken on the European scale. The concentration of $PM_{10}<>f(NO_X)$ has remained relatively stable since January 1999, which is reflected in the stability of $PM_{2.5}<>f(NO_X)$ and $PM_C<>f(NO_X)$. The annual mean $PM_C<>f(NO_X)$ has remained relatively constant at around 5 µg m^{-3}.

Figure 8.8 Regression intercepts for PM_{10} and $PM_{2.5}$.

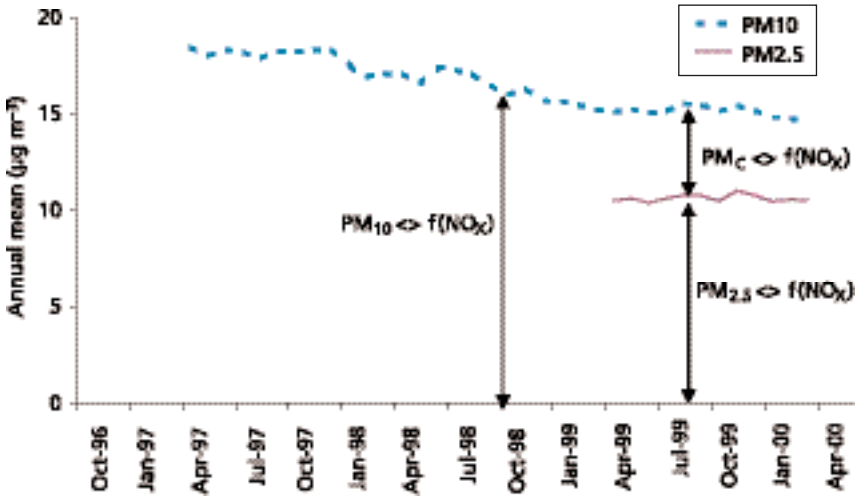

769. A time series of daily means for each of the particulate components was calculated by applying the factors derived from the regression in Equations 1 and 2 to the daily mean NO_X, PM_{10} and $PM_{2.5}$ measured at each of the sites with co-located measurements. This approach allowed the calculation of the NO_X-dependent components. The non-NO_X dependent components were then calculated by subtraction.

770. To enable predictions at other locations, several key assumptions were made. The daily mean NO_X independent components across the area were assumed to be independent of site location. This assumption is probably reasonable for the fraction that includes the secondary aerosol because the sources of these components are distant compared to the size of the London region. The fraction most related to wind-blown dusts, for example, will be influenced by very local conditions, but is also assumed to be constant. The daily mean variation in concentrations of NO_X is required to derive $PM_{2.5}$ $f(NO_X)$ and PM_C $f(NO_X)$.
A time series of daily mean NO_X concentrations can be derived in several ways, depending on the application. For site-specific assessments, use was made of actual NO_X measurements. For the prediction of PM_{10} at locations where NO_X concentrations are not measured (or for predictions into the future), an alternative approach is required that uses a dispersion model to predict the NO_X concentrations. The fraction of $PM_{2.5}$ related to secondary aerosol is reduced in line with that estimated by APEG (1999), that is, a 30% reduction between 1996 and 2010. Further information on the general approach adopted by ERG to modelling concentrations of primary pollutants is considered in the AQEG NO2 report (AQEG, 2004).

771. The PM_C<>$f(NO_X)$ component is relatively small, around one-third of the overall PM_{10}<>$f(NO_X)$, with an annual mean of ~5 µg m^{-3}. Accurate determination of the daily mean PM_C<>$f(NO_X)$ is, therefore, difficult. The PM_C<>$f(NO_X)$ shows no overall trend during 1996–1999. The $PM_{2.5}$<>$f(NO_X)$ derived from separate NO_X and $PM_{2.5}$ measurement sites shows very good agreement, confirming that $PM_{2.5}$<>$f(NO_X)$ is largely invariant over the London region, even on a daily basis.

772. Figures 8.9 and 8.10 show the predictions of PM_{10} at monitoring sites in London for different years.

Figure 8.9 Site-specific annual mean PM_{10} predictions: ERG model compared with measured data.

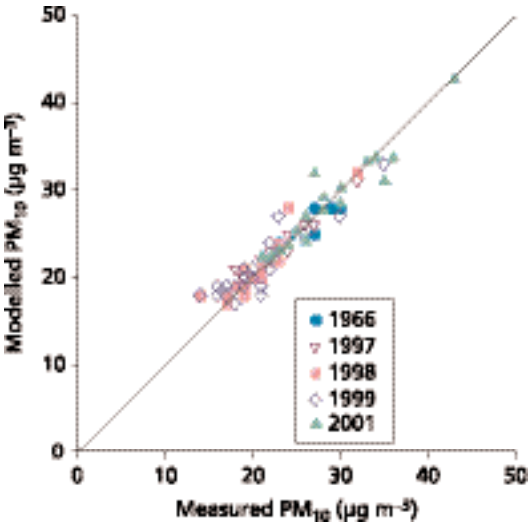

Figure 8.10 Number of days exceeding 50 µg m^{-3} (TEOM * 1.3): ERG model compared with measured data.

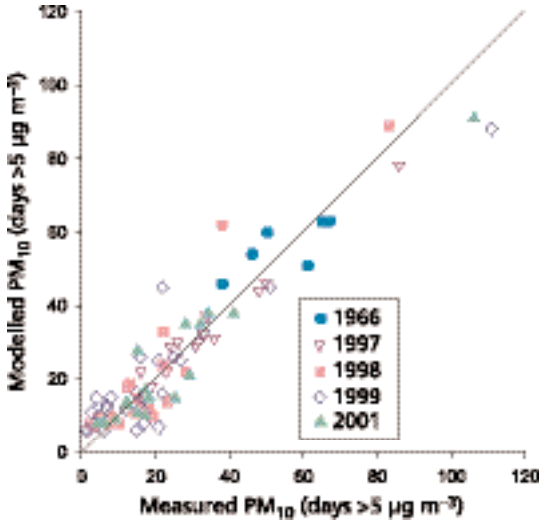

8.2.2.2 *ADMS-Urban*

773. A description and discussion of ADMS-Urban and its application to the calculation of NO_X and NO_2 concentrations in urban areas with specific examples from London has recently been presented in AQEG's report on NO_2 (AQEG, 2004). In this section, only specific aspects of the model relevant to PM calculations will be described together with model validation and verification for PM. Further details may be found in Carruthers *et al*. (2002) and Blair *et al*. (2003). Total concentrations are summed from three components broadly similar to the split used in the Netcen model:

(i) Concentrations of PM arising from the primary emissions specifically accounted for in the emissions inventory for the urban area under consideration. These are calculated from the advection and dispersion algorithms within ADMS-Urban.

(ii) A background component representing secondary PM and PM from other sources (for example, sea salt) transported into the urban area. This component is estimated from measured rural PM concentrations, which – in the case of London – are Harwell and Rochester. Forward projections of the secondary contribution are based on EMEP model calculations; for a base year of 1999 meteorology, the secondary component is reduced by 33% by 2010.

(iii) 'Other' PM representing sources not accounted for in (i) and (ii). These are considered to be coarse PM (for example, non-exhaust traffic emissions, construction dust) arising from within the urban area for which emissions cannot be specified. For the case of PM_{10} this component is taken as a constant 5 µg m^{-3} (gravimetric) across London and is broadly consistent with the observed increment between rural and London background sites. A further coarse component is assumed to be included in the regional background contribution (ii), thus the total coarse contribution for PM_{10} (rural and urban) is 9.9 µg m^{-3} (gravimetric), which is similar to values used in the national model. For $PM_{2.5}$ the 'other' component is assumed to be 30% of that in PM_{10}, consistent with values measured by Harrison *et al*. (2003) and Harrison *et al*. (2004).

774. ADMS-Urban has been used to calculate PM_{10} concentrations in cities both in the UK and elsewhere. Examples of comparisons of model calculations with data from automatic monitoring sites are presented for London, Manchester and York in Figure 8.11: this shows both annual means and percentiles corresponding to 35 exceedences (90.4th percentile) and 7 exceedences (98.1th percentile). The London calculations are for 1999 and utilize the 1999 LAEI for 1999 met data from Heathrow Airport. For Manchester the calculations used are the Greater Manchester Inventory for 2002 and meteorological data from Manchester Ringway Airport for that year. Background data are from Manchester South, Wirral Tranmere, Preston and Ladybower AURN sites. For York the calculations used York City Council's inventory for the year 1999 and meteorological data from Leeds for that year. The background data are from Ladybower and Harwell.

Figure 8.11 PM_{10} Comparison of ADMS-Urban and monitored data.

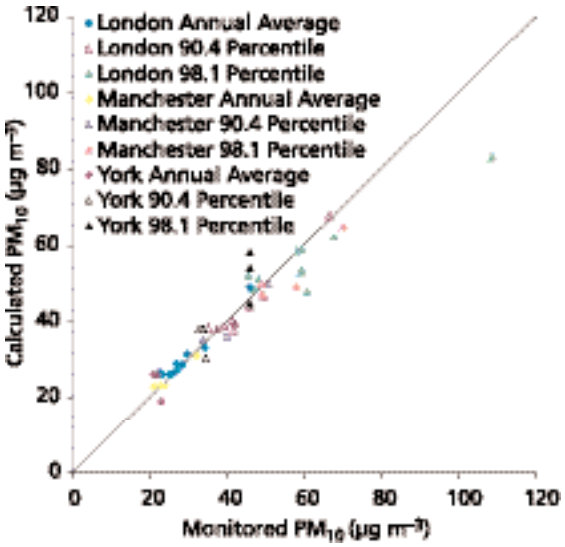

775. The data for London are also presented in Table 8.2. Considering both the figure 8.11 and the table 8.2, the annual average and daily average concentrations corresponding to 35 exceedences and 7 exceedences are well within the requirements of the EU directive. This is despite the fact that the daily average concentration exceeded 7 times is slightly underestimated, as might be expected because no account is taken of the daily variation of the 'other' component ((iii) above) or of other unspecified intermittent sources. Table 8.3 shows the statistics for $PM_{2.5}$ concentrations calculated at two sites within London for 1999. As with PM_{10}, the comparisons are for TEOM-based measurements with a factor of 1.3 for both the London sites and background sites at Rochester and Harwell. Although there is no established factor for this conversion, the average value derived from three sites where TEOMs and gravimetric monitors are calculated for the period 2000–2002 is 1.3 (Johnson *et al.*, 2004).

Table 8.2 1999 Monitored and calculated PM_{10} concentrations (μg m^{-3}) in London, Manchester and York.

	Annual average		90.4th percentile of daily average		98.1th percentile of daily average		Standard deviation	
	Monitored	Calculated	Monitored	Calculated	Monitored	Calculated	Monitored	Calculated
A3	30	31	46	44	59	59	16	13
Camden	34	33	50	47	68	62	18	15
Harringey	28	29	42	41	59	53	15	12
Marylebone Road	46	49	67	68	109	83	42	20
Sutton Roadside	26	26	40	39	48	51	14	12
Bury Roadside	32	31	51	50	70	65	20	18
Fishergate	22	26	34	38	46	54	12	16
Clifton	21	26	33	38	46	58	11	16
Roadside mean	**30**	**31**	**45**	**46**	**63**	**61**	**19**	**15**
Bexley	25	26	42	38	61	48	16	12
Bloomsbury	28	29	42	41	59	54	14	13
Brent	23	26	38	38	46	52	14	12
Eltham	23	27	35	38	47	48	12	12
Hillingdon	27	29	42	41	58	59	17	13
North Kensington	27	27	42	39	59	53	15	12
Bolton	21	23	34	35	49	50	13	13
Salford Eccles	24	23	40	36	58	49	15	13
Stockport Shaw Heath	23	23	34	35	49	47	14	12
Bootham	23	19	35	30	46	45	12	12
Background mean	**24**	**25**	**38**	**37**	**53**	**51**	**14**	**12**
Overall statistic	**27**	**28**	**41**	**41**	**58**	**55**	**16**	**14**

Table 8.3 Monitored and calculated 1999 $PM_{2.5}$ concentrations (μg m^{-3}) in London.

	Annual average		90.4th percentile of daily average		98.1th percentile of daily average		Standard deviation	
	Monitored	Calculated	Monitored	Calculated	Monitored	Calculated	Monitored	Calculated
Marylebone Road	29	37	42	52	53	67	10	11
Bloomsbury	19	19	30	30	43	41	8	7

8.2.3 Regional models

8.2.3.1 The EMEP model

776. The EMEP Centre West in Oslo has developed a new Eulerian model to simulate the dispersal, atmospheric chemistry and deposition of pollutants across Europe. This will be used in forthcoming assessments under the CLRTAP of the UNECE and by the EC within the CAFE programme in revision of national emission ceilings to combat effects of acidification, eutrophication, excess tropospheric ozone and fine particulate concentrations. This single unified model will replace the former Lagrangian models used for acidifying pollutants (SO_X, NO_X and NH_X) and ozone during development of the Gothenburg protocol and National Emissions Ceilings Directive. The estimated concentrations of secondary inorganic aerosol concentrations are substantially different from those of the Lagrangian model available at the time of the APEG report.

777. The model has 20 vertical levels using σ (pressure level) coordinates, with a lowest layer of ~92 m, and the top of the domain at 100 hPa. The horizontal grid is a polar stereographic projection, true at 60° north, with grid-cells approximately 50 km x 50 km. Meteorological data with a 3-h resolution are used from PARLAM-PS, a dedicated version of the High Resolution Limited Area Model (HIRLAM) weather prediction model. National emissions are distributed across the EMEP grid cells and distributed vertically according to SNAP sector. The treatment of boundary conditions, atmospheric chemistry and deposition processes are described in detail in an EMEP report (EMEP, 2003a).

778. The EMEP model domain encompasses the whole of Europe with grid cells of the order of 50 km x 50 km. However, comparison here is limited to a smaller region over the UK.

8.2.3.2 The FRAME model

779. Fine Resolution Atmospheric Multi-pollutant Exchange (FRAME) is a Lagrangian model developed by CEH Edinburgh and the University of Edinburgh (Fournier *et al.*, 2004). It models SO_X, NO_X and NH_X, calculating sulphur and nitrogen deposition to different ecosystem types, and also SO_4, NO_3 and NH_4 aerosol concentrations.

8.2.3.2.1 Model domain

780. The domain of the model covers the British Isles with a grid resolution of 5 km and grid dimensions of 172 x 244 km. Input gas and aerosol concentrations at the edge of the model domain are calculated using FRAME-EUROPE, a larger scale European simulation which was developed from TERN to run a statistical model over the entirety of Europe with a 150-km scale resolution. FRAME is a Lagrangian model that simulates an air column moving along straight-line trajectories. The atmosphere is divided into 33 separate layers extending from the ground to an altitude of 2500 m. Layer thicknesses vary from 1 m at the surface to 100 m at the top of domain. A year-specific wind rose is used to give the appropriate weighting to directional deposition and concentration for calculation of total deposition and average concentration. Diffusion of gaseous and particulate species in the vertical is calculated using K-theory eddy diffusivity and solved with a Finite Volume Method. The vertical diffusivity Kz has a linearly increasing value up to a specified height Hz and then remains constant (K_{max}) to the top of the boundary layer. During day time Hz is taken as 200 m and K_{max} is a function of the boundary layer depth and the geostrophic wind speed. At night time these values depend on the Pasquill stability class.

8.2.3.2.2 Emissions

781. Emissions of NH_3 are estimated for each 5-km grid square using national data for farm animal numbers (cattle, poultry, pigs and sheep) as well as fertiliser application, crops and non-agricultural emissions (including traffic and contributions from human sources and wild animals). The ammonia emissions inventory is described in Dragosits *et al*. (1998). NH_3 is emitted into the lowest layer. Emissions of SO_2 and NO_X are from the NAEI for the UK. For SO_2 ~80% of 1996 and 1999 emissions from the UK are associated with a small number of strong point source emissions. For NO_X, point source emissions account for ~25% of the total. Point source emissions of SO_2 and NO_X are treated individually with a plume rise model that uses stack height, temperature and exit velocity to calculate an 'effective emissions height'.

8.2.3.2.3 Chemistry

782. The chemical scheme in FRAME is similar to that employed in the EMEP Lagrangian model. The prognostic chemical variables calculated in FRAME are: NH_3, NO, NO_2, HNO_3, PAN, SO_2 and H_2SO_4 as well as NH_4^+, NO_3^- and SO_4^- aerosol. The gas phase reactions for oxidised nitrogen include photolytic dissociation of NO_2, oxidation of NO by ozone, formation of peroxyacetyl nitrate (PAN) and the creation of nitric acid by reaction with the OH free radical. NH_4NO_3 aerosol is formed by the equilibrium reaction between HNO_3 and NH_3. A second category of large nitrate aerosol is present and simulates the deposition of nitric acid on to soil dust or marine aerosol. The formation of H_2SO_4 by gas phase oxidation of SO_2 is represented by a predefined oxidation rate. H_2SO_4 then reacts with NH_3 to form ammonium sulphate aerosol. The aqueous phase reactions considered in the model include the oxidation of S(IV) by O_3, H_2O_2 and the metal catalysed reaction with O_2.

8.2.3.2.4 Wet deposition

783. The model employs a constant drizzle approach using precipitation rates calculated from a climatological map of average annual precipitation for the British Isles. Wet deposition of chemical species is calculated using scavenging coefficients based on those used in the EMEP model. An enhanced washout rate

is assumed over hill areas due to the scavenging of cloud droplets by the seeder-feeder effect. The washout rate for the orographic component of rainfall is assumed to be twice that calculated for the non-orographic component.

8.2.3.2.5 Dry deposition

784. Dry deposition of SO_2, NO_2 and NH_3 is calculated individually for five different land categories (arable, forest, moorland, grassland and urban). For NH_3, deposition is calculated individually at each grid square using a canopy resistance model (Fournier *et al.*, 2004). The deposition velocity is generated from the sums of the aerodynamic resistance, the laminar boundary layer resistance and the surface resistance. Dry deposition of SO_2 and NO_2 is calculated using maps of deposition velocity derived by the CEH 'big leaf' model (Smith *et al.*, 2003), which takes account of surface properties as well as the geographical and altitudinal variation of wind-speed.

8.2.3.2.6 Meteorology

785. The depth of the boundary layer in FRAME is calculated using a mixed boundary layer model with constant potential temperature capped by an inversion layer with a discontinuity in potential temperature. Solar irradiance is calculated as a function of latitude, time of the year and time of the day. At nighttime, a single fixed value is used for the boundary layer depth according to Pasquill stability class and surface windspeed. The wind rose employed in FRAME uses 6-hourly operational radiosonde data from the stations of Stornoway, Hillsborough, Camborne and Valentia spanning a 10-year period (1991–2000) to establish the frequency and harmonic mean wind speed as a function of direction for the British Isles.

8.2.3.3 The NAME model

786. The Met Office's Lagrangian dispersion model, NAME simulates the release of atmospheric pollutants by releasing air parcels into a three-dimensional model atmosphere driven by three-dimensional meteorological data from the Met Office's numerical weather prediction model, the Unified Model (UM). The air parcels are carried passively by the UM wind fields and random walk techniques are used to simulate the local turbulent dispersion. Detailed descriptions of the NAME model can be found in Physick and Maryon (1995) and Ryall and Maryon (1998).

787. In order to calculate the species concentrations required for the chemistry scheme, a three-dimensional grid is constructed over the model domain. The model is driven using EMEP[1] 2001 emissions data on a 50-km grid, hence this resolution grid was also used in the horizontal for the chemistry calculations. Five vertical layers are used (0–100 m, 100–300 m, 300–800 m, 800–5000 m and

[1] See http://www.emep.int/

5000–20000 m) and the extent of the model domain for the sulphate nitrate calculations presented in this chapter is 10W to 16E and 44S to 60N. The model emits 13 primary species, including seven VOCs, that are then scaled to represent the full VOC emission inventory. Details of the chemistry scheme can be found in Redington *et al*. (2001).

788. Figure 8.12 presents the model and observed daily particulate sulphate concentrations for Bridge Place in London, Strathvaich in Scotland and Yarner Wood, Devon. An evaluation of model performance is included in Table 8.4 below. The comparison between the model and observations for daily particulate sulphate shows that the model generally predicts peaks when these occur but that the quantitative argument is not good. The correlation coefficients are low. Generally, over all three sites the model over-predicts in January, underpredicts in March and overpredicts in December. The overall performance at Yarner Wood is degraded by the large erroneous peak predicted in December but not seen in the observations. Strathvaich and London show a negative bias that could be removed if a background particulate sulphate contribution was included for air masses advected across the North Atlantic Ocean.

Table 8.4 An evaluation of NAME model performance against the observed daily mean particulate sulphate observations at Stratvaich, London and Yarner Wood during 1996.

Site	Correlation	Bias (μg S m^{-3})	NMSE	Percentage within a factor of 2
Strathvaich	0.36	–0.25	3.23	21.3
Yarner Wood	0.32	1.20	2.93	40.1
London	0.35	–1.94	1.30	45.8

789. Focussing attention on 2002, Figure 8.13 gives a comparison of model and observed daily mean particulate sulphate concentrations for Yarner Wood, Devon for the year 2002. The wintertime underprediction is not seen as strongly as in Figure 8.12 but now the summertime levels appear to be overpredicted. However, during all seasons the model predicts accurately the onset and finish of the regional pollution episodes. This gives some confidence in the ability of the model to represent the long-range transport of particulate sulphate and hence its country attribution.

Figure 8.12 Modelled and observed particulate sulphate in µg SO_4 m^{-3} plotted upwards and model particulate nitrate in µg NO_3 m^{-3} plotted downwards for Strathvaich, Yarner Wood and London for 1996.

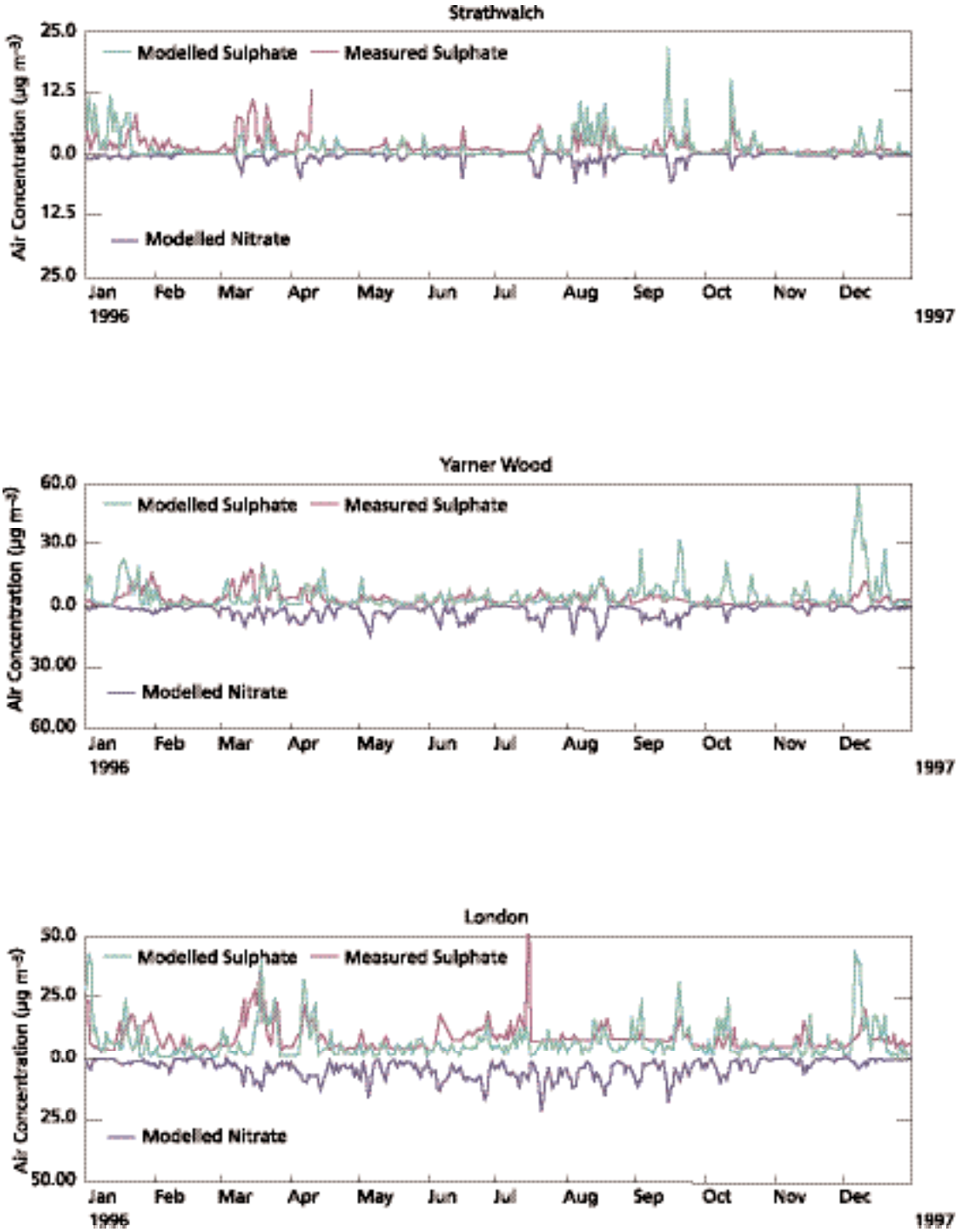

Figure 8.13 A comparison of model and observed daily mean particulate sulphate levels for Yarner Wood during 2002.

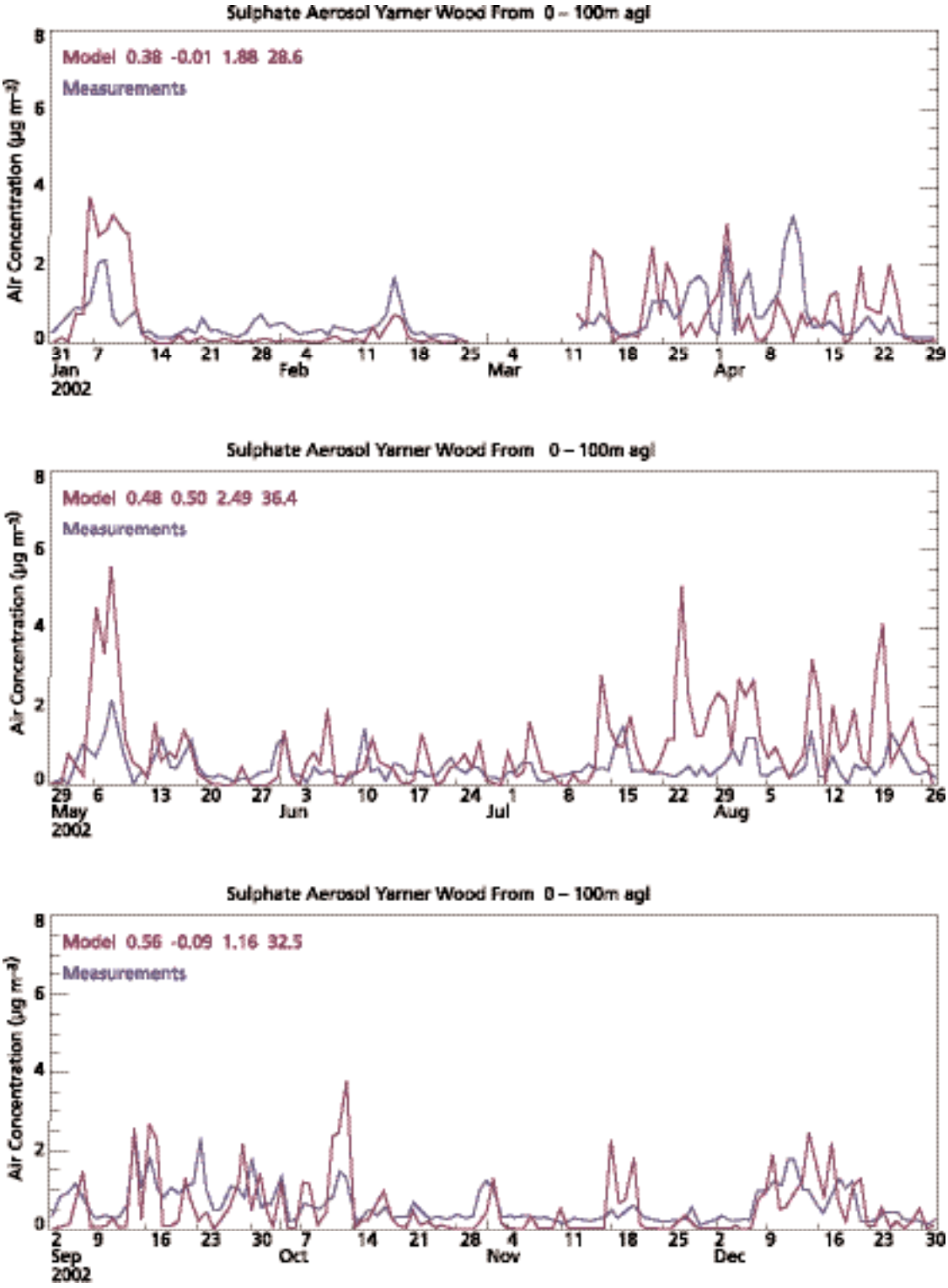

8.2.4 Other models

790. The models discussed in the previous section have been used extensively for policy development in the UK. Of course many other models have been developed for similar purposes and for specific applications, for example DMRB, Caline, ADMS-Roads and OSPM for road traffic emissions. Features of some of these models are presented in Table 8.5 and other models are also discussed in the AQEG NO_2 Report (AQEG, 2004).

8.2.4.1 Models for sources of PM due to wind generation, non-exhaust traffic emissions

791. Although many sources of PM deriving from products of combustion can be estimated from the appropriate emission factors and amount of fuel combusted, speed of process and so on, sources of PM due to mechanical processes such as wind generation and non-exhaust traffic emissions are inherently more difficult to quantify depending for instance on wind speed and turbulence, occurrence of recent rain, road material, weight of vehicles. Theoretical models based on a threshold saltation velocity for the different particle sizes have been developed for uptake of sand particles and the generation of equilibrium shapes for sand dunes (Bagnold, 1941). These ideas have also been applied to other types of surfaces and to stockpiles (Nalparis *et al.*, 1993); however, there are no practically useful models based on well-founded theoretical ideas for resuspension of sources of particles from construction sites. Models that do exist are almost exclusively empirical and based on the AP-42 emission factors of the USEPA estimated from field studies. However, these are generally not appropriate for UK conditions.

8.2.4.2 Advanced transport models including aerosol dynamics

792. In the most advanced atmospheric transport models describing aerosol development, the aerosol size distribution is represented by a number of modes – for example, ultrafine, fine and coarse – and the amount of material in each mode arising as a result of processes – such as emission, condensation and coagulation – is tracked. The chemical composition of the particles is represented by a number of components, such as sulphates, nitrates, organic carbon, mineral dust, sea salt and particle number. It is not practicable in a transport model to represent in detail the multi-mode interactions between each chemical component. Instead, all the components within each mode are assumed to have the same size distribution and the same chemical composition (internally mixed aerosols). The particles within each mode are transported in a similar manner to the gaseous species within atmospheric models and similarly subject to dry and wet deposition appropriate to particles.

793. Even with simplified assumptions, modelling is exceedingly complex and dependent on having good knowledge of processes, such as gas-particle conversion, speciated emission rates and the aggregation of particles. The main benefit of the comprehensive approach, if it can be demonstrated to perform well, is that the particle composition within different size ranges could be predicted. Hence results could be interpreted in terms of the part of the aerosol mass or number which is thought to have an adverse health effect.

794. The approach has been developed as part of the EMEP programme, in order to assess particle concentrations on a regional scale in Europe (Tsyro, 2002). Secondary organic aerosols and natural dust are not yet included. The aerosol dynamics within the Models-3 modelling system (Byun and Ching, 1999) allows

for the interaction of ultrafine particles generated by nucleation and direct emission with aged, fine (accumulation mode) particles. The chemical species include sulphates, nitrates, ammonium, water, manmade and biogenic organic carbon, elemental carbon and other unspecified material of manmade origin. Successful performance of the model clearly depends on a reliable speciated source inventory, which is a challenge in its own right. These models are undergoing continual development. At the present time they cannot be considered sufficiently well tested to be regarded as the basis of a reliable assessment method, not least because speciated aerosol measurements are only just becoming available to test them. Hence in this report simpler empirical approaches have been used to predict trends in particle concentration.

795. It should be recognised that in time these simpler methods may be challenged by the more detailed approaches. An illustration of the potential of comprehensive models is given in the study of Models-3 by Cocks *et al*. (2003), in which Models-3 was run for the whole of 1999 to predict regional acid deposition over England and Wales. The results included hourly concentration fields over the country throughout the year at a spatial resolution of 12 km. Although the purpose of the study was to determine acid deposition not particle concentration, as the comprehensive model is part of an integrated atmospheric modelling system, the 21 components constituting PM_{10} particles were automatically calculated as part of the model run.

796. The mean annual concentration of particulates is shown in Figure 8.14. The resolution means that comparisons can only be made with the few regional background monitoring sites available.

Figure 8.14 Annual mean concentration of total particulates calculated using Models-3.

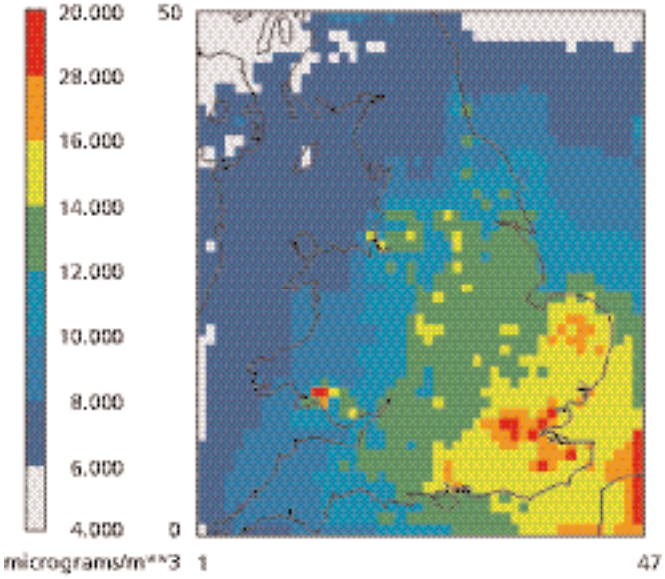

797. To illustrate the kind of comparison that should be possible using comprehensive models, unscaled measured PM_{10} concentrations are compared with the calculated annual average obtained by summing all components (Figure 8.15).

798. The sites at Harwell, Narbeth and Rochester are rural sites within the national network. The remaining sites are rural sites operated by power generation companies as a check to determine concentrations in the neighbourhood of coal and oil-fired power stations. In principle the calculation includes contributions to the rural ground-level PM from power stations, but – as demonstrated elsewhere in this report – the power station contribution is likely to be a small fraction of the total. A strict comparison between measured and calculated concentrations should not be made, as the TEOM instrument is not thought to measure all components, the more volatile components being lost. In future it may be possible to perform more detailed comparisons component by component. This is illustrated in figures 8.16 and 8.17 for sulphate, using data from acid deposition sites in operation in 1999 and calculations from Models-3. The preliminary agreement looks encouraging. However, more research is needed to turn the comprehensive models into reliable, practical assessment tools.

Figure 8.15 Comparison between measured annual average PM_{10} concentration (μg m^{-3}, TEOM) and calculations from Models-3 (year).

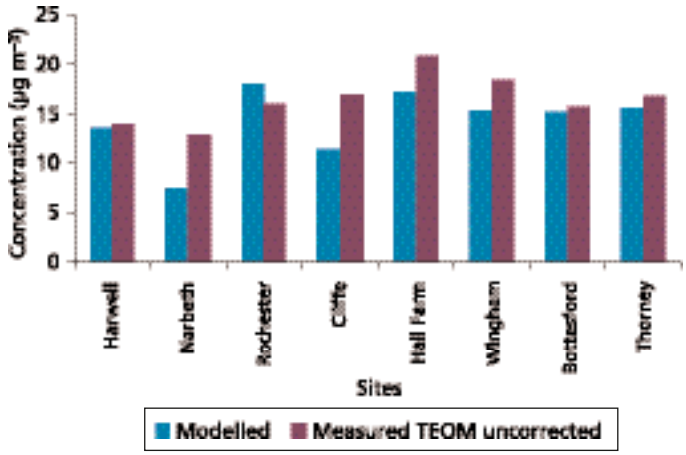

Figure 8.16 Comparison between 1999 measured annual average sulphate concentration and calculations from Models-3 (year).

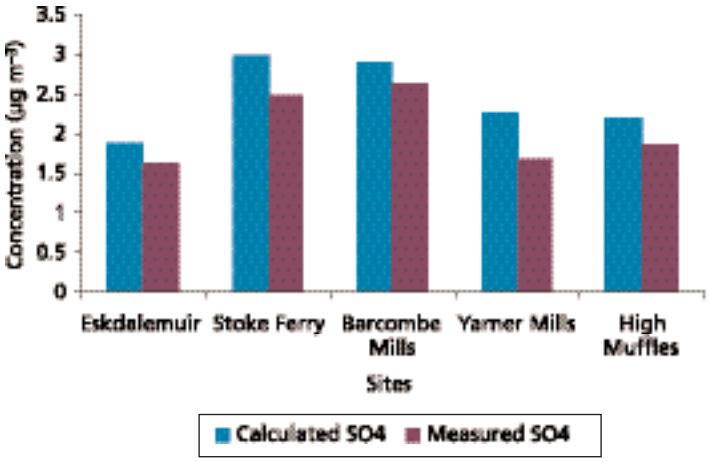

8.3 Comparison of model features

799. The main features of the key models presented in Section 8.2 and some other models are shown in the Table 8.5. This includes and contrasts some basic details of the models and also the methodologies they employ to take account of the coarse component and so on.

8.3.1 Netcen, ERG and ADMS-Urban models

800. These models have some common themes and major differences, which the model intercomparison exercise has discussed in detail (Carruthers *et al*., 2002). Figure 8.17, which compares annual means calculated by each of the models, suggests that the models show broadly similar performance at monitoring sites. However, scatter plots (Figure 8.18) comparing calculated concentrations on road segments calculated by ERG and ADMS show quite different predictions and also illustrate the different treatment of the background (the ERG model exhibits a clear minimum value).

801. Broadly, in the Netcen and ERG models the emphasis, especially for predictions at monitoring sites, is on the use of monitoring data. The performance of these models, therefore, depends critically on the availability of good data coverage, now the case in London for which the ERG approach was developed, but perhaps not in other parts of the UK. The methods do have the disadvantage that their predictions depend to a large extent on the measurement method employed; in addition there is some ambiguity as to what the PM related to NO_X is and in particular how much non-exhaust traffic emission this includes. In ADMS-Urban the emphasis is on modelling the primary emissions in the area of interest; these calculated concentrations are not dependent on the measurement method. The ADMS method is not able to assimilate data but uses broad comparisons with data to refine the physical parameters within the model (for example, surface roughness or minimum Monin Obukhov length). These parameters themselves are subject to uncertainty in urban areas. With regard to the background, Netcen and ADMS use similar general approach in using rural data (Netcen sulphate and nitrate data, ADMS measured PM data) and both approaches could use background data from other sources or employ regional model outputs. ERG derives the background from its analysis of background within the urban area.

Figure 8.17 Measured PM_{10} annual average concentration compared with predicted values (µg m^{-3}).

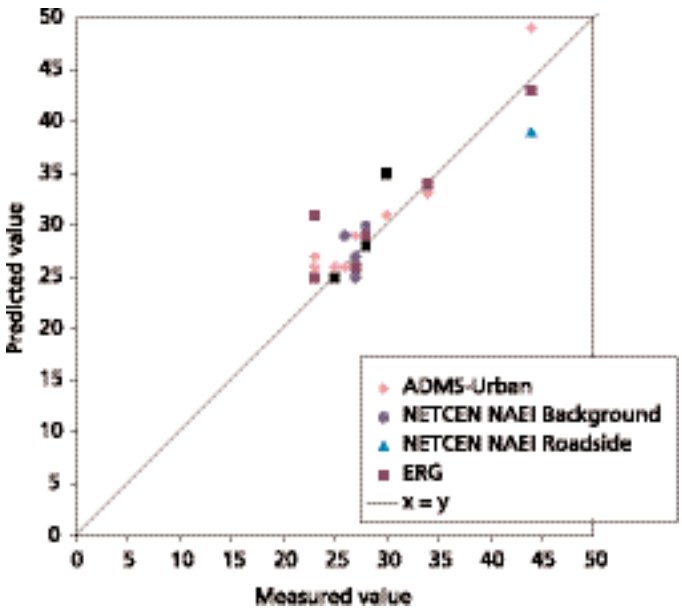

Table 8.5 Description of the main models and modelling techniques used for PM calculations in the UK.

Model	Basic description	Meteorology	Transport and dispersion	Chemistry for particulate formation	Spatial scale	Averaging times	Background, including	Treatment of 'other' projections contributions e.g. non-exhaust traffic emissions
Models used for urban and national assessment against AQ limit values and objectives.								
Netcen Stedman *et al* (2002)	National model for all emission types	Different statistical analyses for different years	Regression analysis based on ADMS 3 calculations and monitoring data for urban background; simple formulation for representative calculation on road segments	None	National to suburban scale representative concentrations for road segments	Annual	Based on measured sulphate and nitrate. Reductions in secondary based on Gottenberg protocol and National Emissions Ceilings Directive	'other' included as 8.8 µg m^{-3} gravimetric. Road contribution implicitly included through roadside only adjustment factor
ADMS-Urban McHugh *et al* (1997)	Models for stationary source emissions and/or road traffic emissions	Hourly sequential data from one site	Quasi Gaussian type model using h/M_{MO} parameterisation of boundary layer. Also includes trajectory model and canyon model based on OSPM approach	Simple sulphate chemistry	Urban down to local, including spatial variation at local street scale	Short term (mins) to annual averages	From rural monitoring sites. Projections based on EMEP calculations (33% reduction 1999-2010 for 1999 base year)	9.9 µg m^{-3} gravimetric for urban background (4.9 µg m^{-3} rural contribution, 5 µg m^{-3} urban increment). Additional roadside contribution only through emissions for PM_C

Model	Basic description	Meteorology	Transport and dispersion	Chemistry for particulate formation	Spatial scale	Averaging times	Background, including	Treatment of 'other' projections contributions e.g. non-exhaust traffic emissions
ERG Carslaw *et al* (2001)	All emission types; set-up for London	Different statistical analyses for different years	Regression analysis based on ADMS 3 calculations and monitoring data	None	Urban down to local scale including spatial variation at local street scale	Annual, daily	Derived as $PM_{2.5}$ not related to NO_X. Reduction of 30% between 1996 and 2010	PM_C derived through regression analysis as 50 µg m^{-3}.
Regional models								
EMEP	Mesoscale model for pollutant dispersion at European scale	Mesoscale model	Eulerian	Inorganic	50 km x 50 km grid cells	Short term/ annual	Modelled	Not considered
FRAME	Regional model for UK	Based on radiosonde data over 10 year period	Straight line trajectory model	Inorganic	5 km x 5 km grid cells	Annual	From FRAME-Europe with 150 km resolution	Not considered
NAME Ryall and Mayor (1998)	Mesoscale model for pollutant dispersion	Mesoscale model	Lagrangian particle model	Inorganic	15 km x 15 km cells	Short term to annual	Models secondary component	Not considered
Road impact models								
DMRB (2003) Highways Agency (2001)	Screening model for road traffic emissions and air quality	Fixed, at $2m/s^{-1}$ equally distributed from all directions	Incorporates a fixed empirically adjusted Pasquill stability category	None	Local	Annual	Uses specific constant value	Implicates through use of road type adjustment factor

Model	Basic description	Meteorology	Transport and dispersion	Chemistry for particulate formation	Spatial scale	Averaging times	Background, including	Treatment of 'other' projections contributions e.g. non-exhaust traffic emissions
CALINE Benson (1979) US-EPA www.EPA.gov /scram001	Road traffic emissions	Hourly sequential data	Gaussian model. Pasquill parameterisation of boundary layer	None	Local	Short term. commercial versions allow short term to annual		
ADMS-Roads	Road traffic emissions model	Hourly sequential data from one site	Quasi Gaussian type model using h/M_{MO} parameterisation of boundary layer. Canyon model based on OSPM approach	None	Local	Short term annual	Specified by user	Within background
OSPM	Street canyon model	Hourly sequential	Combination of plume and box model for concentration within street canyon	None	Canyon	Short term to annual	Specified by user	Within background
CAR	Road traffic emissions		Gaussian model for road network		Street scale	Short term to annual	Specified by user	Within background

Figure 8.18 A comparison of ADMS and ERG of PM_{10} concentrations on road segments in London in 1999 and 2004.

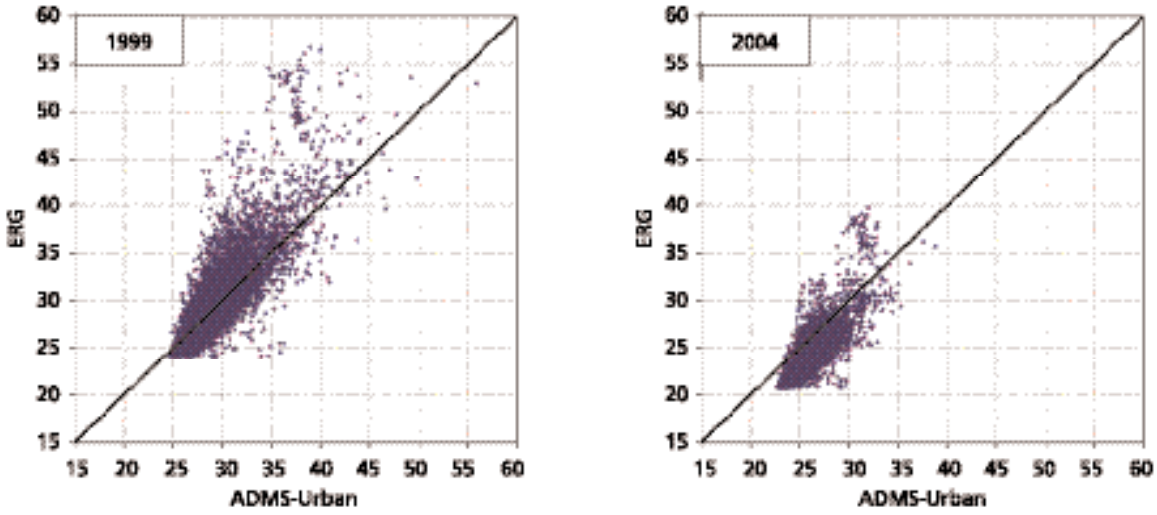

8.3.2 Air pollution models for road traffic

802. An ability to model roadside concentrations is crucial to the management and assessment of roadside PM. Current practical models are generally based on a Gaussian-type dispersion of the pollutants away from the source. At its simplest, the screening model in the Design Manual for Roads and Bridges (DMRB) uses an average dispersion curve to calculate annual mean concentrations downwind of a line source. More detailed models take account of dispersion on a finer time frame, usually of 1-h, which allows for the effect of varying windspeed and direction and atmospheric turbulence, with the annual mean or 24-h means being derived by summing the individual hourly concentrations. Although the models have a broadly similar basis there can still be quite significant differences in detail. For example Figure 8.19 shows hourly average concentration from CALINE and ADMS-Roads for a range of stability conditions and two different wind directions along and perpendicular to a 10-m road. Note that maximum concentration occurs for the wind parallel to the road for CALINE but for perpendicular flow for ADMS-Roads.

803. Recent work using the dispersion model used to derive the DMRB algorithms (Boulter *et al.*, 2003; Figure 8.20) has suggested that dispersion near roads seems to be dependent on road type in ways not generally accounted for in the models. The basic model was overpredicting for rural motorways and underpredicting for non-motorway urban roads. Further investigation showed that the model performance was related to traffic flow and speed, overpredicting more at higher flows and higher speeds. This analysis has led to a calibration relationship based on Annual average daily traffic (AADT) flow (Figure 8.21), which is now applied to the raw DMRB model output. For a given emission rate this results in a fivefold increase in concentration going from very high flows on open motorways to roads with lower flows and lower speeds in towns. Independent work by Netcen (Stedman *et al.*, 2004) has shown a similar behaviour in their empirical model, which relates emission rates (g m^{-1} s^{-1}) to measured roadside concentrations (Figure 8.22). Their work suggests a sevenfold difference between open motorways with high flows and roads with low flows in town centres.

Figure 8.19 Roadside concentrations calculated by ADMS-Roads and CALINE 4; emission rate 0.0171 g km^{-1} s^{-1}. (a) wind perpendicular to road; (b) wind parallel to road. Results shown for three stability conditions: B, unstable; D, neutral; G, very stable.

(a)

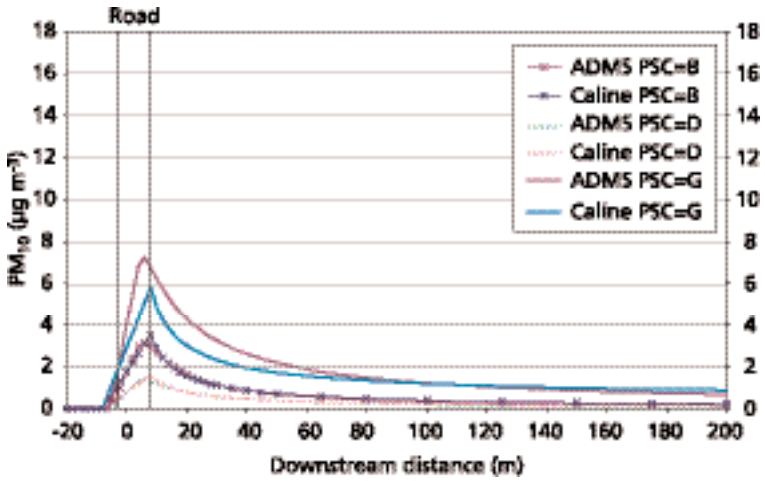

(b)

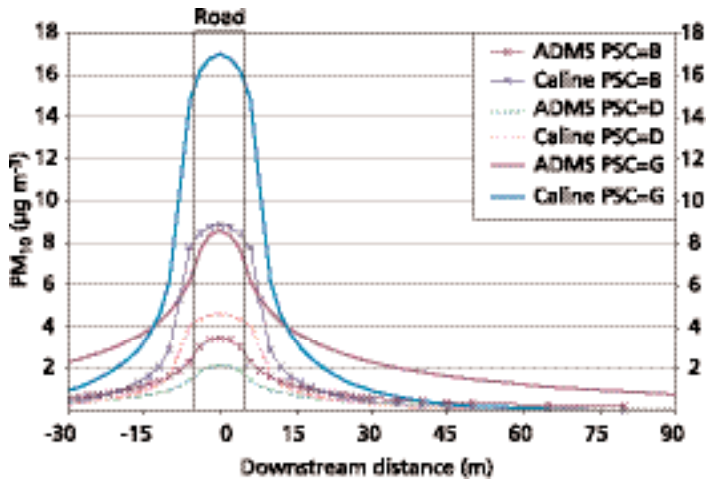

Figure 8.20 Relationship between raw DMRB predictions of annual mean PM_{10} versus measured values as a function of road type (Boulter *et al.*, 2003).

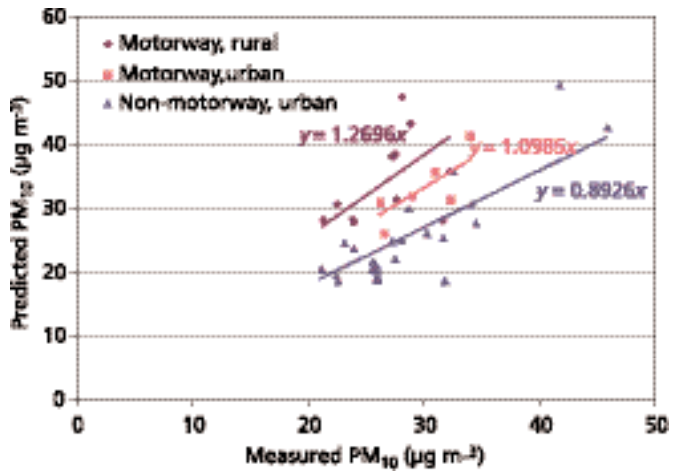

804. Some model verification of more detailed models, where model output is verified with local data from local authority studies for review and assessment purposes, have shown similar patterns (Laxen, 2004). For example CAL3QHC, a variant of the USEPA model CALINE3, appears to perform well for motorways and rural roads (for which it was originally validated), but underpredicts the road contribution significantly, typically by a factor of 4 to 8 in urban settings, where traffic is slower moving and more likely to be congested.

805. Vehicle emissions are sensitive to vehicle speed/vehicle type and so on and may not be well specified; however, there are also many reasons why dispersion is likely to differ significantly in different types of road. These include differing effects of traffic-induced turbulence both mechanically generated by the vehicles and induced by the buoyancy of the exhaust (di Sabatino *et al*., 2003); the impact of surface roughness changes between rural and urban sites (that is, the impact of buildings and other local feature changes), which will change both mean flow and turbulence and hence dispersion; the presence of street canyons; and the impact of the height of vehicle exhaust (for example, exhausts of HGVs are often elevated, whereas bus emissions are close to ground level, and the relative numbers of vehicles of different types will vary with location). In Figure 8.23 ADMS has been used to model the sensitivity of the annual mean concentrations at roadside to some of these different parameters – it is seen that the concentrations vary with all the parameters considered but are very sensitive to the initial vertical mixing height. Thus a specification of how this parameter varies according to vehicle type, vehicle speed and so on is important for improved treatment of sensitivity to road type by dispersion models because currently, in routine calculations, this parameter is held constant in models such as ADMS-Roads and CALINE.

Figure 8.21 Adjustment factors for raw DMRB predictions of annual mean PM_{10} as a function of daily traffic flow (as applied in v1.02 of the DMRB) (Boulter *et al*., 2003).

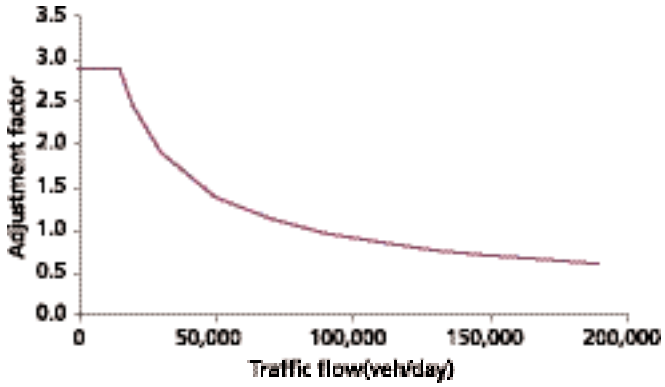

8.4 Model outputs and comparisons

806 This section includes model output firstly for the national and urban scale model and secondly for the regional models. Included are source apportionment calculations both PM_{10} and $PM_{2.5}$; urban, national and regional maps of concentrations for comparison with the air quality limit values for PM_{10}; maps for $PM_{2.5}$; and regional maps of the inorganic components of the secondary particulates. In addition there are summary tables of areas of exceedence and so on for the national and urban models. Where available, different model outputs are presented for comparison purposes.

Figure 8.22 Adjustment factors to apply to vehicle emissions as a function of daily traffic flow (Stedman *et al.*, 2003).

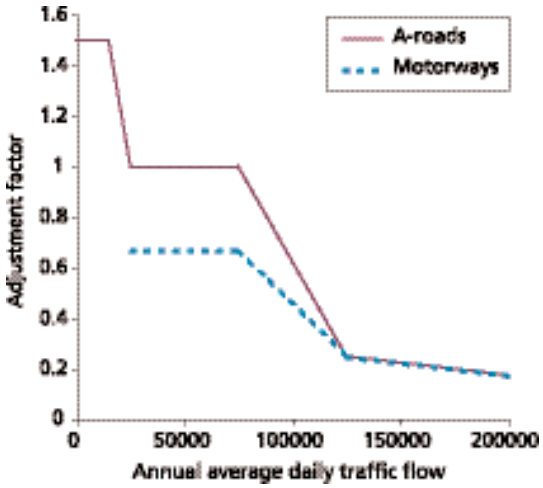

Figure 8.23 Normalised maximum annual average PM_{10} concentration varying with canyon height, road width, roughness length and initial mixing height. (The curves were calculated using ADMS-Roads.)

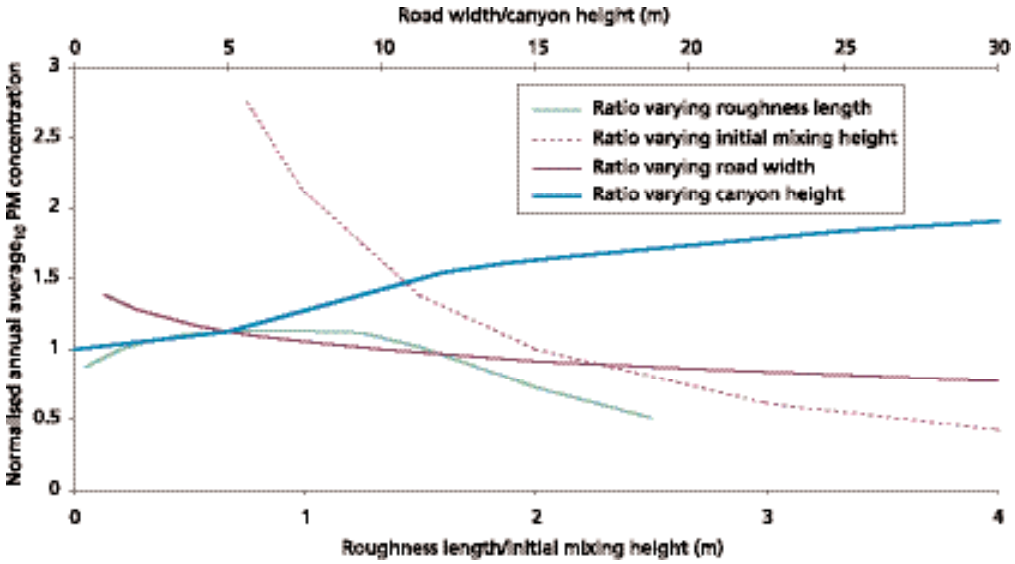

8.4.1 High resolution models up to national scale

8.4.1.1 Site-specific source apportionment

807 Tables 8.6–8.9 present calculations from the APEG source apportionment model (Section 8.2) corresponding to monitoring site across the UK and additional calculations are presented for ADMS-Urban and the ERG model in London (percentages only). Similar tables are presented for $PM_{2.5}$ in Tables 8.10–8.13. Contour maps of the source apportionment of the different components of the traffic fleet in London are shown in Figure 8.24.

808 Modelled PM_{10} concentrations for the current year show that the traffic contribution dominates at roadside locations, but makes a relatively small contribution at urban background and suburban sites. For all sites, there is also a stationary source contribution and a substantial contribution from the regional

Table 8.6 PM_{10} µg m^{-3} source apportionment: concentration from APEG receptor model for 200 NAEI, 2002 measurement, base year.

	Traffic	Stationary	Sulphate	Nitrate	Residual	Total
Marylebone Road TEOM	14.4	3.5	2.7	1.6	12.1	34.3
Marylebone Road KFG	13.2	5.5	2.7	5.5	9.9	36.8
Marylebone Road PART	16.4	6.7	2.7	7.4	10.3	43.5
Haringey Roadside TEOM	4.4	2.1	2.7	1.2	10.6	21.0
M25 Staines TEOM	8.9	1.9	2.6	3.1	6.5	23.0
Bury Roadside TEOM	6.5	3.6	2.1	2.0	9.8	24.0
Harwell TEOM	0.7	0.9	2.5	1.1	7.6	12.8
Harwell KFG	2.4	2.9	2.5	5.0	5.7	18.5
Harwell PART	1.6	2.0	2.5	4.5	8.7	19.3
Rochester TEOM	—	—	—	—	—	—
London Bloomsbury TEOM	—	—	—	—	—	—
London North Kensington TEOM	1.8	2.8	2.7	2.2	10.0	19.4
London North Kensington PART	2.9	4.6	2.7	5.8	9.1	25.1
London Bexley TEOM	1.7	3.7	2.7	2.8	8.0	19.0
Thurrock TEOM	1.1	4.2	2.7	3.7	9.5	21.1
Thurrock KFG	2.0	6.7	2.7	9.0	9.7	30.1
Belfast Centre TEOM	1.4	4.6	1.4	3.0	7.1	17.5
Belfast Centre KFG	2.3	7.2	1.4	6.0	5.9	22.8
Belfast Centre PART	2.0	6.3	1.4	5.4	9.7	24.9
Glasgow Centre TEOM	1.8	2.7	1.4	2.9	6.7	15.5
Glasgow Centre KFG	3.2	4.7	1.4	6.2	2.9	18.4
Glasgow Centre PART	3.6	5.3	1.4	5.5	7.4	23.2
Port Talbot TEOM	—	—	—	—	—	—
Port Talbot KFG	—	—	—	—	—	—
Port Talbot PART	—	—	—	—	—	—
Birmingham Centre TEOM	1.1	3.1	2.4	0.8	9.2	16.7
Birmingham Centre PART	2.7	7.0	2.4	5.1	7.0	24.2
Birmingham Hodge Hill TEOM	1.1	2.3	2.5	0.5	8.7	15.0
Manchester Piccadilly TEOM	2.1	3.7	2.2	2.8	10.7	21.5
Manchester Piccadilly PART	3.2	5.4	2.2	6.5	12.8	30.1

background, including the secondary PM component. The 'residual' component also makes a very significant contribution to the total. By 2010, the traffic component is estimated to fall to about 50–75% of its current contribution, with the secondary component then dominating at non-roadside sites. However, the residual component is assumed to remain unchanged by 2010, and represents 50% or more of the total PM_{10} concentration at non-roadside locations. For $PM_{2.5}$, a broadly similar pattern emerges for both the current and future years, although the residual component is much lower than that assumed for PM_{10}.

Table 8.7 PM_{10} source apportionment expressed as percentages: comparison for sites in London of Netcen 2002 NAEI and ADMS Urban 1999 LAEI.

	Traffic (%)	Stationary (%)	Secondary (%)	Other (%)
Marylebone Road				
ADMS-Urban	50.1	2.7	27.4	19.8
Netcen TEOM	42.0	10.2	12.5	35.3
Netcen KFG	35.9	14.9	22.3	26.9
Netcen PART	37.7	15.4	23.2	23.7
Bloomsbury				
ADMS-Urban	13.5	4.7	47.5	34.3
Netcen TEOM	—	—	—	—
North Kensington				
ADMS-Urban	7.3	5.3	50.7	36.7
Netcen TEOM	9.2	14.4	25.1	51.3
Netcen PART	11.6	18.3	33.9	36.3

Table 8.8 PM_{10} source apportionment projection to 2010: APEG receptor model 2001 NAEI, 2002 measurement base year.

	Traffic	Stationary	Sulphate	Nitrate	Residual	Total
Marylebone Road TEOM	8.0	3.3	2.4	1.4	12.1	27.1
Marylebone Road KFG	7.3	5.2	2.4	4.6	9.9	29.5
Marylebone Road PART	9.1	6.4	2.4	6.2	10.3	34.4
Haringey Roadside TEOM	2.6	2.0	2.4	1.0	10.6	18.5
M25 Staines TEOM	8.9	1.9	2.6	3.1	6.5	23.0
Bury Roadside TEOM	3.6	3.3	1.9	1.7	9.8	20.4
Harwell TEOM	0.4	0.8	2.2	1.0	7.6	11.9
Harwell KFG	1.4	2.5	2.2	4.2	5.7	16.0
Harwell PART	0.9	1.7	2.2	3.8	8.7	17.3
Rochester TEOM	—	—	—	—	—	—

	Traffic	Stationary	Sulphate	Nitrate	Residual	Total
London Bloomsbury TEOM	—	—	—	—	—	—
London North Kensington TEOM	1.0	2.6	2.4	1.8	10.0	17.8
London North Kensington PART	1.7	4.2	2.4	4.9	9.1	22.3
London Bexley TEOM	1.0	3.5	2.4	2.4	8.0	17.3
Thurrock TEOM	0.6	4.0	2.4	3.1	9.5	19.5
Thurrock KFG	1.2	6.4	2.4	7.6	9.7	27.2
Belfast Centre TEOM	0.9	3.4	1.2	2.5	7.1	15.1
Belfast Centre KFG	1.4	5.2	1.2	5.0	5.9	18.7
Belfast Centre PART	1.2	4.5	1.2	4.6	9.7	21.3
Glasgow Centre TEOM	1.0	2.6	1.2	2.4	6.7	14.1
Glasgow Centre KFG	1.8	4.6	1.2	5.3	2.9	15.7
Glasgow Centre PART	2.0	5.2	1.2	4.6	7.4	20.5
Port Talbot TEOM	—	—	—	—	—	—
Port Talbot KFG	—	—	—	—	—	—
Port Talbot PART	—	—	—	—	—	—
Birmingham Centre TEOM	0.6	3.2	2.1	0.7	9.2	15.9
Birmingham Centre PART	1.5	7.2	2.1	4.3	7.0	22.1
Birmingham Hodge Hill TEOM	0.6	2.2	2.1	0.4	8.7	14.1
Manchester Piccadilly TEOM	1.2	3.4	1.9	2.4	10.7	19.7
Manchester Piccadilly PART	1.8	5.1	1.9	5.5	12.8	27.2

Table 8.9 PM_{10} source apportionment projection to 2010: comparison of Netcen NAEI and ADMS Urban LAEI PM_{10} source apportionment for 2010.

	Traffic (%)	Stationary (%)	Secondary (%)	Other (%)
Marylebone Road				
ADMS-Urban	27.8	3.6	32.9	35.7
Netcen TEOM	29.4	12.1	14.0	44.5
Netcen KFG	24.8	17.7	23.8	33.7
Netcen PART	26.5	18.6	25.0	29.9
Bloomsbury				
ADMS-Urban	5.4	4.9	43.0	45.8
Netcen TEOM	—	—	—	—
North Kensington				
ADMS-Urban	3.4	5.3	43.8	47.6
Netcen TEOM	5.6	14.6	23.6	56.2
Netcen PART	7.6	18.8	32.7	40.8

Table 8.10 $PM_{2.5}$ (μg m^{-3}) source apportionment: APEG receptor model 2001 NAEI, 2002 measurement base year.

	Traffic	Stationary	Sulphate	Nitrate	Residual	Total
Marylebone Road TEOM	9.8	1.7	2.7	1.2	5.6	21.0
Marylebone Road PART	9.2	3.6	2.7	4.2	5.4	25.0
M25 Staines	5.5	1.5	2.6	0.6	2.3	12.5
Harwell TEOM	1.1	1.2	2.5	0.3	5.0	10.0
Harwell PART	0.4	0.4	2.5	5.8	3.9	13.0
Rochester TEOM	0.6	2.1	2.7	2.0	3.5	11.0
Bloomsbury TEOM	1.7	2.6	2.7	1.5	5.5	14.0
London North Kensington PART	3.5	4.2	2.7	4.8	2.9	18.0
Belfast Centre PART	1.6	4.7	1.4	4.8	3.5	16.0
Glasgow Centre PART	3.3	4.3	1.4	0.8	4.2	14.0
Birmingham Centre PART	1.8	4.4	2.4	3.4	4.1	16.0
Birmingham Hodge Hill TEOM	1.0	1.8	2.4	0.9	5.9	12.0
Manchester Piccadilly PART	1.6	2.7	2.2	3.1	6.5	16.0

Table 8.11 $PM_{2.5}$ source apportionment: comparison of Netcen 2002 NAEI and ADMS-Urban 1999 LAEI $PM_{2.5}$ source apportionment.

	Traffic (%)	Stationary (%)	Secondary (%)	Other (%)
Marylebone Road				
ADMS-Urban	58.2	2.6	31.1	8.1
Netcen TEOM	46.7	8.1	18.6	26.7
Netcen PART	36.7	14.3	27.5	21.5
Bloomsbury				
ADMS-Urban	17.8	5.2	61.2	15.8
Netcen TEOM	12.1	18.6	30.0	39.3
North Kensington				
ADMS-Urban	9.7	5.9	67.0	17.4
Netcen PART	19.3	23.2	41.4	16.0

Table 8.12 $PM_{2.5}$ (μg m^{-3}) source apportionment projection to 2010: APEG receptor model 2001 NAEI, 2002 measurement base year projections to 2010.

	Traffic	Stationary	Sulphate	Nitrate	Residual	Total
Marylebone Road TEOM	5.4	1.6	2.4	1.0	5.6	16.0
Marylebone Road PART	5.1	3.3	2.4	3.5	5.4	19.7
M25 Staines	3.2	1.4	2.4	0.5	2.3	9.7
Harwell TEOM	0.6	1.1	2.2	0.2	5.0	9.1
Harwell PART	0.2	0.4	2.2	4.9	3.9	11.6
Rochester TEOM	0.4	2.0	2.4	1.7	3.5	10.0
Bloomsbury TEOM	0.9	2.5	2.4	1.3	5.5	12.6
London North Kensington PART	2.0	3.7	2.4	4.0	2.9	15.0
Belfast Centre PART	1.0	3.3	1.2	4.0	3.5	13.1
Glasgow Centre PART	1.8	4.2	1.2	0.6	4.2	12.2
Birmingham Centre PART	1.0	4.5	2.1	2.8	4.1	14.5
Birmingham Hodge Hill TEOM	0.6	1.8	2.1	0.7	5.9	11.1
Manchester Piccadilly PART	0.9	2.5	1.9	2.6	6.5	14.4

Table 8.13 $PM_{2.5}$ source apportionment projection to 2010: comparison of Netcen NAEI and ADMS Urban LAEI $PM_{2.5}$.

	Traffic (%)	Stationary (%)	Secondary (%)	Other (%)
Marylebone Road				
ADMS-Urban	36.8	3.7	42.8	16.6
Netcen TEOM	33.8	10.0	21.3	35.0
Netcen PART	25.9	16.8	29.9	27.4
Bloomsbury				
ADMS-Urban	7.8	5.5	62.4	24.2
Netcen TEOM	7.1	19.8	29.4	43.7
North Kensington				
ADMS-Urban	4.8	6.3	64.1	24.9
Netcen PART	13.3	24.7	42.7	19.3

Figure 8.24 London UK annual mean PM_{10} concentrations by traffic category, 1999.

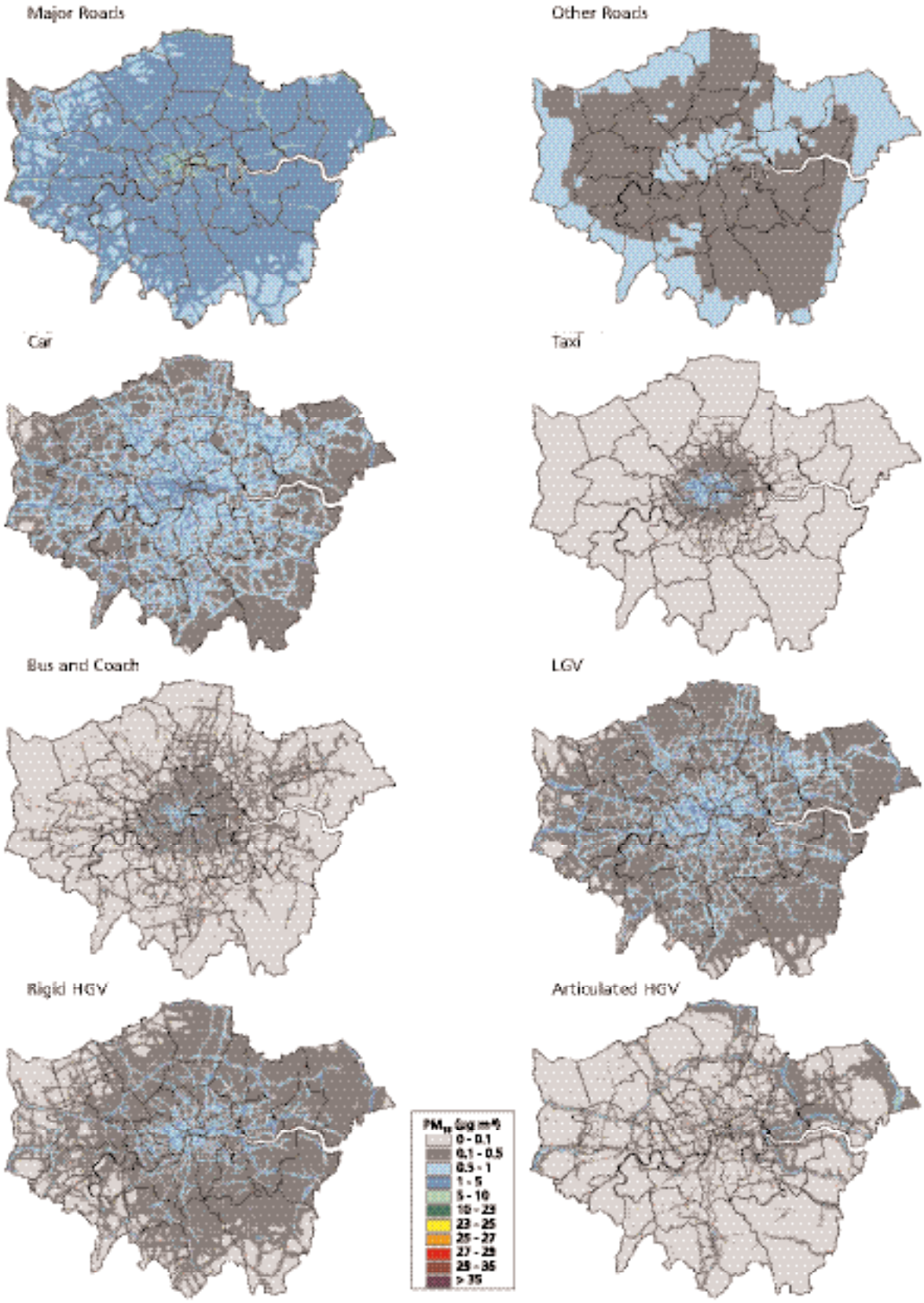

809. The detailed source apportionment maps for the different components of the traffic fleet in London (Figure 8.24) illustrate the large contribution of cars, HGVs and LGVs to PM_{10} concentrations across London and the importance of buses and taxis in the central area.

8.4.1.2 Mapped concentrations of PM_{10}

810 National maps of annual mean PM_{10} calculated using the netcen mapping model are presented in Figures 8.25–8.30 for 2002, 2005 and 2010. Figures 8.25, 8.27, 8.29 present backgound concentrations and Figures 8.26, 8.28 and 8.30 the calculated roadside concentrations determined from summing the roadside increment and background for each major road segment. The background maps generally show higher levels over much of the most populated parts of England with generally lower levels in the North and Southwest of England and Scotland, Wales and Northern Ireland. The levels show only modest declines between 2002 and 2010. The roadside concentrations are as anticipated greatest in the main conurbations and more especially in London. The annual average limit value of 40 μg m^{-3} is broadly achieved; however, there remain widespread exceedences focussed in urban areas of the Stage II indicative limit value of 20 μg m^{-3} in 2010. ADMS-Urban also predicts widespread exceedences of the 2010 limit value in London (Figures 8.32–8.35); however, ERG predicts that the exceedences will mainly be confined to roadside with only small additional areas of exceedence (Figure 8.38).

811 London maps calculated using ADMS-Urban are also presented for daily averaged concentration exceeded 35 times in 2004 and seven times in 2010 (Figures 8.36 and 8.37). These suggest that some exceedence of the 2004 limit values is likely at roadsides but only at roadsides of major roads in 2010, except in adverse meteorological conditions. The main conclusions of the maps are summarised in Tables 8.14 and 8.15.

812 The maps have been analysed by GIS to provide a summary of data relevant to exceedence of the annual mean limit values in Tables 8.14 and 8.15. The tables show the number of road links, total road length and area and population within the area exceeding limit values for 2004/2005 and 2020 for each of the netcen, ERG and CERC models. The Netcen model results cover all regions of the UK, but results from the ERG and CERC models are for London only. Further discussion of the differences and simulations of the different model predictions for exceedence of both annual mean and daily average limit values is given in Chapter 9.

Figure 8.25 Estimated UK annual mean background PM_{10} concentration, 2002, in µg m^{-3} (gravimentric).

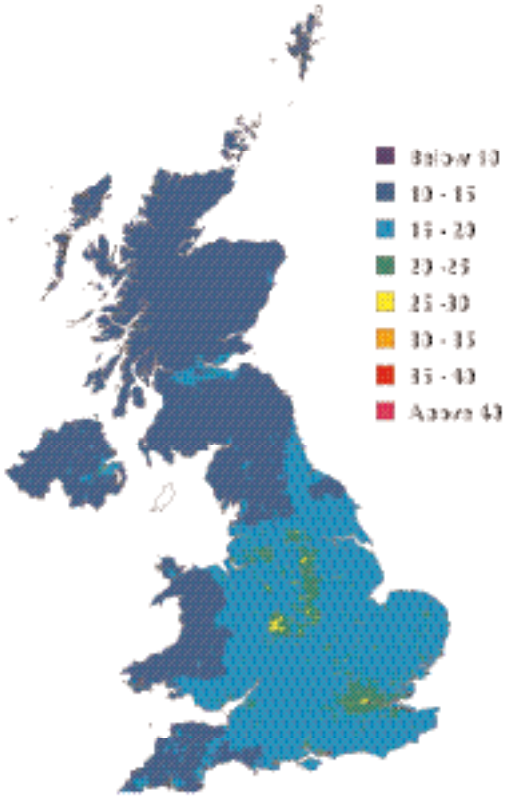

Figure 8.26 Estimated UK annual mean roadside PM_{10} concentrations for major built-up roads, 2002, in µg m^{-3} (gravimetric).

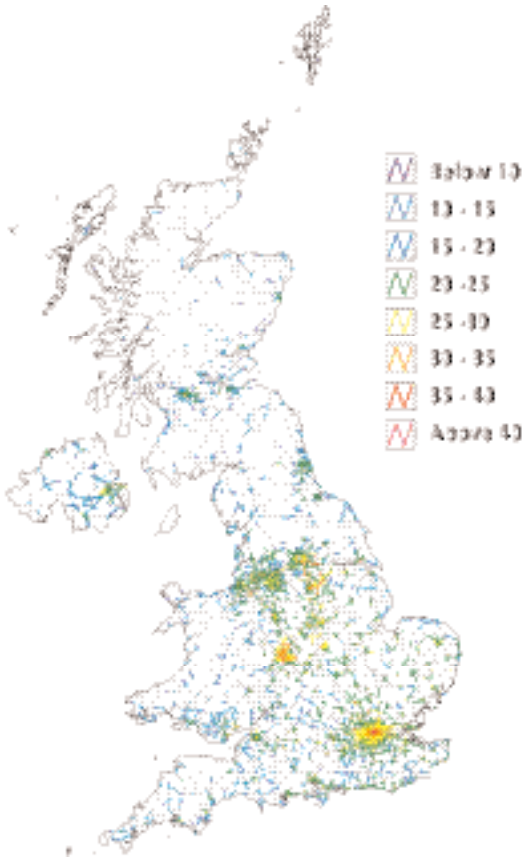

Figure 8.27 Estimated UK annual mean background PM_{10} concentration, 2005, in µg m^{-3} (gravimentric).

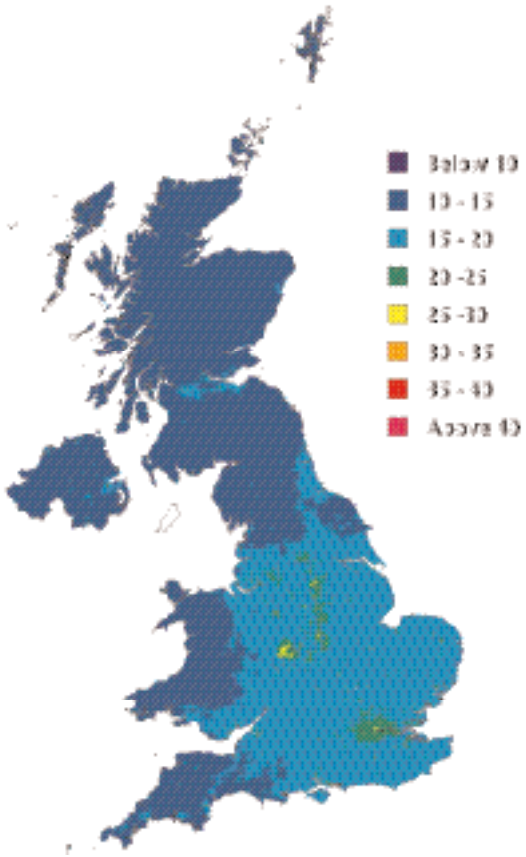

Figure 8.28 Estimated UK annual mean roadside PM_{10} concentrations for major built-up roads, 2005, in µg m^{-3} (gravimetric).

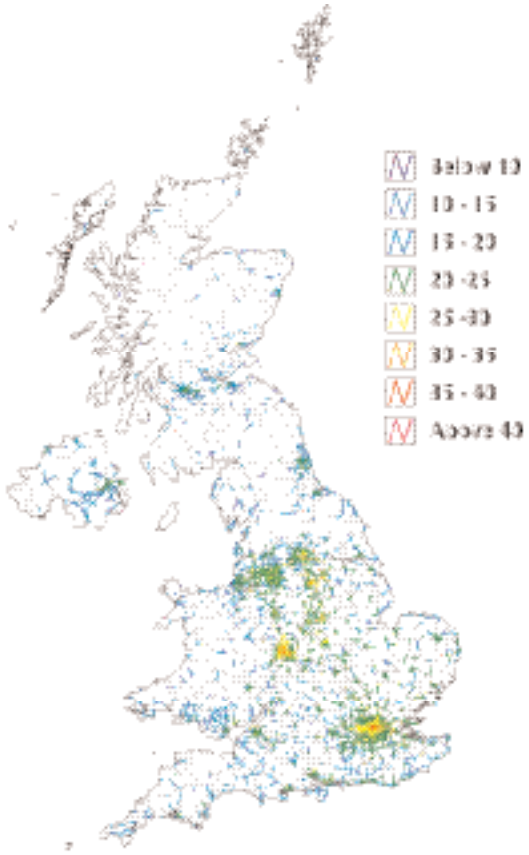

Figure 8.29 Estimated UK annual mean background PM_{10} concentration, 2010 in µg m^{-3} (gravimentric).

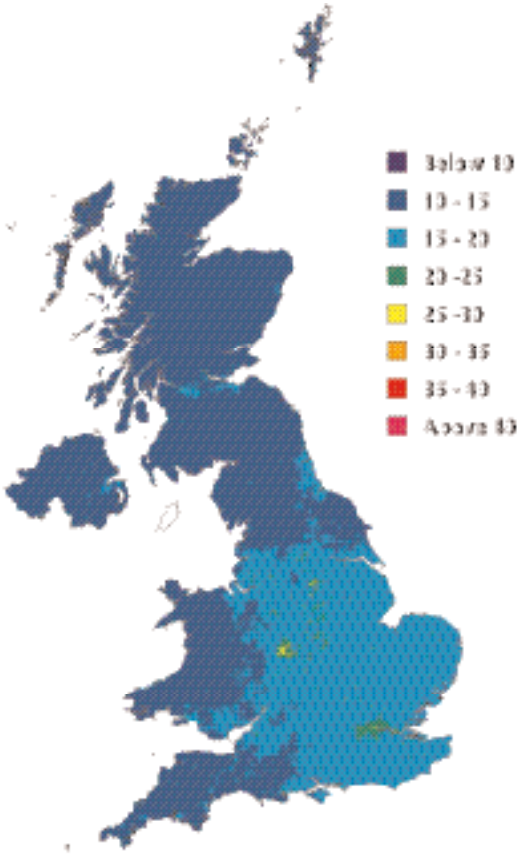

Figure 8.30 Estimated UK annual mean roadside PM_{10} concentrations for major built-up roads, 2010, in µg m^{-3} (gravimetric).

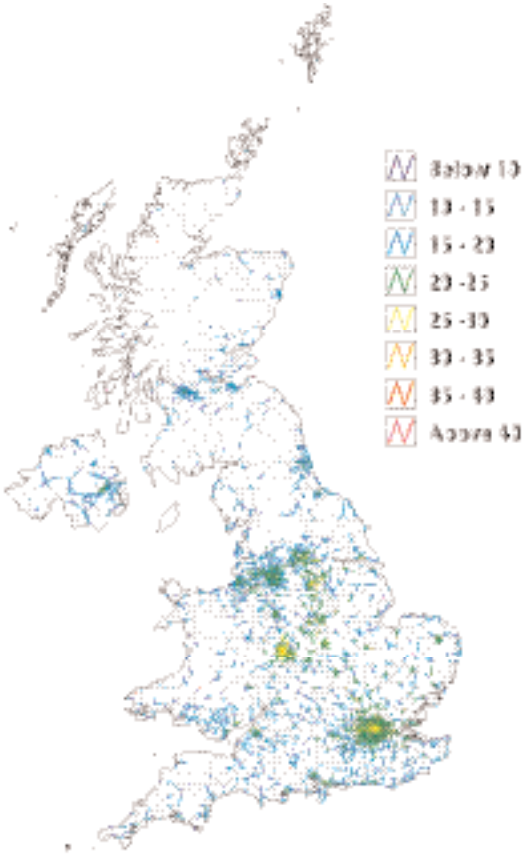

Figure 8.31 Annual average PM_{10} concentrations in London for 1999 calculated by ADMS-Urban (typical meteorology).

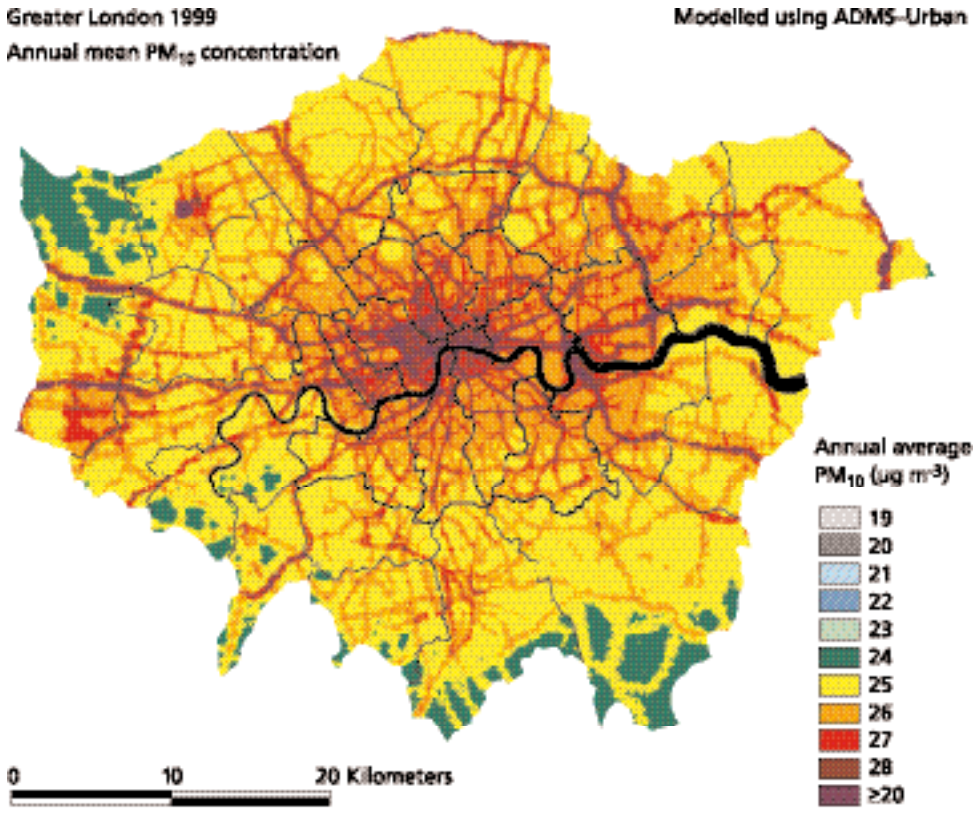

Figure 8.32 Annual average PM_{10} concentrations in London for 2004 calculated by ADMS-Urban (typical meteorology).

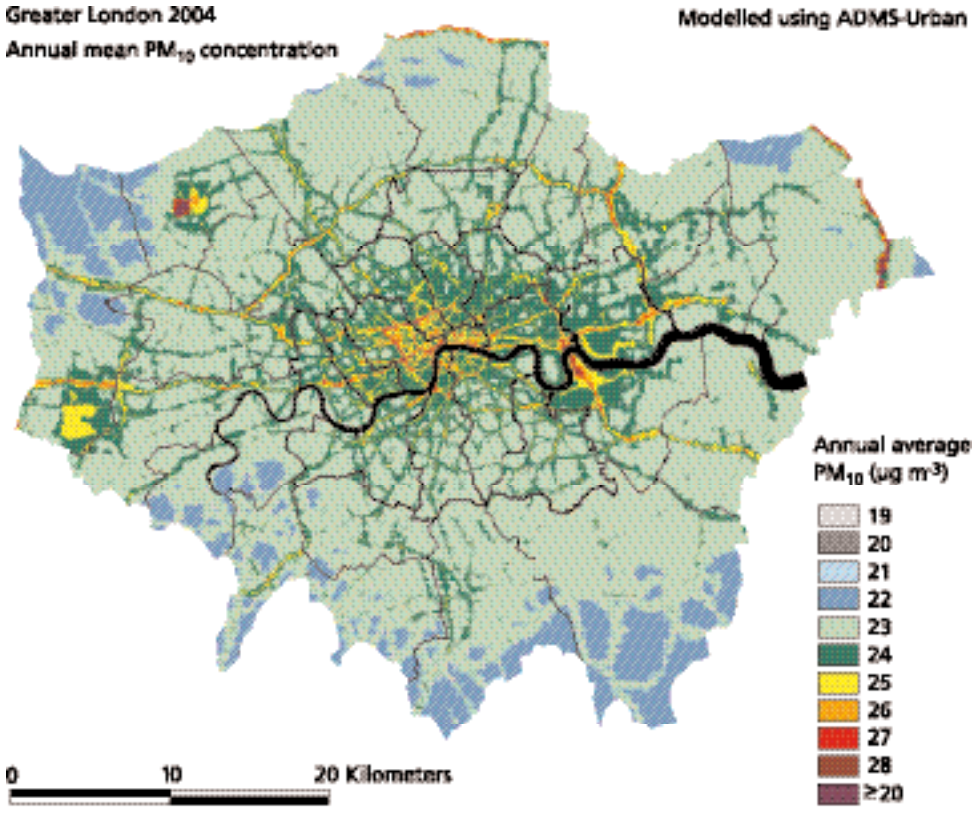

Figure 8.33 Annual average PM_{10} concentrations in London for 2010 calculated by ADMS-Urban (typical meteorology).

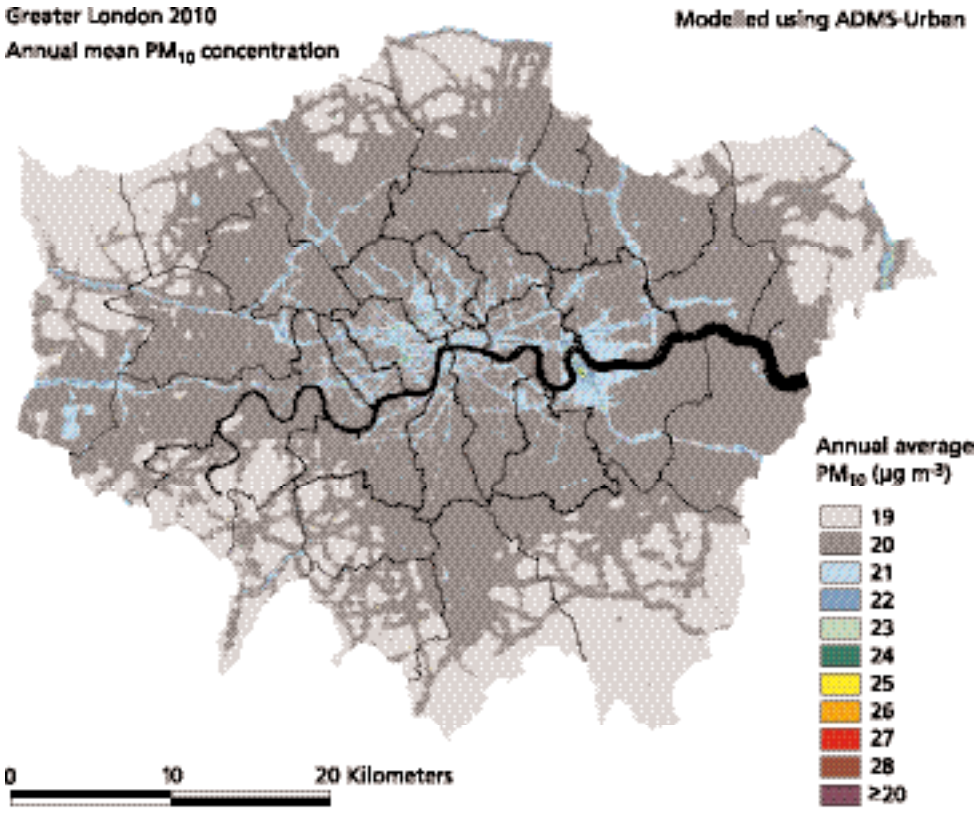

Figure 8.34 Annual average PM_{10} concentrations in London for 2010 calculated by ADMS-Urban (worst case meteorology).

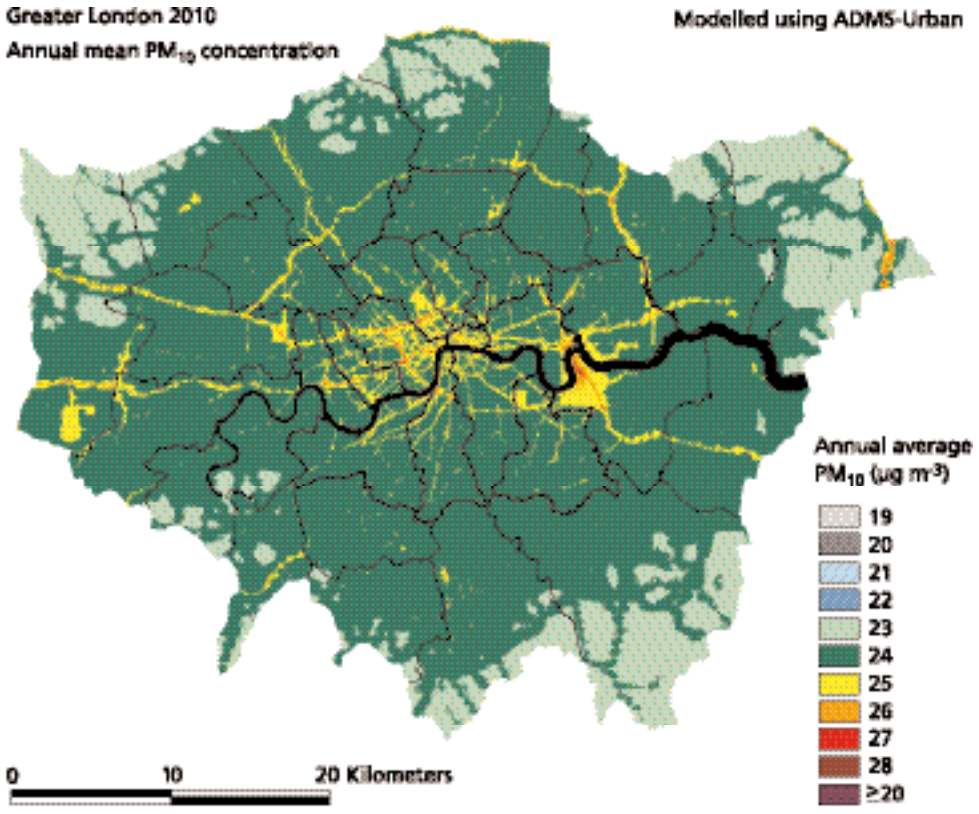

Figure 8.35 The 90th percentile of 24-hourly average PM_{10} 2004 (typical meteorology), corresponding to daily average concentration exceeded 35 times.

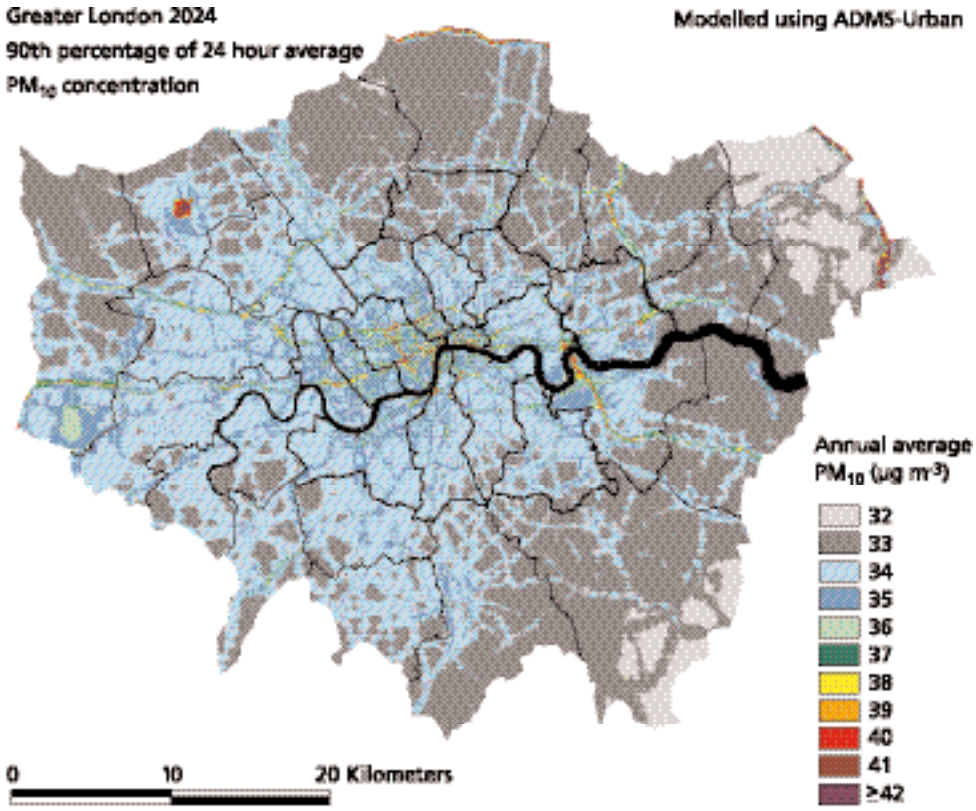

Figure 8.36 The 98th percentile of 24-hourly average PM_{10} 2010 (typical meteorology), corresponding to daily average concentration exceeded 7 times.

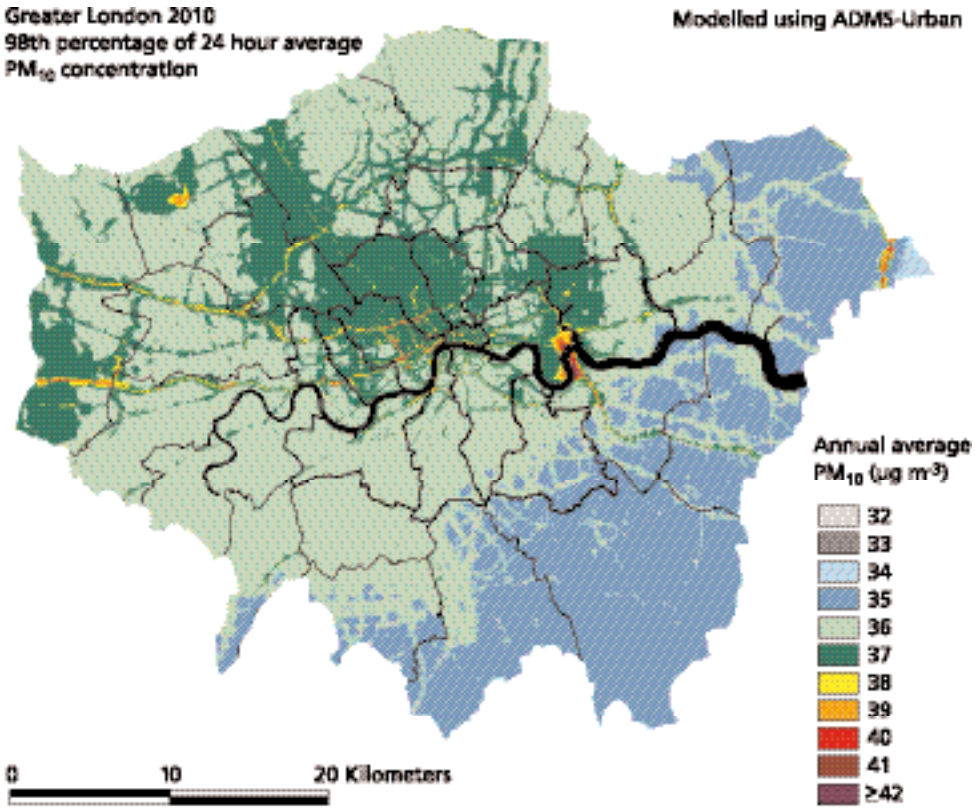

Figure 8.37 London maps predicted using the ERG model (a) Annual mean PM_{10} for 2001; (b) annual mean PM_{10} predicted for 2005 assuming 2001 meteorology; (c) annual mean PM_{10} predicted for 2010 assuming 2001 meteorology (μg m^{-3} (TEOM * 1.3)).

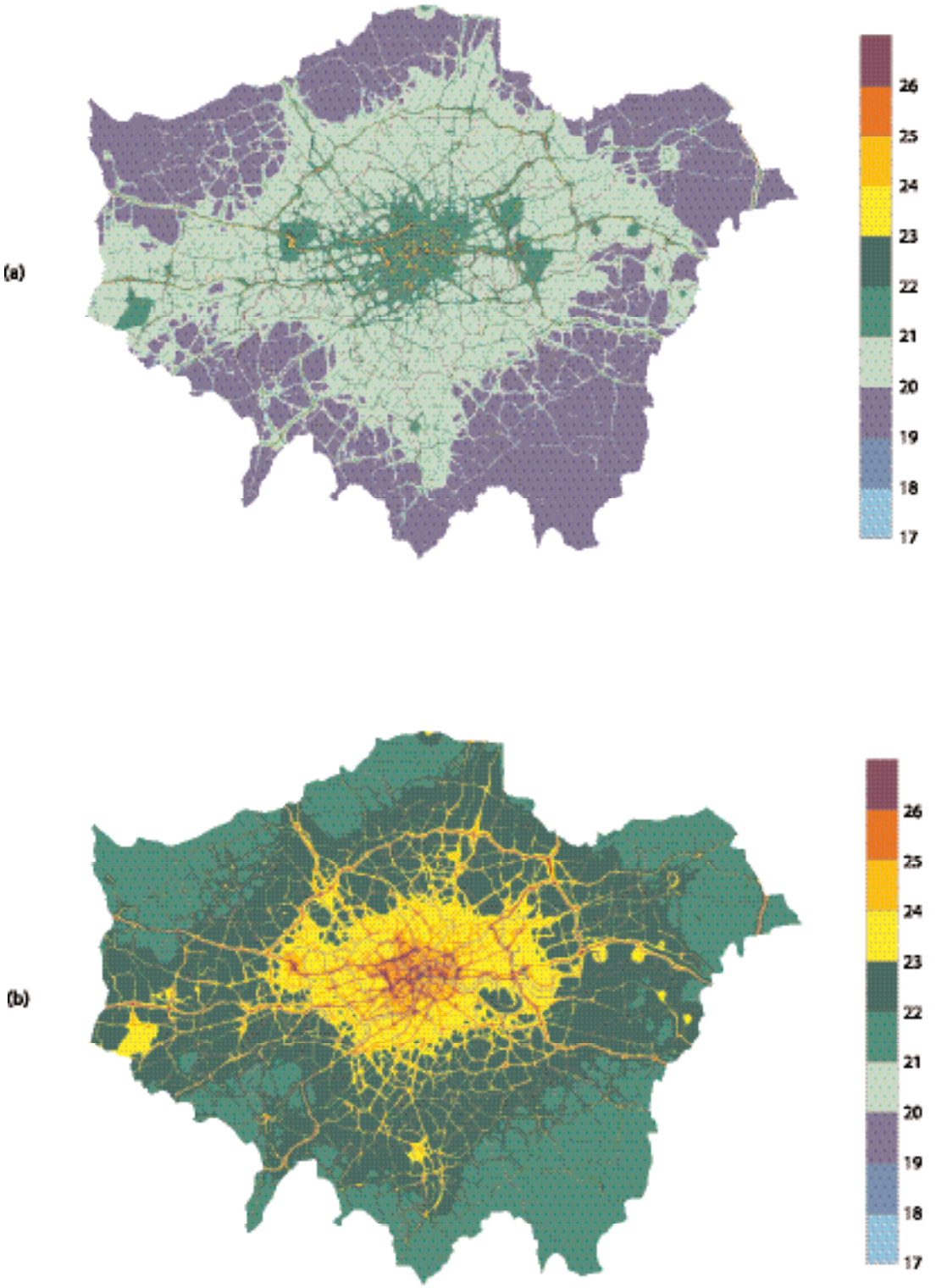

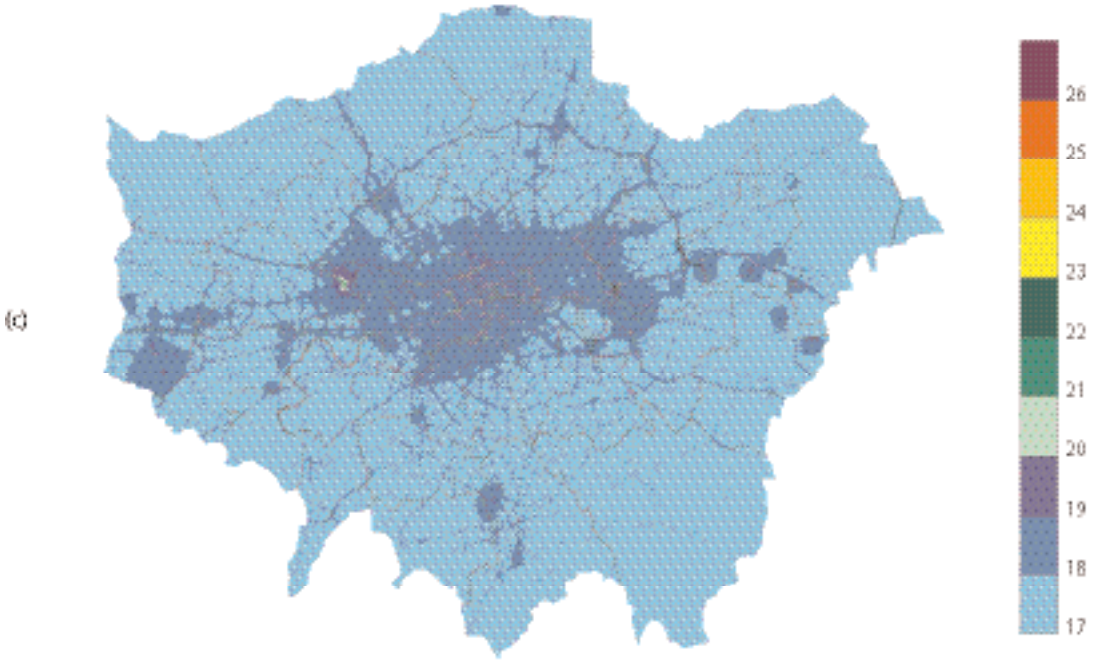

8.4.1.3 Site-specific projections at monitoring sites

813. Figure 8.39 describes the best assessments for annual mean PM_{10} concentrations over the period from 1992–2010 from a combination of observation and site-specific modelling. The observations refer to the average of the annual mean PM_{10} concentrations for 1997–2003 for ten selected background sites: values for earlier years are the average over a subset of these sites in operation in each year. These ten sites comprise one rural site, Rochester and nine urban background sites: London Bloomsbury, Birmingham centre, Cardiff centre, Edinburgh centre, Belfast centre, Liverpool centre, Newcastle centre, Manchester Piccadilly, Bristol centre.

814. The average annual mean PM_{10} concentration declines from 27.6 μg m^{-3} (TEOM) in 1992 to a minimum of 18.5 μg m^{-3} in 2000 before rising again to 20.8 μg m^{-3} in 2003. The upwards trend from 2000 onwards is continued to 2003 but it is likely that 2003 was exceptional as has been indicated in Figure 8.31 by plotting the preliminary result for the first quarter of 2004.

815. Also plotted are the ten-site averages of the annual mean PM_{10} concentrations determined with the site-specific projections model. These model concentrations span the range from 24.1 to 26.5 μg m^{-3} (TEOM) in 1992 and from 15.0 to 17.0 μg m^{-3} in 2010. Each line intersects the observed line at one year during the period 1996 to 2002 (projections from the base years of 2000 and 2003 have not been calculated). The projections reflect the trends in the average concentrations over the ten sites estimated in the site-specific model. Each site has its own source apportionment of current concentrations, which influences the predicted future concentrations, driven by the corresponding emission projections.

Table 8.14 Summary results from Netcen, ADMS-Urban and ERG modelling for PM_{10}. (All calculations outside London and total are for Netcen calculations.)

		Baseline (A)					
		Number of roadlinks with >20 µg m^{-3} (gravimetric) annual mean PM_{10}			Number of roadlinks with >40 µg m^{-3} (gravimetric) annual mean PM_{10}		
	Total assessed	ADMS 1999	Netcen 2002/ 2005	2010	ADMS 1999	Netcen 2002/ 2005	2010
ADMS-Urban London	18195	18195	18195	9042	76	0	0
Netcen London	1926	1923	1922	1883	44	12	0
Rest of England	6267	5321	4825	3130	1	0	0
Scotland	629	197	129	43	0	0	0
Wales	398	135	73	39	0	0	0
Northern Ireland	140	59	37	22	0	0	0
Total	9360	7635	6986	5117	45	12	0

		Road length (km) with >20 µg m^{-3} (gravimetric) annual mean PM_{10}			Road length (km) with >40 µg m^{-3} (gravimetric) annual mean PM_{10}		
	Total assessed	Netcen 2002/ ADMS 1999	2005	2010	Netcen 2002/ ADMS 1999	2005	2010
ERG London	4814	4814	4814	1742	4.2	0	0
ADMS-Urban London	3651	3651	3651	1626	0.6	0	0
Netcen London	1786	1782	1781	1730	24	9	0
Rest of England	10911	7964	6959	4113	0	0	0
Scotland	1348	304	197	59	0	0	0
Wales	982	236	121	55	0	0	0
Northern Ireland	1010	363	244	139	0	0	0
Total	16037	10649	9302	6096	24	9	0

	Total assessed	Area (km^2) with >20 µg m^{-3} gravimetric annual mean PM_{10}			Area (km^2) >40 µg m^{-3} gravimetric annual mean PM_{10}		
		Netcen 2002/ ADMS 1999	2005	2010	Netcen 2002/ ADMS 1999	2005	2010
ERG London	1858	1858	953	39	3	0	0
ADMS-Urban London	1574	1574	1574	1175	0.4	0	0
Netcen London	1624	1491	1342	778	0	0	0
Rest of England	128765	8990	4853	1841	0	0	0
Scotland	77535	35	18	8	0	0	0
Wales	20745	136	52	18	0	0	0
Northern Ireland	13680	101	18	3	0	0	0
Total	242349	10753	6283	2648	0	0	0

	Total assessed	Population with >20 µg m^{-3} gravimetric annual mean PM_{10}			Population with >40 µg m^{-3} gravimetric annual mean PM_{10}		
		Netcen 2002/ ADMS 1999	2005	2010	Netcen 2002/ ADMS 1999	2005	2010
Netcen London	7,650,944	7,034,197	6,665,653	4,526,147	0	0	0
Rest of England	38,037,527	15,052,120	9,402,849	4,139,160	0	0	0
Scotland	4,905,019	60,549	27,981	3,362	0	0	0
Wales	2,916,782	174,391	73,786	31,515	0	0	0
Northern Ireland	1,577,855	319,520	58,715	13,326	0	0	0
Total	55,088,127	22,640,776	16,228,984	8,713,511	0	0	0

816. There is good correspondence between the time profiles of the observed and site-specific model annual mean concentrations over the period up to 2003. Both the observations and the predicted concentrations show a steeply declining trend followed by a levelling off and an increase from 2000 to 2001. It is noted that the projections from the site-specific model tend to show monotonic declines over the period from 2004 up to 2010. The model estimates for 2010 come close to, but still exceed, the indicative Stage II limit value of 20 μg m^{-3} (gravimetric), equivalent to 15.3 μg m^{-3} (TEOM), as an annual mean concentration. To have achieved the indicative limit value in 2010, the measured annual mean concentrations would have needed to have shown a decline of –4 % per year over the entire 1997–2010 period, which is close to that observed for the long-running urban background sites over the period 1992–2003.

817. Several factors have been identified that may lead to systematic over or underestimates by 1 to 2 μg m^{-3}. The influence of a perturbation of plus or minus such amounts has been investigated within the Netcen and ERG models, and the effect is indicated in the tables giving a factor of up to 2 on the extent of exceedence relative to the base case. The tables imply good agreement between the Netcen and ERG estimates allowing for such uncertainties.

Figure 8.38 Observed annual mean PM_{10} concentrations over the period 1992–2003 for the background sites for which results are available from the site-specific model and their projections through to 2010.

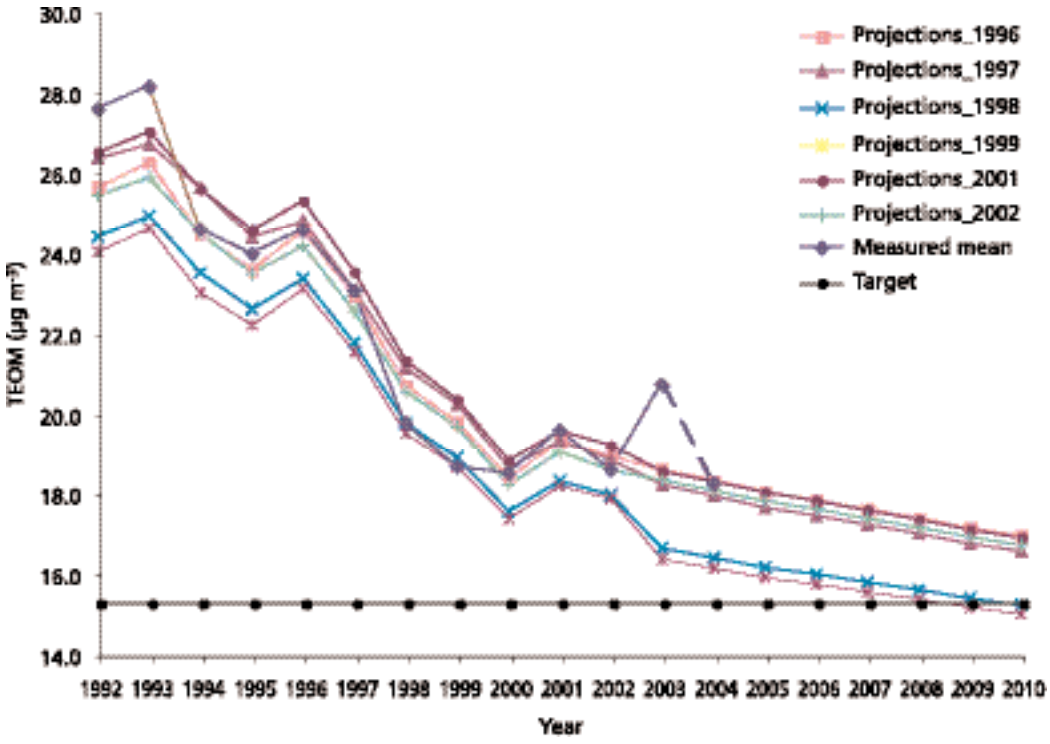

8.4.1.4 *Mapped concentrations for $PM_{2.5}$*

818. Two sets of national maps for $PM_{2.5}$ have been calculated, calibrated using TEOM (Figures 8.39 and 8.40) and gravimetric measurements (Figures 8.41 and 8.42). The TEOM maps were calibrated using measurements from four national network sites. The gravimetric maps were calibrated using data from seven national network sites. The maps for $PM_{2.5}$ show similar spatial patterns to PM_{10}; however,

Figure 8.39 Estimated UK annual mean background $PM_{2.5}$ concentration, 2002, in µg m^{-3} (TEOM).

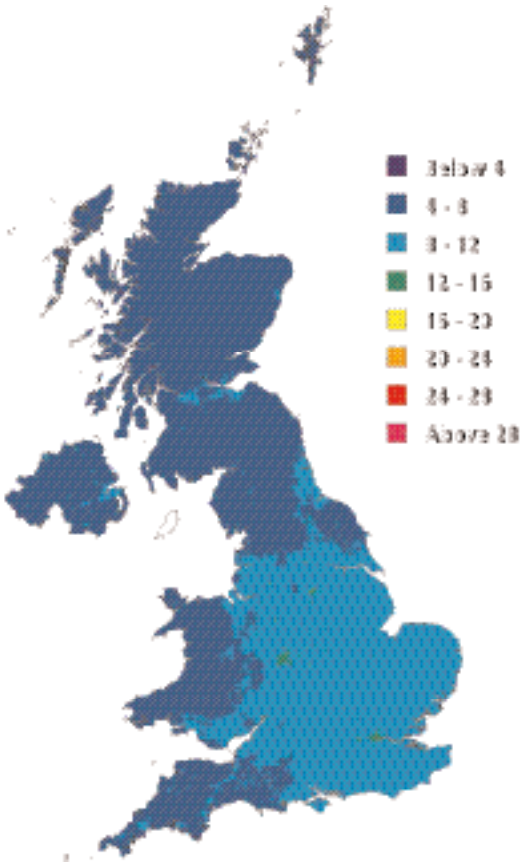

Figure 8.40 Estimated UK annual mean roadside $PM_{2.5}$ concentrations for major built-up roads, 2002, in µg m^{-3} TEOM).

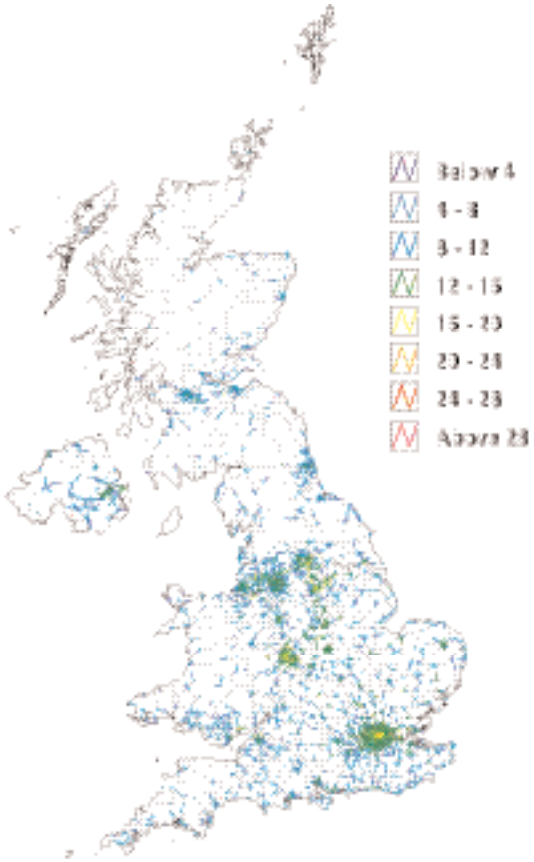

Figure 8.41 Estimated annual mean background $PM_{2.5}$ concentration, 2002, in µg m^{-3} (gravimentric).

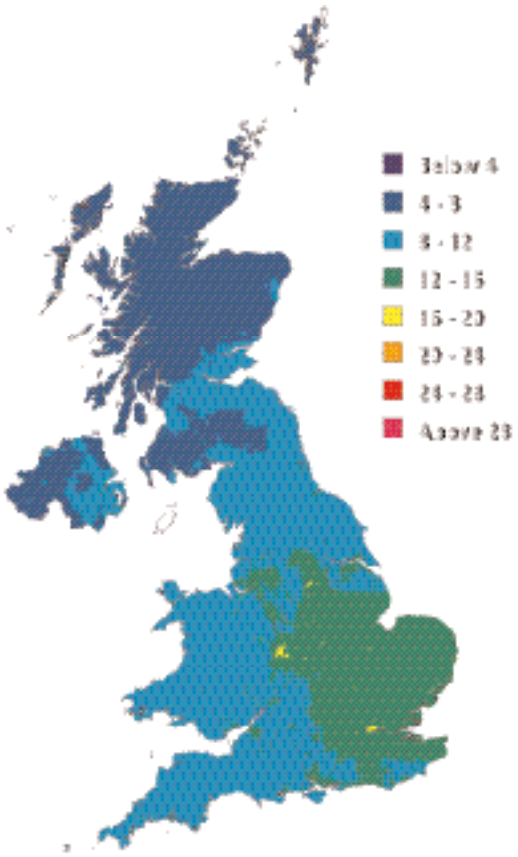

Figure 8.42 Estimated UK annual mean roadside $PM_{2.5}$ concentrations for major built-up roads, 2002, in µg m^{-3} (gravimetric).

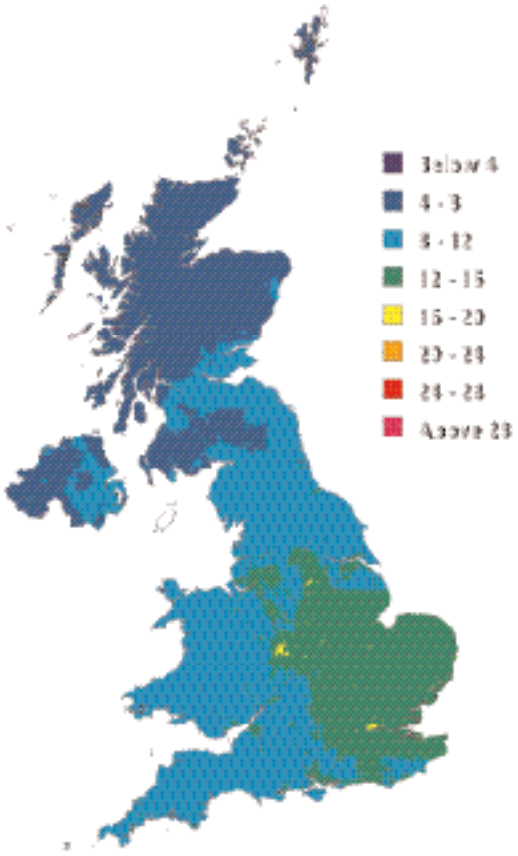

Figure 8.43 Annual average $PM_{2.5}$ mean concentration calculated using ADMS-Urban for (a) 2004 and (b) 2010.

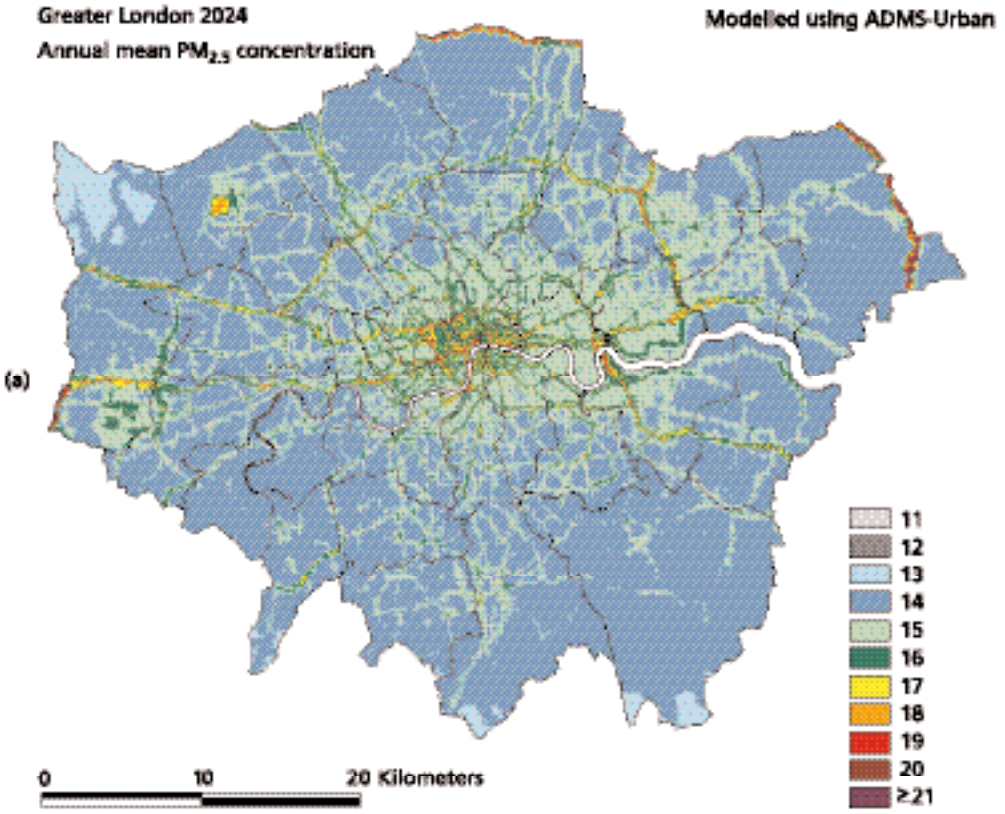

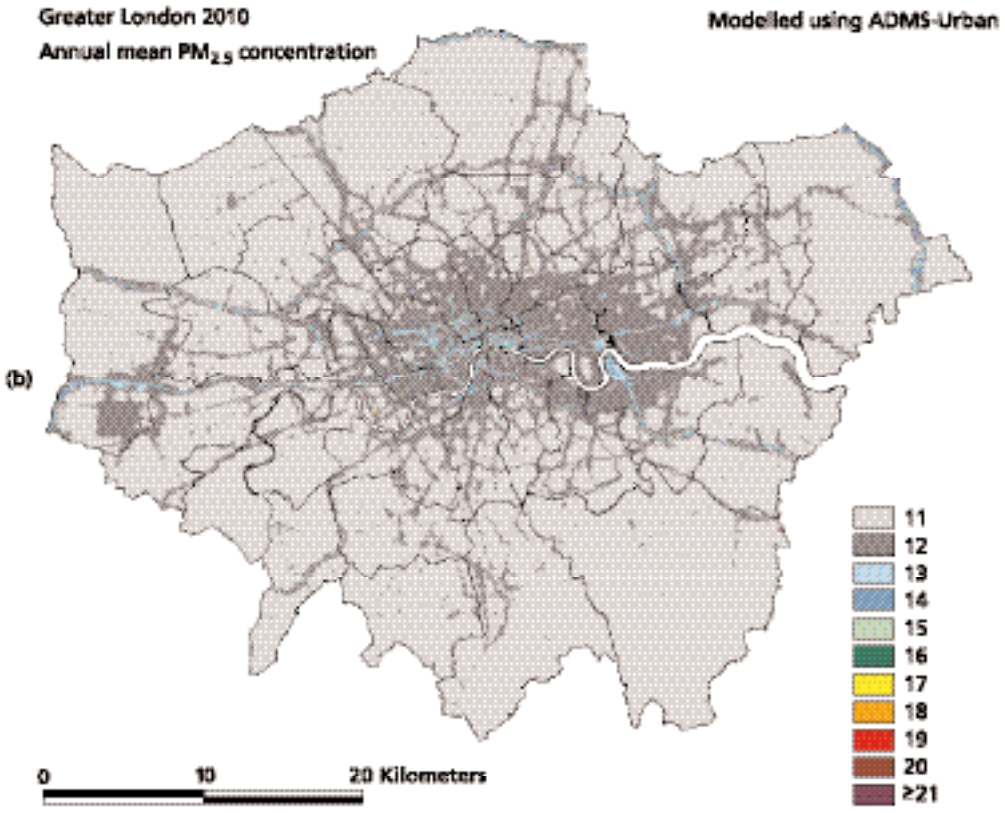

Table 8.15 Summary results from Netcen and ADMS-Urban mapping for $PM_{2.5}$. (All areas outside London and total are for Netcen calculations.)

	Total assessed	Number of roadlinks with >12 µg m^{-3} annual mean $PM_{2.5}$				Number of roadlinks with >16 µg m^{-3} annual mean $PM_{2.5}$				Number of roadlinks with >20 µg m^{-3} annual mean $PM_{2.5}$			
		Netcen 2002/ ADMS		1999		2010		Netcen 2002/ ADMS		1999		2010	
ADMS-Urban London	18195	18195		5047		17303		64		3409	463	0	35
		TEOM	Grav.	TEOM	Grav.	TEOM	Grav.	TEOM	Grav.	TEOM	Grav.	TEOM	Grav.
Netcen London	1926	1821	1926	1035	1923	548	1742	79	629	82	141	1	3
Rest of England	6267	2710	5866	752	4553	257	1665	17	321	10	0	0	0
Scotland	629	53	168	2	15	0	2	0	0	0	0	0	0
Wales	398	38	187	8	45	1	10	1	0	0	0	0	0
Northern Ireland	140	32	50	3	13	1	7	0	0	0	0	0	0
Total	9360	4654	8197	1800	6549	807	3624	97	950	92	604	1	38

	Total assessed	Number of roadlinks with >12 µg m^{-3} annual mean $PM_{2.5}$				Road length (km) with >16 µg m^{-3} annual mean $PM_{2.5}$				Road length (km) with >20 µg m^{-3} annual mean $PM_{2.5}$			
		Netcen 2002/ ADMS		1999		2010		Netcen 2002/ ADMS		1999		2010	
ADMS-Urban London	3651	3651		815		3289		7		433		0	
		TEOM	Grav.	TEOM	Grav.	TEOM	Grav.	TEOM	Grav.	TEOM	Grav.	TEOM	Grav.
Netcen London	1786	1663	1786	719	1782	306	1547	39	358	40	245	1	19
Rest of England	10911	3505	9595	998	6861	424	2223	26	420	13	236	0	2
Scotland	1348	74	264	3	27	0	3	0	0	0	0	0	0
Wales	982	53	262	15	61	2	16	0	0	0	0	0	0
Northern Ireland	1010	208	318	21	65	4	38	0	0	0	0	0	0
Total	16037	5503	12325	1757	8795	736	3828	65	778	53	481	1	21

	Total assessed	Area (km²) with >12 µg m⁻³ annual mean $PM_{2.5}$				Area (km²) with >16 µg m⁻³ annual mean $PM_{2.5}$				Area (km²) with >20 µg m⁻³ annual mean $PM_{2.5}$			
		Netcen 2002/ ADMS 1999		2010		Netcen 2002/ ADMS 1999		2010		Netcen 2002/ ADMS 1999		2010	
ADMS-Urban London	1574	1574		410		1440		1		51		0	
		TEOM	Grav.	TEOM	Grav.	TEOM	Grav.	TEOM	Grav.	TEOM	Grav.	TEOM	Grav.
Netcen London	1624	213	1624	27	1531	0	111	0	9	0	0	0	0
Rest of England	128765	580	54866	239	12660	2	292	1	52	0	0	0	0
Scotland	77535	2	26	0	4	0	0	0	0	0	0	0	0
Wales	20745	5	212	1	53	0	0	0	0	0	0	0	0
Northern Ireland	13680	9	52	0	1	0	0	0	0	0	0	0	0
Total	242349	809	56780	267	14292	2	403	1	61	0	0	0	0

	Total assessed	Population with >12 µg m⁻³ annual mean $PM_{2.5}$				Population with >16 µg m⁻³ annual mean $PM_{2.5}$				Population with >20 µg m⁻³ annual mean $PM_{2.5}$			
		Netcen 2002/ ADMS 1999		2010		Netcen 2002/ ADMS 1999		2010		Netcen 2002/ ADMS1999		2010	
ADMS-Urban London	7,172,407	7,172,407		1,907,378		6,604,814		640		171,045		9	
		TEOM	Grav.	TEOM	Grav.	TEOM	Grav.	TEOM	Grav.	TEOM	Grav.	TEOM	Grav.
Netcen London	7,650,944	1,590,589	7,269,158	114,880	7,120,938	0	935,757	0	25,529	0	0	0	0
Rest of England	38,037,527	1,465,710	28,913,434	645,334	13,640,192	2,900	774,943	944	123,226	0	0	0	0
Scotland	4,905,019	354	33,805	0	1,068	0	0	0	0	0	0	0	0
Wales	2,916,782	8,975	328,012	76	55,387	0	0	0	0	0	0	0	0
Northern Ireland	1,577,855	29,959	157,259	0	4,926	0	0	0	0	0	0	0	0
Total	55,088,127	3,095,587	36,701,668	760,290	20,882,510	2,900	1,710,700	944	148,755	0	0	9	0

the actual concentration calculated depends a great deal on the measurement method, as no scaling factor has been used for the TEOMs. The ADMS-Urban calculations of $PM_{2.5}$ for London (Figure 8.43) are more similar to the partisol-based values from the national models. In Table 8.15 GIS has been used for each of the model runs to calculate the number of road links, roadlength, area and population within the area exceeding the annual means of 12, 16 and 20 μg m^{-3}. It can be seen that by 2010 all models predicted almost no exceedence of 20 μg m^{-3} and limited exceedence (none in some cases) of 16 μg m^{-3}.

8.4.2 Regional models

8.4.2.1 Comparison of modelled sulphate, nitrate and ammonium concentrations for the UK

819. EMEP and FRAME were both originally developed for sulphur and nitrogen deposition, and work on the secondary particulates has evolved more recently as increased emphasis has been placed on the health effects of fine PM. Both FRAME and EMEP provide concentrations of sulphate, ammonium and aerosol nitrate, although EMEP provides further subdivision into coarse and fine size fractions for the nitrate. Results from a detailed intercomparison study in progress are available from two versions of EMEP, EMEP (1) and EMEP (2), from a current version of FRAME plus the previous data provided for use in UKIAM. The illustrations given below include maps of FRAME with one EMEP version in each case.

820. Figure 8.44 shows a comparison of the estimated sulphate concentrations from FRAME and EMEP. In the EMEP model the variation across the UK is less marked than in FRAME, which indicates rather lower values in the more remote areas and the higher values close to the major sources on the eastern side of the country. Such locally enhanced concentrations are very sensitive to the assumed fraction of sulphur emitted as sulphate.

821. In Figure 8.45 the model results are compared with measurements from the 12 background monitoring sites as scatter plots.

822. Figure 8.46 shows the corresponding results for ammonium. The FRAME model indicates somewhat smaller values than the EMEP model. Figure 8.47 again gives comparison, with the measurements showing good agreement with the EMEP model, but some underestimation with FRAME. In all the maps there is a clear gradient from the southeast to the remote northwest.

823. Figure 8.48 compares model results for maps of aerosol nitrate concentrations, and Figure 8.49 shows the corresponding scatter plots comparing with measurements. (Here the EMEP results correspond to a more recent version of the model in April 2004 with some revised nitrate chemistry.)

824. The aerosol nitrate will depend both on the overall rate of oxidation to nitrate and the partitioning between the aerosol nitrate and the gaseous nitric acid. For the latter, both models differ from measured values over the UK network with the EMEP values being particularly low. There is ongoing work on the nitrate chemistry to resolve these discrepancies. However, for the nitrate aerosol component the models are generally in good agreement both with each other and the measurements.

Figure 8.44 Calculated sulphate, by EMEP and FRAME.

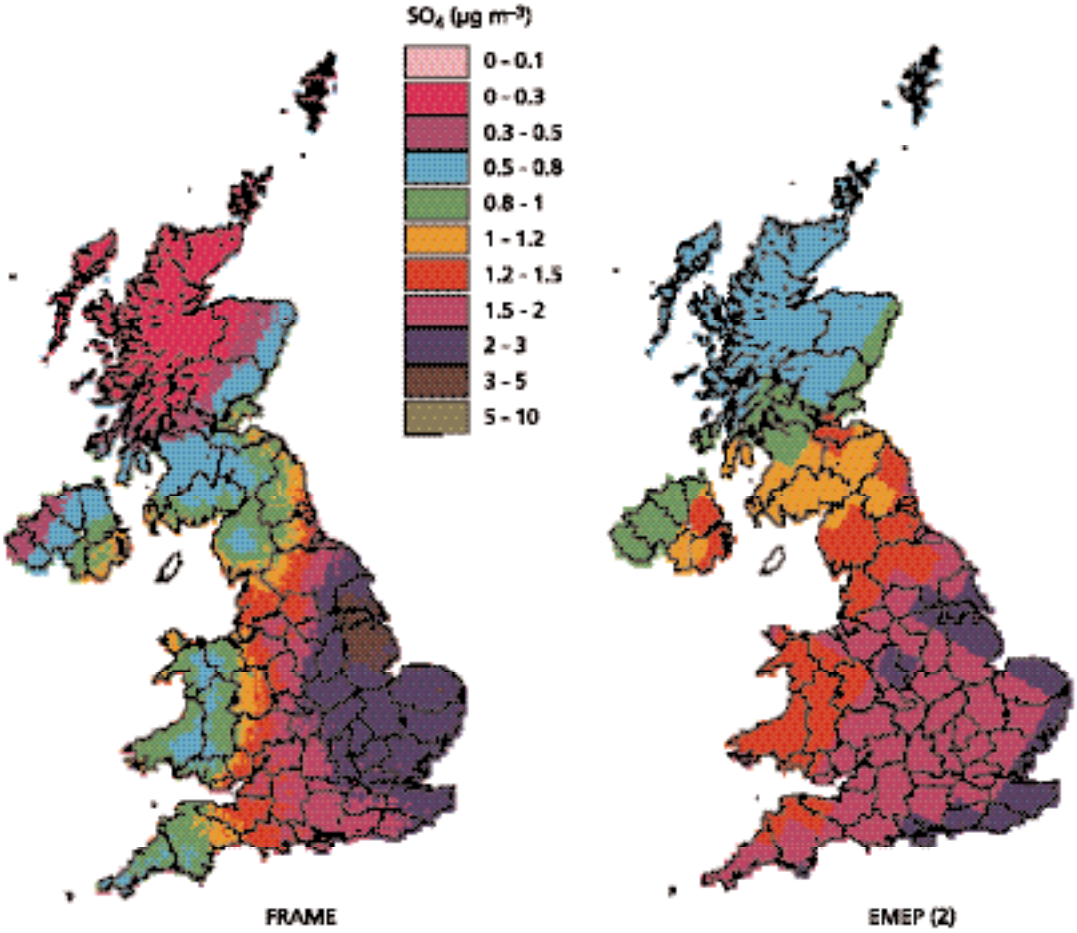

Figure 8.45 Comparison between models and measurements of sulphate.

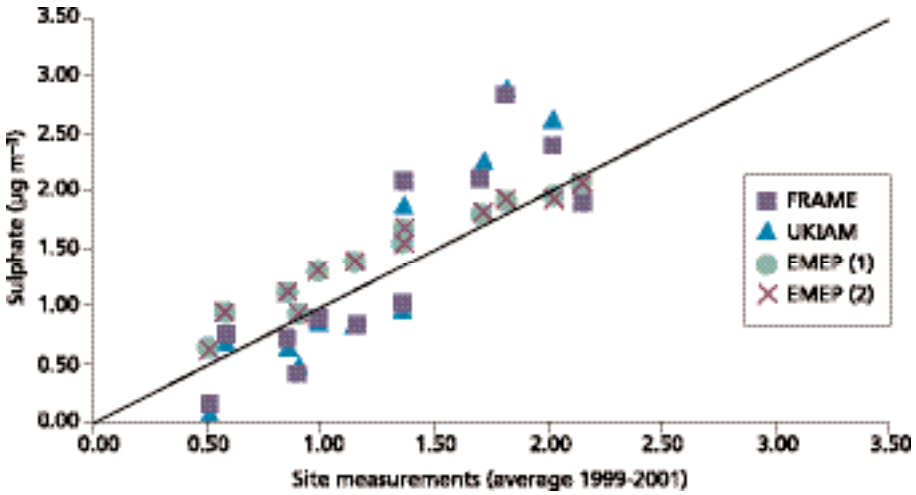

825. The reason why the secondary inorganic aerosol concentrations are of concern is the health effects attributed to exposure to fine PM. As a measure of risk we have calculated population exposure to the combined total sulphate plus nitrate plus ammonium concentrations. In Figure 8.50 maps of total secondary inorganic aerosols from the FRAME and EMEP model are compared with the estimates from

Figure 8.46 Calculated ammonium aerosol, by EMEP and FRAME.

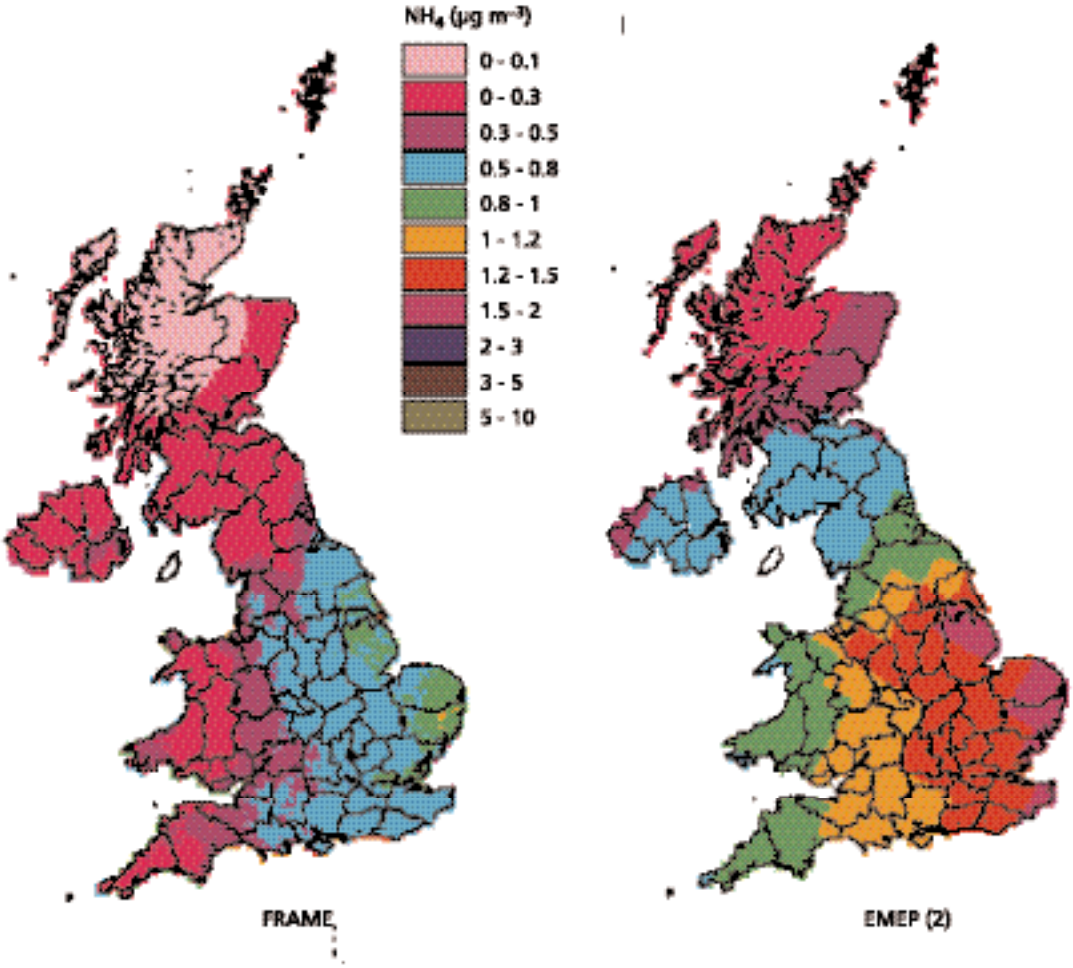

Figure 8.47 Comparison between models and measurements of ammonium concentrations.

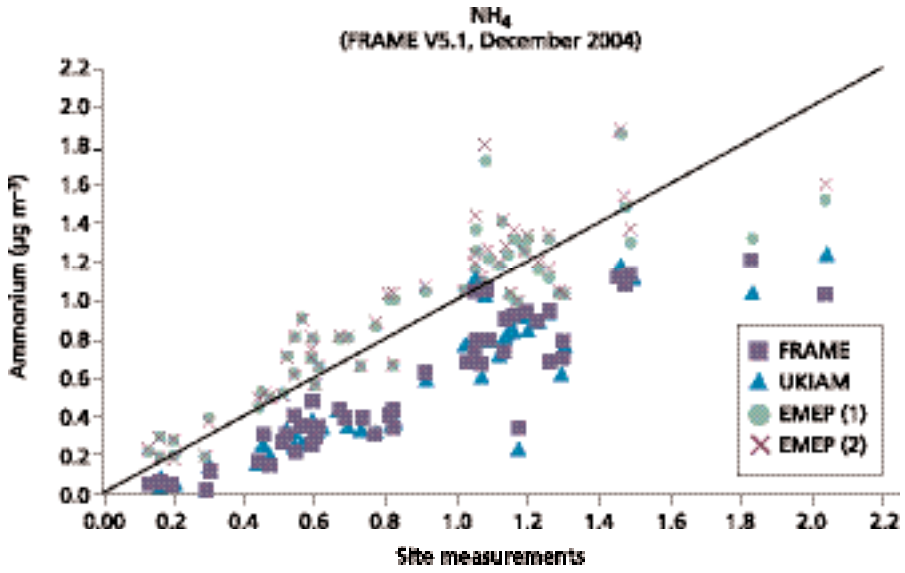

the Netcen mapping model. Table 8.16 shows the corresponding estimates of population exposure in person g m^{-3} (derived by summing over the grid squares the population from census data times the annual average concentration in µg m^{-3}).

Figure 8.48 Calculated nitrate aerosol, by EMEP and FRAME.

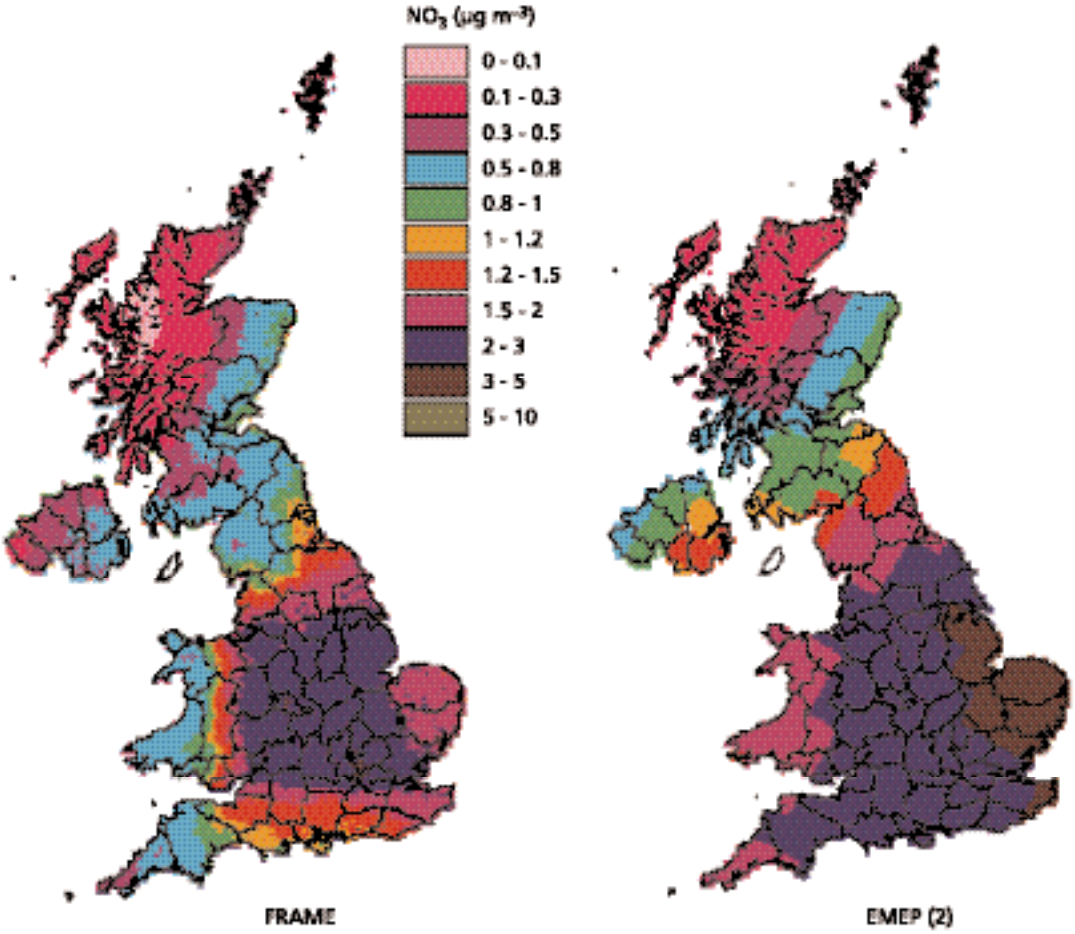

Figure 8.49 Comparison between models and measurements of nitrate aerosol.

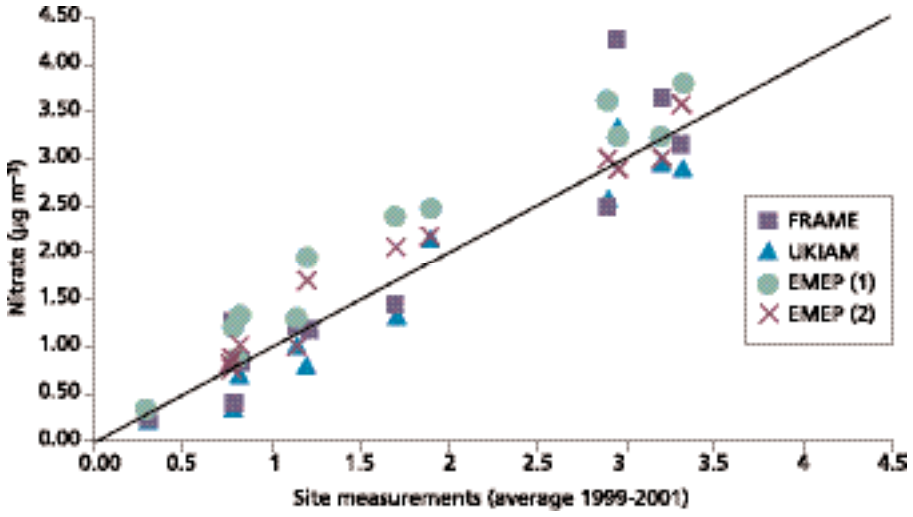

Figure 8.50 Calculated total secondary inorganic aerosol, by EMEP, FRAME and Netcen.

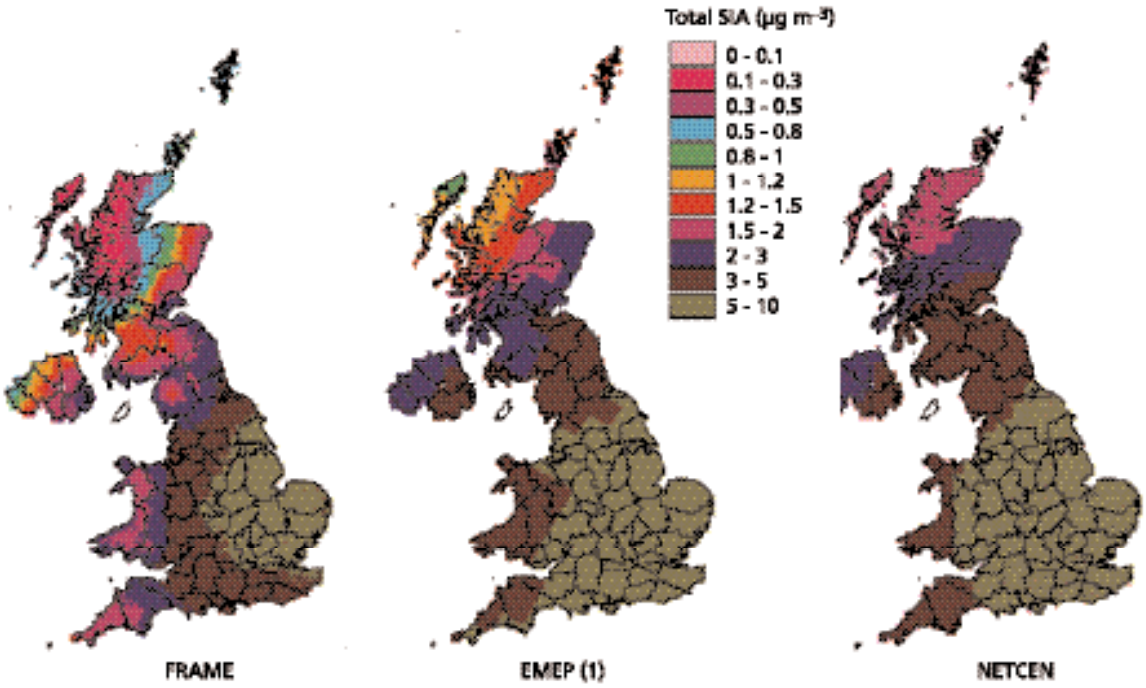

Table 8.18 Total UK population exposure to secondary inorganic aerosol (SIA) (in person µg m^{-3}) calculated from year 2000 annual average concentrations (2002 for Netcen data).

	SO_4	NO_3	NH_4	Total SIA
FRAME	95.54	154.88	32.85	283.27
UKIAM	100.06	140.93	42.04	283.04
EMEP (1)	97.28	149.61	63.82	310.71
EMEP (2)	95.52	129.98	64.25	289.74
Netcen	—	—	—	337.12

8.4.2.2 Europe-wide calculations

826. Figure 8.51 presents the annual average boundary layer concentration map for particulate sulphate for 1996. The map shows a widespread distribution over much of Northwest Europe with a maximum over Northern France, Belgium, the Netherlands and Northern Germany. A second maximum is found over Northern Italy, separated from the rest of Europe by the Alps. The 1.5 µg S m^{-3} contour spreads into the UK from Northwest Europe, showing the influence of long-range transport both out of and into the UK.

827. The spatial pattern obtained from the NAME model is in broad agreement with the spatial pattern obtained from the observations within the EMEP network, as described by Hjellbrekke *et al*. (1997). The model and observed maps are similar over the UK and Scandinavia but they are markedly different over the rest of

Europe. The model values are consistently higher than those measured over the region extending from Northern France into Northern Germany. The observed maximum is further east, over Poland and the Czech Republic. The model agrees well with the observations of Ottley and Harrison (1992) over the North Sea.

828. Figure 8.52 presents the corresponding map for particulate nitrate expressed as the sum of both fine ammonium nitrate and coarse nitrate formed by displacement reactions. This shows a maximum over Belgium and The Netherlands and a secondary maximum over Northern Italy. Again the moderately polluted contours spread into the UK.

829. The spatial pattern generated by the NAME model compares well with the map derived from observations (Hayman *et al*. 2001). The model overestimates levels across Scotland, 0.2–1.5 μg NO_3 m^{-3} in the model compared with 0.2–1.0 μg NO_3 m^{-3} in the observations. Similarly in the Southeast of England the model gives 3–5 μg NO_3 m^{-3} in the region where the observations report concentrations of NO_3 of greater than 1.5 μg m^{-3}.

830. By adding together the total mass of ammonium nitrate, ammonium sulphate and coarse particle nitrate – excluding the contribution to the mass from ions such as sodium and calcium – it is possible to map the modelled secondary inorganic particulates as PM_{10} and this is shown in Figure 8.53. The maximum over Northern Italy is now clearly the strongest with the maximum over the low countries a secondary one. The 10 μg m^{-3} PM_{10} contour spreads across Northwest Europe and into the UK. This can be compared with the observed regional background over London of 16.5 μg m^{-3} inferred from the observations in the LAQN. The pattern predicted by NAME for 1996 can also be broadly compared with calculations of the EMEP model (Figure 8.54). This also shows the highest levels of sulphate and nitrate over the low countries and Northern Italy; however, the areas of highest concentration are much less focussed.

Figure 8.51 Annual average particulate sulphate concentrations during 1996 across Northwest Europe, as calculated by NAME.

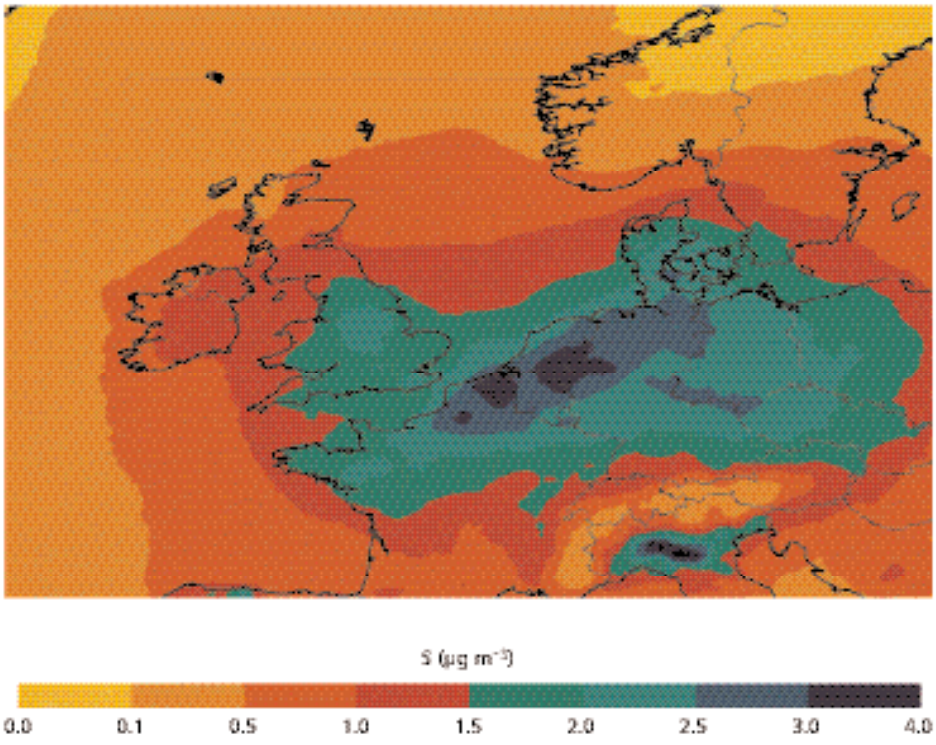

Figure 8.52 Annual average particulate nitrate concentrations during 1996 across Northwest Europe, expressed as the sum of both fine and coarse components.

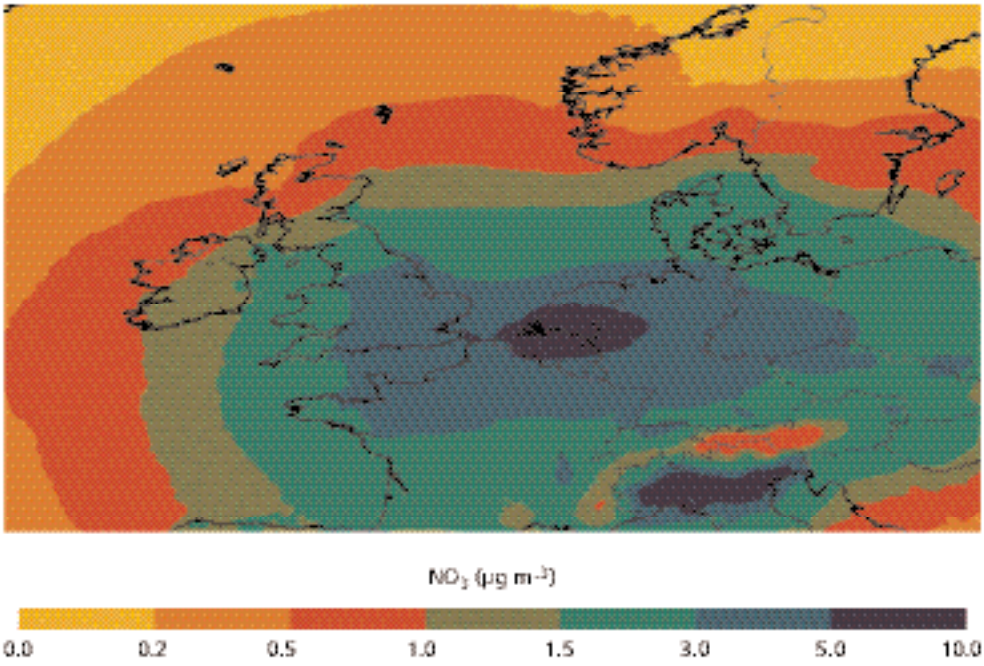

Figure 8.53 Annual average secondary inorganic particulate concentrations plotted as PM_{10} for 1996.

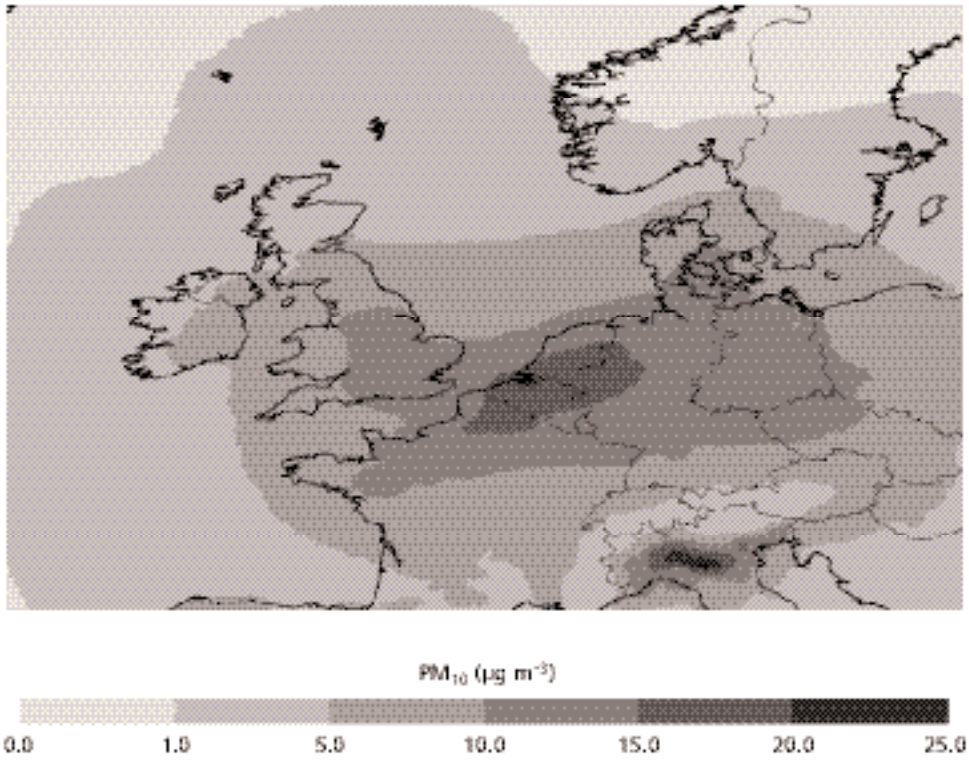

Figure 8.54 Secondary inorganic aerosol concentrations across Europe estimated using EMEP (2), 2003 emissions and 2000 meteorology.

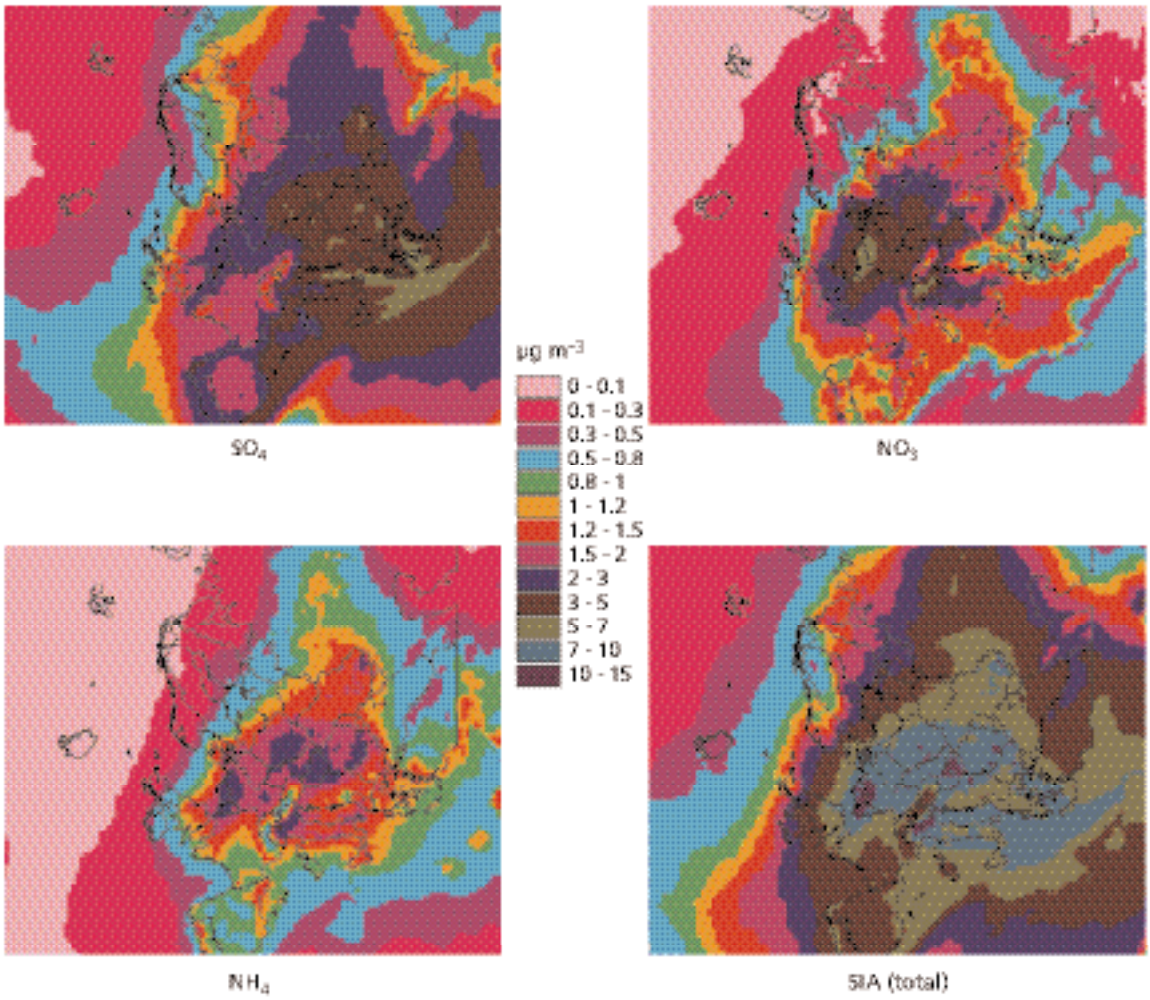

831. Figure 8.55 shows how the NAME model can give an indication of the likely country attribution of the SO_2 emissions that acted as precursors to the model particulate sulphate. Each of the main observed pollution episodes is represented as vertical bars in Figure 8.55. The bar is sectioned according to the country of origin of the SO_2 that had been transformed into particulate sulphate *en route* to Yarner Wood.

832. During the January 2002 episode, the particulate sulphate appears to have originated from the UK, France and the Benelux countries. During the prolonged episode during March 2002, however, the UK appears to have been the dominant source. The May 2002 episode appears to have involved the UK, the Benelux countries and Germany. During the summer period from July to August, the UK appears to have been the dominant source. The episode during September is characteristically different, with contributions from France, Germany, Poland and the Baltic. This is the time when long-range transport brought elevated PM_{10} levels to much of the UK from the forest fires near Moscow. The episodes during December 2002 brought particulate sulphate from the UK and Germany to Yarner Wood.

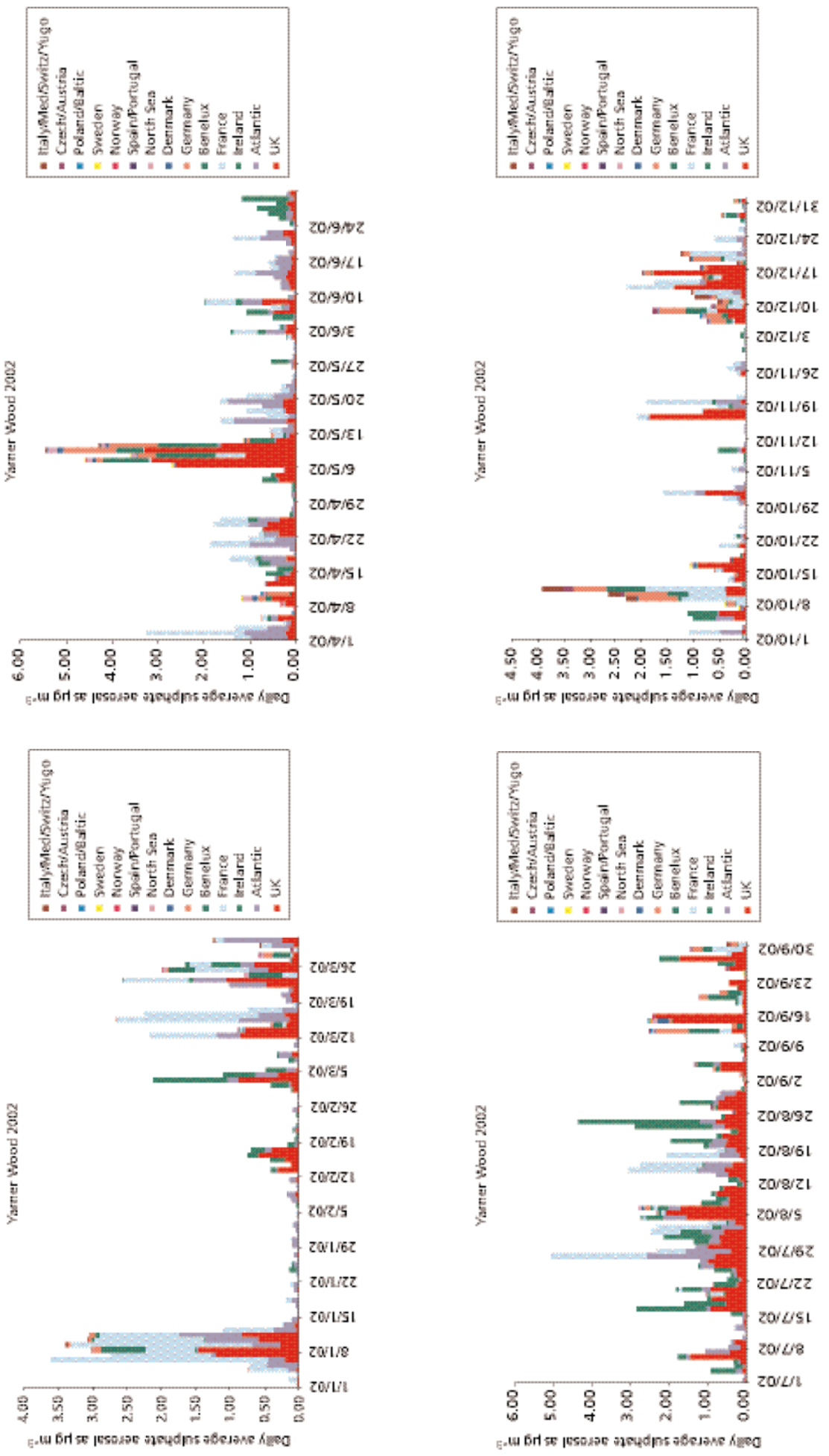

Figure 8.55 Daily attribution of sulphate aerosol at Yarner Wood for 2002.

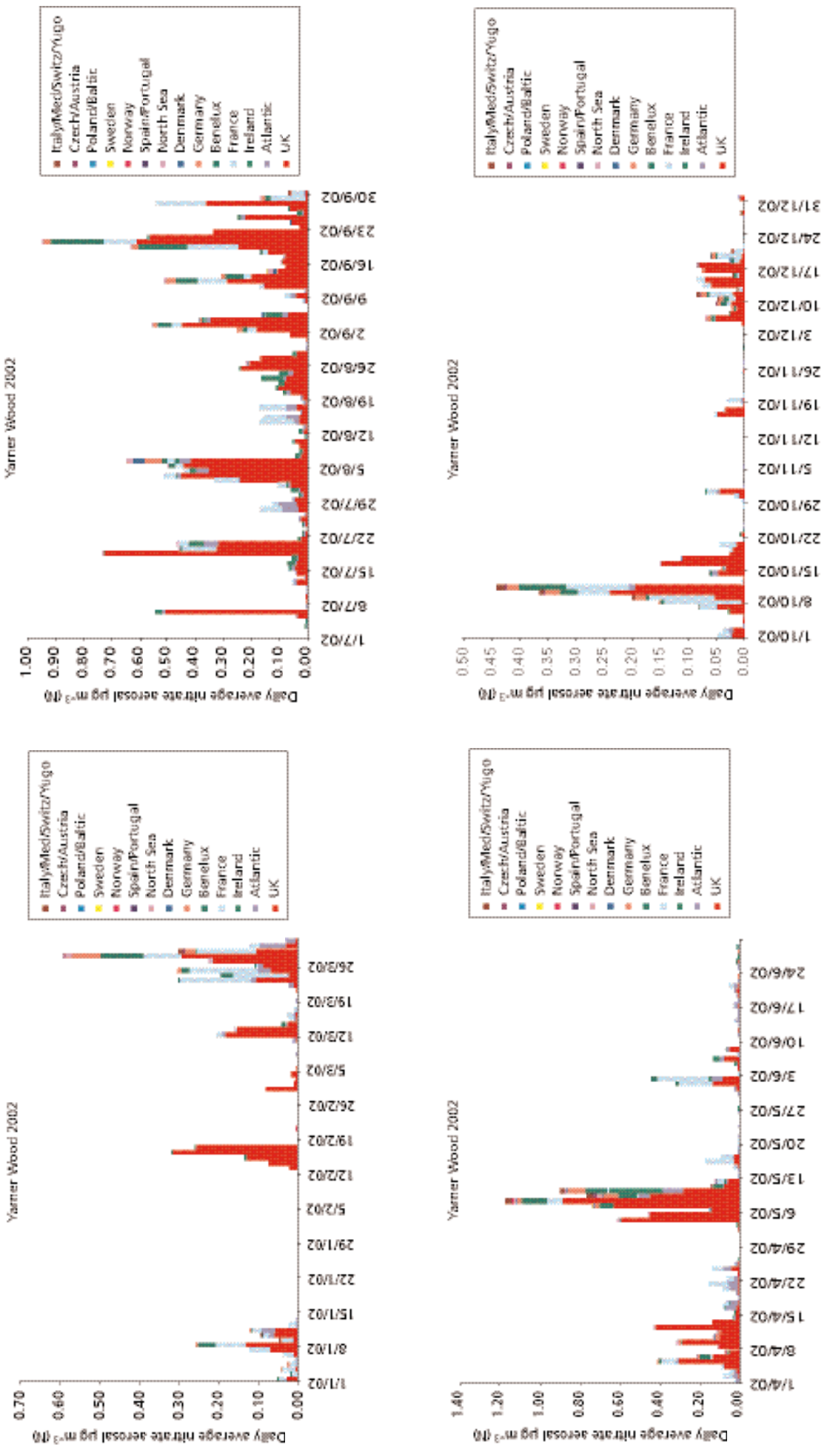

Figure 8.56 Daily attribution of nitrate aerosol at Yarner Wood for 2002.

833. Integrating over the entire year 2002, about 25% of the particulate sulphate modelled at Yarner Wood has been derived from SO_2 sources outside of the UK. Figure 8.56 shows a series of graphs for the attribution of nitrate aerosol at Yarner Wood for the same period. There are no measurement data available for nitrate aerosol at Yarner Wood. It is thought, based on previous work, that the NAME model underpredicts nitrate aerosol, particularly in the winter, and that these results are indeed very low with a maximum of <1.2 μg m^{-3} in May and values very close to zero through much of the winter.

834. Similar calculations to those described for Yarner Wood have been conducted at 30 sites across the UK and Ireland to obtain the percentage contributions to the annual average for each country or group of countries.

835. Tables 8.13 to 8.15 show, respectively, the percentage contribution to modelled sulphate aerosol, nitrate aerosol and sulphur at a subset of these sites. Some countries have been grouped and it should be noted that the model domain does not fully extend into some countries, for example Norway, Sweden and Italy.

836. Looking at the tables, the model is predicting that (as a percentage of the total for that species) the greatest import from outside the UK is by sulphate aerosol. Sites to the south and east of the UK see greatest import from other countries of which the larger part originates from France. Lough Navar and Belfast (Northern Ireland) and Mace Head (Ireland) have large contributions from Ireland, as would be expected. Substantial Irish contributions are also seen at northern and western UK sites, for example, Eskdalemuir and Narberth.

837. The contribution from other European countries falls off markedly with distance from the UK, as would be expected.

838. In contrast to Table 8.16, the percentages shown in Table 8.17 for sulphur dioxide show that UK emissions are much more dominant. France has quite a big effect on the London sites and in the south and east generally, reaching a maximum of 19.4% of sulphur dioxide at Barcombe Mills. The percentage of sulphate aerosol arriving at Barcombe Mills is 38.1%, however, which demonstrates how generation of the secondary aerosol can actually have a more dominant effect than the primary species. It should be noted that the attribution for the secondary species includes aerosol formed during the travel time from the country of origin of the primary species (sulphur dioxide in this case).

839. The percentage contributions for nitrate aerosol in Table 8.18 show that sites are, generally speaking, less influenced by European nitrate aerosol than they are by European sulphate aerosol. For example, 63% of nitrate aerosol at Barcombe Mills is of UK origin compared with 38% of sulphate aerosol.

Table 8.19 Percentage contributions to sulphate aerosol in 2002 at the listed sites.

Site	UK	Atlantic	Ireland	France	Benelux	Germany	Denmark	North Sea	Norway	Sweden	Poland/ Baltic	Czech/ Austria	Italy/ Med/ Switz/ Yugo
Barcombe Mills	38.2	7.6	3.5	38.1	5.1	4.8	0.7	1.0	0.0	0.1	0.1	0.3	0.5
Belfast	37.7	5.8	40.9	6.7	2.4	4.2	0.8	0.8	0.0	0.2	0.2	0.3	0.1
Birmingham	60.3	6.1	6.8	15.3	4.7	4.2	0.9	0.8	0.0	0.1	0.2	0.3	0.2
Bloomsbury	46.7	6.4	3.6	28.8	6.5	5.1	0.9	1.1	0.0	0.1	0.2	0.4	0.4
Edinburgh	65.8	3.5	14.0	7.3	2.5	3.7	1.2	1.2	0.0	0.2	0.3	0.2	0.1
Mace Head	23.4	9.3	43.9	10.1	3.8	6.4	1.0	0.9	0.1	0.2	0.2	0.4	0.2
Narberth	39.9	15.1	19.8	13.9	4.2	4.9	0.6	0.8	0.0	0.1	0.1	0.4	0.3
Stoke Ferry	51.4	4.7	4.3	20.8	8.1	7.0	1.2	1.6	0.0	0.1	0.2	0.4	0.2
Strathvaich	54.7	5.6	17.9	8.6	3.2	4.4	2.5	2.0	0.1	0.3	0.5	0.2	0.1
Yarner Wood	36.0	17.7	12.4	23.3	4.2	4.3	0.5	0.7	0.0	0.1	0.1	0.2	0.5

Table 8.20 Percentage contributions to nitrate aerosol in 2002 at the listed sites.

Site	UK	Atlantic	Ireland	France	Benelux	Germany	Denmark	North Sea	Norway	Sweden	Poland/ Baltic	Czech/ Austria	Italy/ Med/ Switz/ Yugo
Barcombe Mills	63.1	1.1	0.4	22.7	8.2	2.6	0.3	1.2	0.0	0.0	0.0	0.2	0.2
Belfast	66.6	3.5	12.8	6.8	4.4	2.8	0.5	2.1	0.1	0.1	0.0	0.2	0.1
Birmingham	80.2	1.3	0.7	7.5	5.5	2.5	0.6	1.4	0.0	0.0	0.0	0.2	0.2
Bloomsbury	70.3	0.9	0.4	15.1	8.6	2.8	0.3	1.3	0.0	0.0	0.0	0.2	0.2
Edinburgh	81.7	1.1	2.0	4.3	4.1	2.4	0.7	3.2	0.0	0.1	0.0	0.1	0.1
Mace Head	43.3	7.3	31.4	6.6	5.2	4.0	0.3	1.0	0.1	0.2	0.0	0.3	0.3
Narberth	71.5	6.9	5.0	8.0	4.1	2.6	0.5	0.8	0.0	0.0	0.0	0.2	0.3
Stoke Ferry	70.4	0.6	0.4	10.6	10.7	4.0	0.4	2.7	0.0	0.0	0.0	0.2	0.1
Strathvaich	76.3	2.8	3.4	5.1	3.9	2.8	1.0	4.3	0.1	0.2	0.0	0.1	0.1
Yarner Wood	66.4	6.0	3.0	15.5	5.1	2.5	0.3	0.7	0.0	0.0	0.0	0.1	0.4

Table 8.21 Percentage contributions to sulphur dioxide in 2002 at the listed sites.

Site	UK	Atlantic	Ireland	France	Benelux	Germany	Denmark	North Sea	Norway	Sweden	Poland/ Baltic	Czech/ Austria	Italy/ Med/ Switz/ Yugo
Barcombe Mills	72.8	2.0	0.5	19.4	3.4	1.2	0.1	0.4	0.0	0.0	0.0	0.2	0.0
Belfast	64.3	1.9	30.9	1.3	0.4	0.6	0.1	0.3	0.0	0.0	0.1	0.1	0.0
Birmingham	95.6	0.9	0.6	1.5	0.7	0.5	0.0	0.2	0.0	0.0	0.0	0.1	0.0
Bloomsbury	84.2	1.4	0.5	9.3	2.9	1.1	0.1	0.4	0.0	0.0	0.0	0.2	0.0
Edinburgh	98.1	0.2	0.8	0.3	0.2	0.2	0.0	0.2	0.0	0.0	0.0	0.0	0.0
Mace Head	15.5	1.7	79.8	0.9	0.8	0.8	0.1	0.2	0.0	0.0	0.0	0.1	0.0
Narberth	66.5	20.8	5.2	4.5	1.4	1.0	0.1	0.3	0.0	0.0	0.0	0.2	0.0
Stoke Ferry	86.4	1.0	0.7	5.8	3.5	1.5	0.1	0.8	0.0	0.0	0.1	0.2	0.0
Strathvaich	84.1	2.8	5.2	2.4	1.2	1.6	0.6	1.6	0.1	0.1	0.3	0.1	0.0
Yarner Wood	67.5	15.0	2.2	11.7	2.0	1.0	0.1	0.3	0.0	0.0	0.0	0.1	0.0

8.5 Uncertainty in modelling PM

840. This section considers the accuracy and precision with which the models described in Section 8.2 are able to calculate airborne PM concentrations at sampled and unsampled locations, at locations similar and different to those where measurements are made, in the past, present and future. The focus will be on PM_{10} and the model results for PM_{10} that were presented in Section 8.4, but the ability to consider other PM metrics will also be considered. The larger amount and variety of uncertainty in PM_{10} modelling compared with NO_2 merits more detailed consideration of uncertainty in this report than was included for similar models in AQEG's NO_2 report (AQEG, 2004).

8.5.1 Methods for quantification of uncertainty and error

841. Sources of information on model uncertainty can be divided into the following three categories.

- Scientific assessment of the assumptions made in each model, compared with the theory of PM processing that was presented in Chapter 2 and elsewhere.
- Empirical quantification of error:
  - ❑ by comparison with measured data, necessarily in past years (but including retrospective assessment of the model's past ability to make future predictions, for example, model runs completed in 1998 predicting 2002 concentrations that can now be compared with measurements); or
  - ❑ by comparison between models for past or future scenarios.
- Sensitivity analysis of the extent to which varying model inputs causes the output to change (which can include inputs such as user choice of model assumptions and tunable parameters). In cases where a large number of parameters and/or inputs can be varied, a Monte Carlo approach to sensitivity analysis can be adopted.

842. Ideally, scientific assessment can confirm the results of sensitivity analysis, which, in turn, should be able to explain the results of empirical evaluation of model performance. In practice, full sensitivity analysis is impossible for the more complex models because of the number of parameters that can be varied. In theory a full scientific assessment, is possible for any well-documented model, but again, model complexity often renders this impossible to do completely and quantitatively. All three sources of information have, therefore, been used here.

843. In theory, it would be instructive to perform an analysis of the error due to the model itself, separately from the effects of error in emissions data or error in measurements that feed through into the modelling. In practice, it is usually impossible to separate these three main sources of error. The contributions of errors in measurement, emissions and modelling are discussed separately in relation to their impact on our confidence in the overall conclusions of this report in Chapter 9 but here, all three sources of error will be considered together.

8.5.2 Results of uncertainty analysis

8.5.2.1 Annual average past concentrations of PM_{10}

844. Figure 8.57 summarises the results of the uncertainty analysis. The format is taken from IPCC's analysis of causes of climate change. For a detailed discussion of these different types of error and uncertainty, refer to copious explanatory text and footnotes throughout IPCC (2001). The source apportionment of total annual average PM_{10} in Figure 8.56 is based on the general levels and source apportionment reported in Section 8.4. Estimates of the magnitude of the error in the calculated contribution of each component are based on the model evaluation information in Section 8.2. The level of scientific uncertainty described is based on information drawn from Sections 8.2 and 8.3 as well as earlier chapters of this report.

Figure 8.57 Contributions to PM_{10} and uncertainty therein at the most polluted point in the UK, 2001.

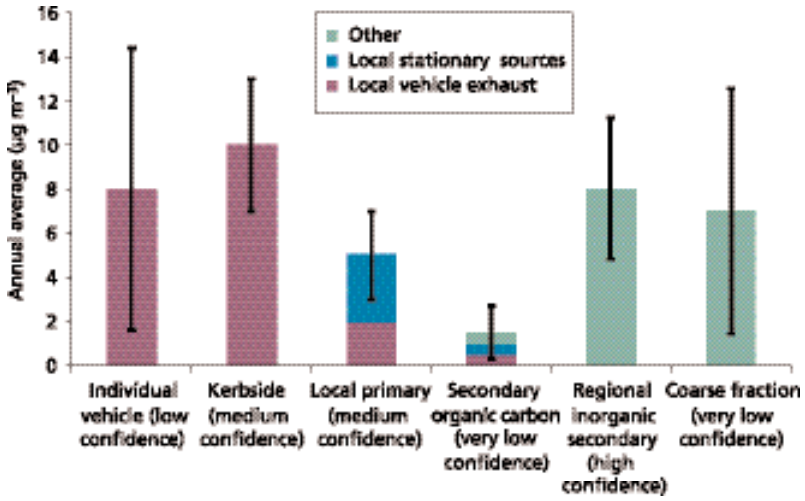

845. Figure 8.58 refers to the hypothetical 'most polluted point in the UK'. This is taken to be closer to traffic sources than kerbside, that is, on the carriageway of a heavily-trafficked, canyon-type city centre road, close to individual highly-emitting vehicles. At such a location, the total PM_{10} concentration is the sum of all the bars in the chart. Other locations can be considered by combining the summary data differently. For example, an urban background location is the sum of the four bars to the right of the chart. A rural motorway could similarly be considered as the sum of bars one, two, four, five and a non-urban part of six.

Figure 8.58 Variability in annual average PM_{10} as a function of distance for traffic sources.

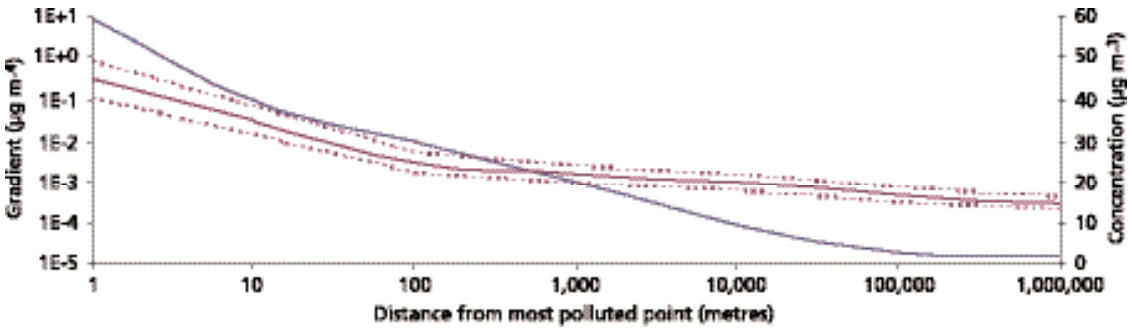

846. Bar one of Fig. 8.58 represents the contribution of traffic emissions to the concentration of PM_{10} at a receptor on the carriageway (Gomez-Perales *et al*., 2003). On-street concentrations are highly variable (Arnold *et al*., 2005) and regulatory model paramaterisation dispersion on the carriageway is currently restricted to a parameter describing the gross effect of traffic-induced turbulence designed to correct the kerbside and roadside contributions not the on-street pollution levels. Nevertheless, this contribution is an important part of commuters' daily experience of pollution, but is not accurately determined by models. Being a component of exposure means current air quality management policy does not require it to be included.

847. Bar two represents the contribution of traffic on the nearest road to PM_{10} at a typical kerbside or roadside location. Our ability to quantify this is described as 'medium confidence' since Gaussian Plume and Street Canyon models are believed to contain most of the necessary science to model this, and there is sufficient roadside monitoring to allow empirical models to perform well in this area. The emissions from traffic averaged over the fleet and over a length of road are also relatively well known. The major source of error arises from the discrepancy between roadside models discussed in Section 8.3.1.

848. Bar three represents the local combustion of primary PM_{10} emissions, further away than the nearest road, to urban concentrations. It is described as 'medium confidence' since Gaussian Plume and empirical models have well-characterised reliable performance at this scale. A major contribution to the uncertainty in this component is the lack of consensus on an appropriate emissions factor for domestic and commercial combustion of natural gas that was noted in Chapter 4.

849. Bar four, secondary organic carbon, is highlighted as a component subject to large uncertainty. This is because neither the precursor emissions nor the identification of the important chemical reactions are well known, and the speciated hydrocarbon chemistry with three-dimensional mixing and oxidation reactions is inherently difficult to model. Note that primary particulate organic carbon is not included here, but probably forms a significant part of the roadside and kerbside contributions.

850. Bar five, regional inorganic secondary PM_{10}, is described as 'high confidence' since the basic chemistry and physics are well known, as described in Chapters 2 and 4. Nevertheless, the complexity of models required to quantify this, and debate on the effect of interannual variability of meteorological conditions and photo-oxidant availability, means that the actual error involved in calculating this component is larger than otherwise might be expected. The general level of agreement between models of this component showed in Section 8.4 is encouraging, but there are marked differences in spatial variability and source apportionment that can give rise to a larger error at specific locations. For this component, empirically deriving the concentration from measured speciation or rural sites can be more accurate than indicated in Figure 8.58.

851. Bar six, coarse fraction, is described as 'very low confidence' with large error since its source is not quantified and its spatial distribution from roadside to background and urban to rural is unknown. The size of the bar merely indicates that its contribution could be large, at least at some locations.

852. When the total PM_{10} contribution is computed from the sum of its components, the magnitude of the total error is critically dependent on the extent to which errors in individual components are correlated with each other. Model evaluation exercises reported in Section 8.2 indicate that it is possible to reproduce past measured PM_{10} annual average concentrations at monitoring sites with an accuracy of the order of ±2 μg m^{-3} or about ±10%. This is a much smaller percentage error than that in individual components. The smallness of the error in total PM_{10} arises partly because some of the larger errors are in components that make a small contribution at the monitoring sites used for model evaluation. But AQEG has concluded that in addition to this, nearly all modellers adopt a process of iteratively comparing their model with measured PM_{10} concentrations and selecting model improvements that tend to reduce differences between measurement and model results. This introduces some empiricism, even into the least empirical models. The resulting tendency is for errors of opposite sign in the modelling of individual components to cancel out to a greater extent than would be the case if they were simply uncorrelated.

8.5.2.2 Future projections

853. Since most models achieve small errors in total PM_{10} at the expense of correct source apportionment, model performance will tend to deteriorate considerably when moving from mapping of past conditions to projection into the future. Where all sources are abated by similar amounts, model performance will be preserved. But where one source is abated much more strongly than others, model performance should be reassessed to take into account explicitly the implications of a factor of two error in the contribution of the most strongly abated component.

8.5.2.3 Other metrics of PM concentration

8.5.2.3.1 90th percentile

854. Model evaluation shows models that calculate daily PM_{10} concentrations before deriving long-term average metrics calculate the 90th percentile concentration with errors no larger than the annual average.

855. Examination of the fit between measured data and the relationships used empirically to convert annual average to 90th percentile in other models shows that an additional error can be introduced at this step, which is the same magnitude as the error in the annual average concentration. The resulting difference in total error in 90th percentile is, however, not large. The difference between ±10% and ±15% is smaller than the difference between one and three standard deviations of model error. Air quality management policy is sufficiently insensitive to the exact probability of exceedence as to demand the more detailed error analysis that would be required to resolve such a small difference.
The convenient rule of thumb that we can calculate the annual average or the 90th percentile both within about ±10% using an empirical or deterministic model therefore still holds.

856. A note of warning, however, needs to be made when modelling the effect of abatement of only one source of PM_{10} instead of all sources together. Analysis of monitoring data discussed by AQEG, but not included in this report, confirms that different components of PM_{10} are often not highly correlated with each other at a given location. The result of this is that the relative change in the 90th percentile

will usually (but not always) be smaller than the relative change in the annual average. For example, halving the transboundary secondary component without any local emissions abatement typically might result in a decrease of around one-third in the 90th percentile of total PM_{10}. Models that fail to take account of this can, therefore, systematically over-predict the effects of abatement.

8.5.2.3.2 Higher percentiles

857. Moving towards less than 35 days exceedence gives much more cause for concern over model performance than the change from annual average to 90th percentile. One of advantages of allowing a certain number of days exceedence of a daily air quality standard is that it allows unrestricted emissions from temporary sources such as national and cultural celebrations involving fireworks. This also has an important advantage for quantitative air quality management since emissions from such temporary sources are inherently very difficult to quantify.

858. AQEG, therefore, recommends that decreasing the number of days exceedence allowed should be done only very deliberately and carefully and not simply as a convenient way of tightening an air quality objective. Reducing the number of days exceedence changes the source apportionment of PM_{10} on the days when the relevant exceedences occur and also increases the error involved in modelling the extent and severity of the exceedence. The kind of source that currently can be ignored in air quality management but starts to contribute or even dominate the analysis when the number of exceedences allowed is reduced from 35 per year to seven, is one that might be responsible for 500 μg m^{-3} of PM_{10} for 90 min per day, two days per week throughout 3 months of the year. It is difficult to assess how widespread sources, such as repeated barbecues or bonfires, are that produce this amount of smoke. Nevertheless, such a source certainly would make a major contribution to exposure and potential health effects of people who are at home at the times when the emissions occur, and so arguably they should be included in air quality management and not merely considered to be a nuisance. Some detailed investigations of intermittent source emissions are, therefore, required to support a reduction in the number of days exceedence allowed.

8.5.2.3.3 $PM_{2.5}$

859. The smaller quantity of monitoring data for $PM_{2.5}$ compared with that for PM_{10}, and the lesser amount of experience modelling this fraction, makes $PM_{2.5}$ somewhat more difficult to model currently than PM_{10}. We note the lack of realism in some of the assumptions in the emissions inventory, especially the lack of fairly obvious changes in particle size with time. But excluding the coarse fraction of PM_{10} from the assessment removes some major areas of scientific uncertainty. AQEG's conclusion overall is therefore that $PM_{2.5}$ can be modelled with accuracy comparable with that of PM_{10}.

8.5.2.3.4 Finer particle size fractions and particle number

860. The availability of measurement data and our understanding of the spatial and temporal variability as well as some of the basic science all decrease on moving to smaller particles than $PM_{2.5}$. Ultrafine particle concentration is more sensitive than $PM_{2.5}$ to the amount of time people spend in close proximity to combustion sources. It would, therefore, be relatively straightforward to consider exposure reduction measures for ultrafine particles, although quantifying these with a high

degree of precision is more challenging. Emissions factors for ultrafine particles from some vehicle classes exist, and on-street as well as roadside measurements have been made in a few locations. There is also some debate over the implications of formation of large numbers of ultrafine particles in clean air.

8.5.2.4 *Sensitivity of air quality management outcome to model uncertainty*

861. Figure 8.58 shows schematically the rate of change of PM_{10} concentration with distance away from a heavily-trafficked city centre location. It is based on a synthesis of the graphs of PM_{10} as a function of distance away from a road, and maps of PM_{10} across London, presented earlier in this chapter.

862. The left side of the graph represents a point on the carriageway of a busy canyon-type road close to the centre of a large city in Southeast England. The right side represents a rural location in the Northwest of Britain. The red line represents a typical annual average PM_{10} concentration at such a location (base year circa 2002) with ±10% considence intervals on a linear scale. The blue line shows the rate of change in concentration with distance on a logarithmic scale. Note the steep gradient, up to 10 μg m^{-3} change in PM_{10} over distances as short as 1 m very close to traffic sources, falling to a rather shallow gradient less than 0.01 μg m^{-3} per m 100 m away.

863. A peculiar phenomenon of PM_{10} is how the gradient decreases much more rapidly with distance than the concentration because of the large contribution of distant sources to the secondary accumulation mode particle mass. Because of this, PM_{10} concentration isopleths enclosing areas between 100 m^2 and 10 km^2 are most sensitive to small errors in concentration – easily a factor of 10 or more for a ±10% concentration error. Even isopleths that are smaller or larger than this can vary in area by a factor of five for the same change in concentration. This should be kept in mind when considering policy implications based on area of exceedence as presented in Chapter 9.

864. Given this sensitivity, and the possibility discussed above that source apportionment errors could be exacerbated in future projections, any policy based on future projection of area of exceedence of an air quality standard is inherently difficult to support quantitatively using modelling.

865. Projected changes in average population exposure can be modelled rather more robustly than the absolute area itself. Numbers of lives saved by air quality management policies can, therefore, perhaps be estimated more easily than absolute numbers of people living at locations where air quality standards are exceeded.

866. Health end-points that are sensitive to short periods of exposure to high concentrations are more strongly influenced by air pollution 'hotspots' through which large numbers of people travel per day. In principle, the steeper PM_{10} concentration gradients at such locations make quantification of exposure reduction benefits inherently easier for such short-term effects than is the case for effects of exposure over 24 h or longer, even though the detailed modelling of concentrations very close to traffic is currently an area of some difficulty.

867. If short-term peak exposures to ultrafine particles can be shown to be important, these are subject to even steeper gradients than PM_{10} close to traffic sources, although our understanding of their origin and fate is less strong. On balance, it is, therefore, unclear to what extent assessment of short-term peak exposure to ultrafine particles might be more or less difficult than short-term peak exposure to PM_{10}.

868. Health end-points that can be shown to be caused by exposure to secondary inorganic aerosol can also be quantitatively assessed relatively easily, as large numbers of people are exposed to the same concentration irrespective of the time they spend at more or less polluted locations within an urban area.

869. The regime in which it is most complicated and difficult to draw the boundary of an area of exceedence is the urban background. The combination of high concentration, shallow gradient and contribution of sources at a wide range of distances means that indicators of air quality of pollution impact in these areas need to be selected with care, to avoid making impossible demands on model performance. This is discussed at length in Colvile *et al*. (2002). This is also the environment in which most of our population live, so that moving the boundary of an area of exceedence results in very large numbers of people being excluded or included. Place of residence is not a good indicator of PM_{10} exposure variability for these people, and so greater consideration of the influence of lifestyle and daily movement on their exposure to outdoor sources of air pollution might allow much better use to be made of the ability of current modelling and mapping techniques to identify opportunities to reduce exposure.

8.6 Conclusions and recommendations

870. The chapter has presented details of a range of models of varying complexity for different spatial scales that are used for air quality assessment and policy development in the UK. Although there is significant divergence between the models, especially for future projections, the following general conclusions can be reached regarding the limit values for 2005 and 2010.

871. In 2005 the annual limit value 40 μg m^{-3} is likely to be achieved throughout the UK. However, the daily limit value of 35 exceedences of 50 μg m^{-3} may not be achieved near major roads in urban areas in particular in London and, more especially, in meteorological conditions that lead to high background levels transported from mainland Europe.

872. In 2010 the Stage II indicative annual limit value will be exceeded in many urban and roadside areas. Models diverge significantly on the likely exceedence of the indicative daily limit value of seven exceedences of 50 μg m^{-3}.

873. The model descriptions and uncertainty analysis have highlighted significant areas where the reliability of model calculations is limited. These include the coarse fractions – both urban background and roadside, the treatment of secondary organic carbon and the variability of roadside concentration with road characteristics. In contrast, the secondary component is well modelled at least for annual averages.

874. Model development is best focussed on areas of model uncertainty that have significant impacts on calculated concentrations.

875. It is recommended that models are developed for the coarse component both from the urban background, for example, from construction sites and from traffic – both direct emissions and non-exhaust traffic emissions. Any significant development will require improved parameterisation of these emissions. Secondly improved modelling and understanding of the impacts of road characteristics including traffic induced turbulence, vehicle exhaust height, urban topography etc. These will both increase confidence of the road type adjustment factors and improve the reliability of dispersion models adjacent to roads.

876. Further modelling of $PM_{2.5}$ should also be conducted in anticipation of new air quality standards. However, reliable model validation will require appropriate resolution of the difference between the different measurement techniques (for example, stipulation of appropriate conversion factors and so on).